The unsolved mystery of human ADP-dependent glucokinase

A thesis presented in partial fulfilment of the requirement for the degree of Master of Science in Biochemistry at Massey University, Palmerston North, New Zealand.

Amanda Gribble

1/1/2010

Acknowledgements

I would like to express my appreciation to my supervisor Dr. Kathryn Stowell who has supported me and driven me throughout my research. Without your faith and encouragement I would have not have believed in myself or achieved all that I did. I would also like to thank my co-supervisors Ron Ronimus and Andrew Sutherland-Smith for their support and advice through my work.

I would like to acknowledge and thank my parents for their never-ending love and support through the good and tough times. Your hardworking and passionate attributes have been an inspiration to me and without you I would not have completed this work. Thank you to all my friends who have stuck by me on this journey, especially to Jazz, you have been my rock and my sanity.

A huge thank you must be given to everyone in the Twilight zone, it has been a pleasure working with such passionate and dedicated people. I would like to specially thank Natisha for putting up with my endless questions, and for your continual advice and friendship. Without your wisdom and encouragement I couldn't have done this.

Thank you to Dmitry for his technical support and to Massey University for their financial support.

Abstract

Human ADP-dependent glucokinase (hADP-GK) is the most recently discovered glycolytic enzyme that has been shown experimentally to phosphorylate glucose to glucose-6-phosphate. This reaction is catalysed using ADP as the phosphoryl donor, which is uniquely different from the traditional ATP-dependent hexokinase type I-IV enzymes that were initially shown to carry out the first step of glycolysis.

The functional role of hADP-GK within the cell and the significance of utilizing an ADP-dependent glucokinase have yet to be elucidated experimentally. It has been hypothesised that the unique characteristic of ADP utilisation may provide cellular advantages during times of limited energy and oxygen (hypoxia), as ATP is able to be conserved during anaerobic glycolysis. Cellular survival and sustainability may be increased during disease states as ADP is invested into the first step of glycolysis instead of ATP. AMP is also produced during this reaction, and may activate AMP-activated protein kinase (AMPK), an energy sensor within the cell, which may regulate energy metabolism during times of low energy and/or hypoxia.

Prior to this research no experimental work had been carried out on the regulation of hADP-GK at the transcriptional level. The main objectives of this project were to investigate the effect of glucose concentration on the expression of hADP-GK at the transcriptional level, and to investigate the promoter and potential transcription factors responsible for promoter activity. The cellular localisation of hADP-GK was also briefly investigated through microscopy. This experimental work has opened up a new path for future research, and therefore the continuation of this project would be important in understanding the role of hADP-GK.

Abbreviations

ADP-GK	ADP-dependent glucokinase
Amp	Ampicillin
AMP	Adenosine monophosphate
APS	Ammonium persulfate
ATP	Adenosine triphosphate
bp	Base pairs
BSA	Bovine serum albumin
cDNA	Complimentary DNA
CDTA	1,2-disminocyclohexane-N,N,N',N-tetraacetic acid
ChREBP	Carbohydrate response element-binding protein
CRE	cAMP response element
CREB	cAMP response element binding protein
cpm	counts per minute
Cq/Ct values	PCR crossing points
CV	Coefficient of variance
DAPI	4',6-diamidino-2-phenylindole
DEPC	Diethylpyrocarbonate
DMSO	Dimethyl sulfoxide
DNA	Deoxyribose nucleic acid
dNTP	Deoxynucleoside triphosphate (dATP, dCTP, dGTP, dTTP)
DTT	Dithiothreitol
E	Amplification efficiency
E. coli	*Escherichia coli*
EDTA	Ethylene diamine tetra-acetic acid
EMSA	Electrophoretic Mobility Shift Assay

ER	Endoplasmic reticulum
FCS	Fetal calf serum
FITC	Fluorescein-5-isothiocyanate
GAPDH	Glyceraldehyde 3-phosphate dehydrogenase
gDNA	Genomic DNA
GSB	Gel shift buffer
GR	Glucocorticoid receptor
hADP-GK	Human ADP-dependent glucokinase
HCl	Hydrochloric acid
HeLa	Human cervical cancer cell line
HEPES	N-[2-hydroxyethyl]piperazine-N'-[2-ethane sulfonic acid]
HRP	Horse radish peroxidase
IgG	Immunoglobulin G
IPTG	Isopropyl β-D-thiogalactoside
KCl	Potassium chloride
kDa	Kilodaltons
LB	Luria Bertani bacteriological media
mADP-GK	Mouse ADP-dependent glucokinase
mM	Milli Molar
µL	Micro Litre
µg	Micro Gram
mRNA	Messenger RNA
mt	Mutant
Mw	Molecular weight
NaCl	Sodium chloride
NADH	Nicotinamide adenine dinucleotide
ng	Nano Gram

NS	Non-specific
NTC	Non-template control
ONPG	o-nitrophenyl 1-β-D- galactopyranoside
PAGE	Polyacrylamide gel electrophoresis
PBS	Phosphate buffered saline
PCR	Polymerase chain reaction
PDI	Protein Disulfide Isomerase
PM	Plasma membrane
RNA	Ribonucleic acid
RNase	Ribonuclease
rpm	revolutions per minute
RT-qPCR	Reverse transcription-quantification polymerase chain reaction
SDS	Sodium dodecyl sulfate
SDS-PAGE	SDS-polyacrylamide gel electrophoresis
Sp1	Specificity factor 1
TAE	Tris acetate EDTA buffer
TBE	Tris borate EDTA
TBST	Tris-buffered saline-Tween 20
TE	Tris-EDTA buffer
TEMED	N,N,N',N'-Tetramethylethylenediamin
Tm	Melting temperature
Tris	Tris (hydroxymethyl)-aminomethane
TRITC	Tetramethyl Rhodamine Isothiocyanate
TSP	Transcription start point
UV	Ultra violet
Wt	Wildtype
X-gal	5-bromo-4-chloro-3-indoyl-β-D-galactosidase

List of Figures

Page number

List of Tables

Table of Contents

Chapter One: Introduction

The phosphorylation of glucose upon entry into the cell is the first step in the crucial pathway that utilises glucose for energy production. It is widely known that this step is catalysed by a family of enzymes called hexokinases (Katzen and Schimke, 1965). Hexokinases phosphorylate glucose to glucose-6-phosphate using ATP in the first step of glycolysis. More recently the discovery of a new mammalian glycolytic enzyme called ADP-dependent glucokinase (ADP-GK) has been shown to catalyse an alternative reaction (Ronimus and Morgan, 2004). The alternative reaction involves the phosphorylation of glucose via a different phosphoryl donor as shown in the following reaction:

Glucose + ADP ⟶ Glucose-6-phosphate + AMP

The significance of this reaction is that ADP is utilised rather than ATP in conventional glucose phosphorylation reactions and therefore has the potential to conserve ATP. The role of ADP-GK in mammalian systems is currently unknown and is the focus of the research carried out for this thesis.

1.1 Glycolysis

ATP is the energy currency of the cell, providing fuel for hundreds of reactions required for cellular function. Glycolysis is a catabolic process that results in the production of ATP through the degradation of glucose. Glycolysis was first investigated by Louis Pasteur in 1860 when he observed the fermentation of grape sugars (Pasteur, 1861). Later in the 20th century three German scientists Warburg, Embden and Meyerhof elucidated the entire pathway, and hence the ten enzyme-catalysed glycolysis pathway is often referred to as the Embden-Meyerhof pathway (Warburg, 1956). The glycolytic pathway is highly conserved in all plants, microorganisms and animals including humans with only minor variations in individual steps. Glycolysis is thought to be an important biological pathway conserved during evolution when oxygen and nutrients were limited.

The ten enzyme-catalysed steps can be broken down into two phases. The first phase involves five of the enzyme-catalysed reactions. In the first phase glucose enters the cytosol of the cell and is converted to two molecules of glyceraldehyde-3-phosphate (refer to Figure 1.1, steps 1 & 2). During the first phase two molecules of ATP are invested into the pathway to allow the phosphorylation of glucose to glucose-6-phosphate and D-fructose-6-phosphate to D-fructose-1,6-bisphosphate, respectively (refer to Figure 1.1, steps 3 & 4). Phosphorylation of glucose in the first step ensures that glucose molecules can no longer diffuse back across the plasma membrane due to the negative charge of the phosphate.

The second phase of glycolysis involves the conversion of glyceraldehdye-3-phosphate to pyruvate (refer to Figure 1.1, steps 5a-10). During these five steps four molecules of ATP are produced resulting in a net gain of two ATP for every molecule of glucose utilised. This is known as substrate level phosphorylation. The overall aerobic reaction is shown below:

$$\mathbf{Glucose + 2NAD^{+} + 2ADP^{3-} + 2P_i^{2-} \rightarrow 2\ NADH + 2pyruvate^{-} + 2ATP^{4-} + 2H_2O + 2H^{+}}$$

When oxygen is available, the pyruvate produced during glycolysis is then transported to the mitochondrion where acetyl coenzyme A is formed and then metabolised within the tricaryboxylic acid (TCA) cycle and the electron transport chain to produce large quantities of ATP. CO_2 and NADH are produced upon pyruvate oxidation. The electron transport chain involves a series of electron carriers which reoxidise $NADH/H^+$ to NAD^+, with each conversion resulting in the production of ~3 ATP. This occurs through the generation of a proton gradient across the mitochondrial inner membrane which produces free energy upon dissipation. This free energy can be used to form ATP from ADP and inorganic phosphate. The final electron acceptor is oxygen, making the process aerobic. The overall outcome of aerobic glycolysis is the net production of 30-38 molecules of ATP for every glucose molecule oxidized (Flurkey, 2010).

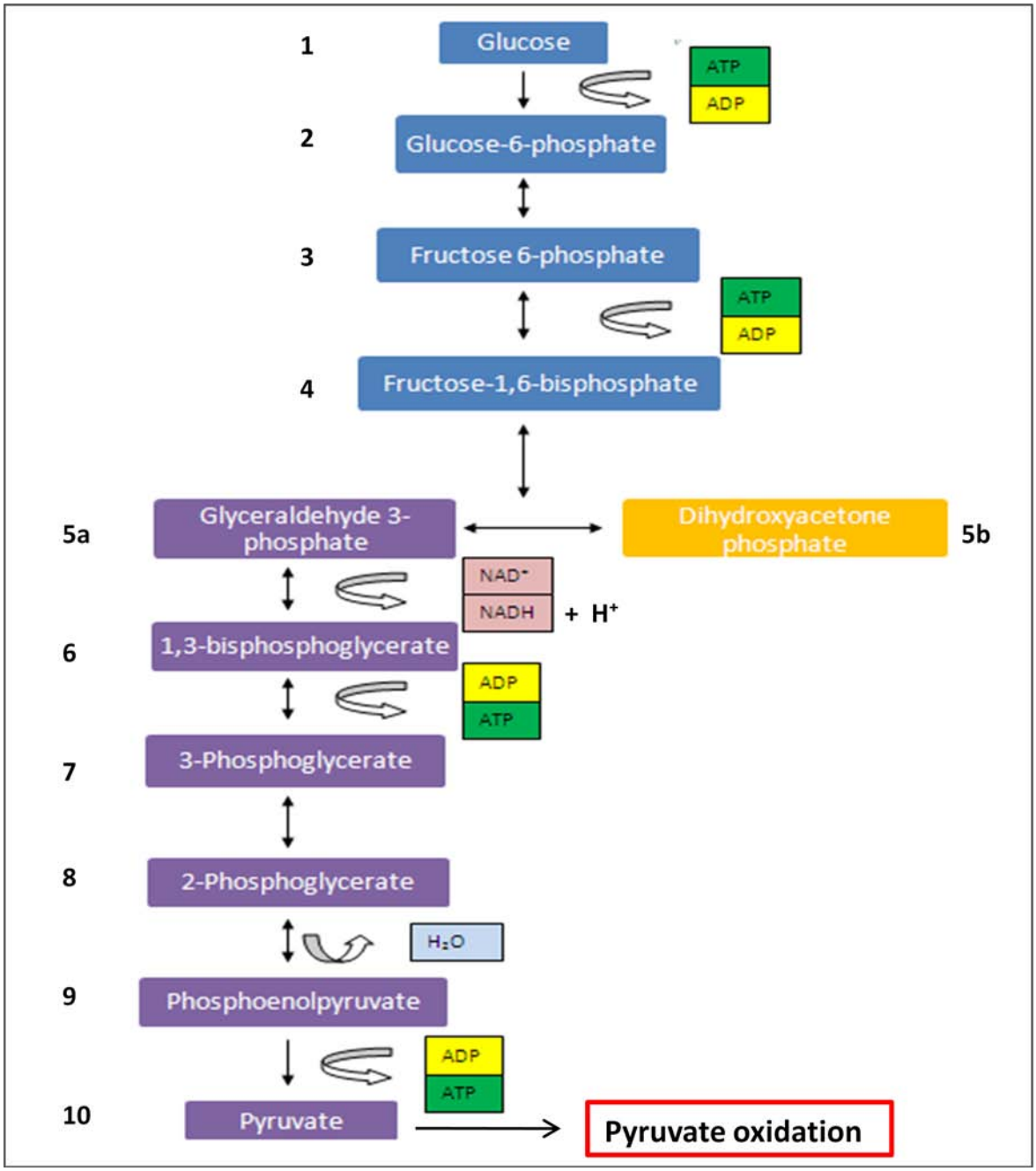

Figure 1.1 Schematic diagram of glycolysis

The glycolytic pathway involves the conversion of one molecule of glucose to two molecules of pyruvate, during which two molecules of ATP are synthesised from ADP and P_i in two substrate level phosphorylation reactions.

In conditions when oxygen is limiting, such as anaerobic metabolism in the muscle, the pyruvate produced from glucose utilisation is converted to lactate. This enables the

reoxidisation of NAD^+ from NADH without the input of oxygen (Semenza, 2007). The lactate is transported from the muscle to the liver where is it converted back to pyruvate and finally glucose. The overall anaerobic reaction is shown below:

$$\mathbf{Glucose + 2ADP^{3-} + 2P_i^{2-} \rightarrow 2lactate^{-} + 2ATP^{4-} + 2H_2O}$$

Due to the decrease in oxygen availability the electron transport chain is compromised, and the production of additional ATP is reduced. This demonstrates how ATP production is heavily dependent on glycolysis. During anaerobic processes, the enhancement of glycolysis called the Pasteur Effect is carried out. This effect is essential when cells undergo stressful conditions, such as hypoxia, and energy demands need to be met to maintain cellular function. There is only an overall net gain of 2 ATP during anaerobic glycolysis, this means the amount of ATP is greatly reduced and could compromise the chance of cell survival during hypoxia and low glucose conditions, such as that exhibited during cancer, stroke and ischemic heart disease (Zu and Guppy, 2004).

1.2 Hexokinase Family I-IV

The hexokinase (ATP: D-hexose 6-phosphotransferase) family is a group of enzymes that can catalyse the first step in the pathway of glycolysis where glucose is phosphorylated. The hexokinase family includes four isozymes each distinct from each other by its electrophoretic, kinetic, chromatographic and enzyme stability properties. The amounts and enzyme activity of each hexokinase isozyme differs from tissue to tissue depending on age, nutritional factors and enzyme stability (Katzen and Schimke, 1965). Hexokinase type I, II and III are similar in molecular properties including size, inhibition by its products and affinity for glucose. They are found in almost all tissues including the brain. Hexokinase type IV, also known as the ATP-dependent glucokinase, is much smaller than its relatives, and has its own set of unique characteristics including a low affinity for glucose, inhibition by regulatory proteins and the binding of glucose shown by a sigmoidal saturation curve. Hexokinase type IV is found mostly in the liver where it has a key role in maintaining blood glucose levels (Van Schaftingen *et al*., 1994).

The hexokinase types I, II and III have a molecular weight of approximately 100 kDa and are thought to have evolved from the ancestral 50 kDa type IV hexokinase. It has been proposed that the fusion of the gene encoding hexokinase type IV may have led to the formation of the other hexokinase isozymes, which explains the similarity in the internal and the N- and C-terminal sequences among all hexokinases across various species (Cardenas *et al*., 1998). Multiple duplication of the ancestral gene is thought to have produced variability amongst the isozymes. The high degree of conservation of these enzymes suggests that each enzyme may play an important role within the mammalian cell. Differences may have arisen to support specific metabolic roles determined by the various regulatory and catalytic properties of each enzyme; tissue specific functions may cause variations in gene expression depending on environmental conditions, and finally localisation of various pathways may require compartmentalisation of certain enzymes involved in glycolysis for the further utilisation of by-products (Wilson, 1997).

The four hexokinase enzymes carry out the same reaction that phosphorylates glucose to glucose-6-phosphate (Glu-6-P). Hexokinase type I-III exhibit sensitivity to inhibition by Glu-6-P which is the key product involved in enzyme activity regulation. This is the initial step of glucose metabolism, where the product Glu-6-P can be utilised in multiple pathways. Firstly, Glu-6-P is utilised through the pathway of glycolysis to produce energy in the form of ATP. Secondly Glu-6-P is used for storage purposes via glycogen and starch, and finally Glu-6-P is used through the pentose phosphate pathway to provide NADPH which can be used in reductive biosynthesis of nucleotides and glycolytic intermediates (Wilson, 2003). The breakdown of Glu-6-P in the pentose phosphate pathway is shown in the following reaction:

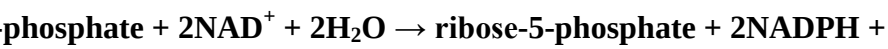

Hexokinase type I is expressed in all tissues with a high prevalence in brain tissue. Its major functional role is glycolytic through the phosphorylation of glucose. It has a characteristic N-terminal sequence that is hydrophobic, which allows the association between the outer mitochondrial membrane to occur by selective targeting (Tsai and Wilson, 1997). Within the

mitochondrial membrane a voltage dependent anion channel (VDAC), called Porin, controls the metabolites that cross through the membrane, and interacts with hexokinase type I. The Porin channel facilitates the phosphorylation of glucose by providing a quick supply of ATP from the process of oxidative phosphorylation that occurs within the mitochondria (Arora and Pedersen, 1988). The two halves of the hexokinase type I isozyme are different in comparison with the other hexokinase enzymes. The catalytic activity is predominantly found in the C-terminal half, while the N-terminal half is associated with the regulatory function, i.e. the binding site for Glu-6-P. Evolutionary studies of hexokinase type I predict that mutations in the N-terminal half resulted in the production of the isozyme (Tsai and Wilson, 1995).

Hexokinase type II is found in insulin-responsive tissues including cardiac and skeletal muscle, adipocytes and liver with only minimal levels of expression. It is found within cytosolic fractions, as well as exhibiting the hydrophobic sequence within the N-terminal half allowing the association with the mitochondrial outer membrane. It has been hypothesised that the association between hexokinase type II and the mitochondrial membrane facilitates the survival of cancerous tissue by enabling efficient catabolism of glucose for energy production. It is thought that association with the mitochondrial membrane changes the kinetic properties of the enzyme, which result in a reduction in sensitivity to product inhibition. Unlike its relatives, hexokinase type II is involved in both catabolism and anabolism, therefore also contributing to the synthesis of glycogen and lipids *(*Nakashima *et al*., 1988, Pedersen, 2007, Sebastian *et al*., 2001).

Hexokinase type II is believed to be the first of the three enzymes that evolved through gene duplication from hexokinase type IV because the sequences of the C- and N-terminal halves share greater similarity with each other when compared to the amino acid sequences of the other hexokinase enzymes. Both halves have equivalent functions for catalysis and regulation, with very little interaction between the two halves (Tsai and Wilson, 1996). Hexokinase type II is the most commonly expressed hexokinase found in tumours and is thought to be responsible for the increase in glycolytic activity observed in some cancerous cells (Marin-Hernandez *et al*., 2006). In tissues such as the liver and pancreas, a 'switch-over' from hexokinase type IV to hexokinase type II expression has been observed. This has

been further elucidated by studies involving hexokinase promoter activity and regulation. Within the promoter region of the hexokinase type II gene a 4.3 kbp region has been shown to be responsive to glucose concentration. A positive correlation has been observed where glucose concentrations are high an increase in promoter activity is observed. Glucose has also been implicated with a role in up-regulating other glycolytic enzymes such as pyruvate kinase, as well as lipogenic enzymes. It is likely that this mechanism is required to ensure adequate glucose utilisation during stressful conditions by increasing the activity and distribution of glycolytic enzymes. A second regulatory effect of glucose is observed through the activation of the cAMP-dependent protein kinase (PKA) signal transduction pathway, which is switched on during times of low glucose. Once again the promoter is activated resulting in an up-regulation of the hexokinase type II gene (Rempel *et al*., 1996, Lee and Pedersen, 2003).

Another function of hexokinase type II within tumour cells involves the inhibition of apoptosis and cell death through the association with the mitochondrial membrane. This mechanism involves the binding of proteins, which are involved in apoptotic events, to the membrane, such as Bax which has been shown to inhibit the release of cytochrome c in HeLa cells. This potentially would provide an advantage for tumour cells over normal cells (Pastorino *et al*., 2002, Mathupala *et al*., 1997, Pedersen *et al*., 2002).

Hexokinase type III enzymes share characteristics with both hexokinase type I and hexokinase type II enzymes. It has very low levels of expression across a wide range of tissues. It lacks the N-terminal hydrophobic sequence and therefore does not exhibit binding with the outer mitochondrial membrane. It is found in soluble extracts and is therefore located within the cytosol of the cell. It has however been shown to associate with the nuclear membrane and is believed to carry out a similar metabolic advantage as that seen with hexokinase type I and hexokinase type II when associated with the mitochondrial membrane. It also exhibits the same amino acid similarities for the C- and N-terminal halves in terms of catalytic and regulatory properties as observed for hexokinase type I (Preller and Wilson, 1992, Tsai and Wilson, 1997).

Hexokinase type IV, or ATP-dependent glucokinase as it is more commonly known, is the only member of the hexokinase family that has been found to have tissue specific distribution. Hexokinase type IV is found in hepatocytes, insulin-secreting β-cells of the pancreas, neurons of the brain, endocrine and pituitary cells. The major function of hexokinase type IV within the liver and pancreas is to maintain glucose homeostasis, while its functions in other tissues have yet to be determined. Within the liver, glucokinase controls the storage of glucose in the form of glycogen through the initiation of gluconeogenesis; while in the islets of Langerhans the role of glucokinase is to monitor the concentration of glucose (Zelent *et al*., 2006, de la Iglesia *et al*., 2000).

Experiments focused on gene expression and promoter analysis have identified tissue specific promoter elements specific for hexokinase type IV expression which accounts for the differences in enzymatic activity of glucokinase between tissues. The downstream promoter regions control the β-cell form, while the up-stream promoter regions control the liver form. Binding sites on the two promoters differ resulting in specific regulation of each glucokinase form. Within the liver, insulin controls the regulation of glucokinase type IV and the activity of the enzyme is affected by nutritional status. This differs with the β-cell enzyme which has constant activity despite changes in nutrition. Glucagon acts via cyclic AMP-dependent protein kinase (AMPK) to repress glucokinase type IV expression within the hepatocytes while the β-cell form is only minimally regulated by hormones (Magnuson and Shelton, 1989, Matschinsky *et al*., 2006).

Along with the regulation of the liver glucokinase by insulin, regulation of enzyme activity is also controlled by a 68 kDa glucokinase regulatory protein (GKRP). When glucose is low GKRP binds to the glucokinase and causes inactivation by sequestering the hexokinase type IV within the endoplasmic reticulum. When the nutritional status returns to normal the association between the regulatory protein and the hexokinase type IV is removed, and the hexokinase is translocated back to the cytosol where it is once again active (Matschinsky *et al*., 2006, Anderka *et al*., 2008).

1.3 The Pasteur Effect

During diseased states such as cancer, heart attack, sepsis and stroke, stress is placed upon cellular functions due to limited oxygen (hypoxia) and limited nutrient availability. To ensure cell survival, adaptation to changes in the cellular environment must occur, or cell death from apoptosis or necrosis will result. On a short term basis up-regulation of glycolysis and the switch from aerobic to anaerobic metabolism can be carried out to support the energy demands of the cell during diseased conditions (Guppy, 2005). This process can occur through the alteration of gene expression, which involves the down-regulation of genes encoding enzymes active in the electron transport chain and the up-regulation of the genes encoding components of the glycolytic pathway (Semenza *et al*., 1994).

The Pasteur Effect was first described by Louis Pasteur in 1860 when he observed an increase in glycolysis under anaerobic conditions using grapes undergoing fermentation. Pasteur observed that fermentation was inhibited by the presence of oxygen and that there was an inverse correlation between glucose consumption and the availability of oxygen (Pasteur, 1861). Overall the number of molecules of ATP produced per each unit of substrate is reduced during anaerobic glycolysis; however the rate at which ATP is produced is increased. During states of low oxygen and glucose, anaerobic processes can maintain an adequate energy supply by the up-regulation of glycolytic enzymes and glucose transporters (Semenza *et al*., 1994). Changes in enzyme availability and activity through alteration in gene expression are primarily mediated through the transcriptional regulator hypoxia-inducible factor-1 (HIF-1). HIF-1 has been implicated in the maintenance of free ATP levels through the observation that HIF-1 mutants exhibit a notable drop in ATP levels. ATP levels drop due to the loss of glycolytic enzyme induction seen during the Pasteur Effect. Therefore HIF-1 can be considered as a key mediator of the Pasteur Effect (Seagroves *et al*., 2001).

AMP-activated protein kinase (AMPK) is likely to have a role in the induction of the Pasteur Effect, as its activity is known to be induced during hypoxia and low glucose conditions. AMPK increases glucose absorption from the blood supply, and enhances glycolysis promoting ATP production, all characteristics of the Pasteur Effect. It is likely that a combination of increased AMPK and HIF-1 activity induces the Pasteur Effect exhibited during stressful conditions related to hypoxia (Laderoute, 2006).

1.4 The "Warburg Effect"

Under hypoxic conditions glucose metabolism switches from aerobic to anaerobic glycolysis to maintain adequate energy production. Lactic acid is converted back to glucose within the liver and further metabolised. Cancerous tumours were shown to utilise the process of anaerobic glycolysis even in the presence of oxygen (Warburg, 1956). This phenomenon was termed the "Warburg Effect" after the German scientist Otto Warburg who discovered that tumours could produce a higher rate of ATP by converting glucose to lactic acid by modifying aerobic glycolysis. These modifications exhibited by cancerous cells could potentially provide advantages over normal cellular functions during stressful conditions, and explain why cancerous tissue can undergo rapid cell division and metastasis. The mechanisms involved during the Warburg Effect are both biochemical and molecular, and involve a combination of oncogene alterations, malfunctioning of mitochondrial processes, and tumour environmental adaptations (Dang and Semenza, 1999, Wallace, 2005, Gatenby and Gillies, 2004).

There are a number of benefits obtained by tumours that exhibit the Warburg phenotype, including an increase in biosynthesis, protection from immune responses, induction of negative effects on surrounding tissue to allow invasion and survival. Firstly, an increase in glycolytic rate results in an increase in the biosynthesis of carbon precursors. Building blocks such as cholesterol, phospholipids, nucleic acids and fatty acids are provided for rapid growth and increased cell survival. Secondly, the increased production of lactic acid results in an environment of lowered pH. This may provide protection against immune responses elicited by the body, and cause surrounding healthy cells to become weakened allowing further spread of the cancer. Finally, if oxygen does become limited, the components of the

modified glycolytic pathway can already function adequately without the need for oxygen, and therefore providing cancer cells with an advantage over normal cells (Pedersen, 2007, Guppy, 2002).

A number of key components have been identified that are responsible for the Warburg Effect. These include hexokinase type II, a voltage-dependent anion channel (VDAC) and the transcription factor hypoxia inducible factor one (HIF-1). These components contribute to the rapid glucose uptake and lactate production that occurs in tumours that exhibit the Warburg phenotype (Pedersen, 2007). The mechanisms underlying the involvement of HIF-1 are not fully understood, but evidence suggests that insulin and growth factors, such as vascular endothelial growth factor (VEGF), are able to induce HIF-1 in a hypoxia-independent manner. Numerous oncogenes have been implemented in the onset of the Warburg Effect through the up-regulation of proteins such as hexokinase type II, glucose transporters as well as the activation of glycolysis. One particular example is the Myc oncoprotein which is found to bind to Myc-binding sites found within promoter sequences and activates glycolytic enzymes even in the presence of oxygen (Kim and Dang, 2006). p53 is another oncoprotein shown to up-regulate glycolysis and also enables the re-direction of glucose from energy production to biosynthesis, characteristic of the Warburg Effect (Bensaad *et al*., 2006).

The characteristics exhibited by the Warburg Effect involve an increase in glycolysis, glucose uptake and lactate production, and a decrease in respiration. These characteristics have become key identifiers used to clinically diagnose metastatic disease. Positron-emission tomography (PET) imaging is used to visualise the transport of glucose across the cell membrane and its subsequent phosphorylation by hexokinase. PET can be used to identify the characteristics of the Warburg Effect often exhibited by cancerous tissue and therefore is used to diagnose cancer. There is however some uncertainties towards the method of PET for cancer detection, as a high variability in cancer type and progression exist between patients (Mankoff and Bellon, 2001).

1.5 Hypoxia and Clinical Implications

During oxygen deprivation, cells become hypoxic which can lead to a number of clinical conditions. Hypoxia causes cells to reduce energy production capabilities, and therefore compromises overall cellular function. Hypoxia can occur through a number of different processes including normal physiological and pathological situations. A well studied example of hypoxia is observed in tumours when abnormal blood vessels are formed to supply oxygen and nutrients for rapid cell division, a process known as angiogenesis (Guppy, 2005). Furthermore, it is possible that the increase in metabolic demand exhibited by tumours is responsible for the hypoxic conditions that are often observed (Giatromanolaki, 2001).

An extensive range of clinical implications exist for patients that exhibit hypoxic conditions within tissues compared with patients that have normal oxygen levels. The first is a difference in drug clearance rates which occurs due to a change in expression patterns of genes encoding metabolising enzymes. This has the potential to cause a reduction in drug effectiveness or drug efflux with the possibility of toxicity. Secondly, hypoxia often changes the distribution of blood flow which can alter the rate of drug metabolism by the liver, thereby reducing clearance rates (Lee, 2007). Finally, hypoxia can affect the efficiency of chemotherapy and radiotherapy treatments for cancer patients by reducing the ability of radiation or chemical reactions to create oxygen free radicals, and the subsequent induction of further damage. Hypoxic cells can become radiation- and drug-resistant due to abnormal angiogenesis and consequent lack of oxygen, with the patient's disease-free survival time being directly related to the oxygen tension of the tumour (Guppy, 2005, Guppy, 2002).

1.6 Hypoxia-inducible Factor 1

During disease states, cells must undergo adaptation to stressful conditions to ensure that cellular function continues and cell death is avoided. Regulation of the glycolytic pathway induced during hypoxia and/or low glucose conditions, allows such adaptation to occur. A group of transcription factors called the hypoxia-inducible factors (HIF) carry out regulation through a wide range of gene expression alterations. HIF proteins are known to target a wide range of genes via a *cis*-acting element called the hypoxia-responsive element (HRE) found

within the promoter region. HREs consist of a transcription factor binding site containing the sequence 5´ RCGTG 3´ which is recognised by HIF proteins (Lee, 2007, Caro, 2001, Maxwell *et al*., 2001).

HIF-1 is the most commonly known protein of the HIF family which is up-regulated during hypoxia, and is involved in up-regulating genes involved in glycolysis, iron transport, cell survival, angiogenesis and apoptosis. Tumours that undergo changes from normoxic to hypoxic environments exhibit elevated levels of HIF-1. Both *in vivo* and *in vitro* models have shown that HIF-1 can be responsible for initiating the switch from aerobic to anaerobic glycolysis (Vissers *et al*., 2007, Chen, 2001). HIF-1 is a heterodimer containing an α subunit (HIF-1α) and a β subunit (HIF-1β). The HIF-1α subunit is undetectable during normoxia, but rapidly appears during hypoxia exposure. During normoxic conditions HIF-1α is unstable and degraded via the ubiquitin-proteasomal pathway, which is mediated through the von Hippel-Lindau tumour suppressor protein (VHL). VHL binds with other proteins to form the E3 ligase complex which mediates ubiquitination of HIF-1α along with E1 and E2 enzymes (Guppy, 2002, Kamura *et al*., 2000).

HIF-1α mutants exposed to hypoxia exhibit a decrease in the expression of glycolytic enzymes as well as a reduction in cellular ATP levels. In renal carcinoma cells VHL function is diminished resulting in an increase in active HIF-1α, and the up-regulation of genes encoding enzymes involved in glycolysis. These results indicate the importance of HIF transcriptional factors in the switch from aerobic to anaerobic glycolysis during hypoxia, and that they play a key role in up-regulating glycolytic enzymes required to sustain sufficient ATP levels during disease states such as cancer (Seagroves *et al*., 2001, Mandriota *et al*., 2002).

1.7 AMP-activated Protein Kinase

AMP-activated protein kinase (AMPK) is a regulator of glucose utilising pathways, and is known to be up-regulated during hypoxia and glucose deprivation. AMPK is a heterotrimeric serine/threonine protein kinase that is comprised of an α subunit containing the catalytic site,

a β subunit responsible for regulation and a γ subunit. AMPK is highly conserved within eukaryotes and has been termed a "sensor of cellular energy status". Changes in the cellular AMP/ATP ratio result in the allosteric regulation and phosphorylation of AMPK. This occurs through an increase in AMP which directly activates AMPK via phosphorylation, inhibits dephosphorylation and finally activates further upstream kinases which can also activate AMPK, making the AMPK cascade highly sensitive to changes in AMP concentration (Hardie, 2004). During times of cellular stress, such as hypoxia, ischemia and glucose deprivation, ATP concentrations drop which leads to a change in the AMP/ATP ratio. This results in the activation of AMPK. The activation of AMPK results in the switch of pathways from ATP utilisation to ATP synthesis and conservation by switching on alternative catabolic and switching off anabolic pathways (Hardie, 2004, Carling, 2004).

Targets of AMPK phosphorylation include transcription factors which bind to the cAMP-response element (CRE) and the activating transcription factor (ATF-1) binding sites. Both the CRE and ATF-1 sites are found within the promoters of glycolytic enzymes such as hexokinase and fructose-1, 6-bisphosphate, glucose transporters GLUT1 and 4, and metabolic enzymes such as acetyl-coenzyme A carboxylases (ACC) 1 and 2 involved in fatty acid synthesis. AMPK phosphorylates the proteins that bind to these elements within the promoter. This results in a reduction in ATP utilisation for fatty acid synthesis, and an increase in fatty acid storage, thus conserving ATP (Rattan *et al*., 2005, Laderoute, 2006, Thomson *et al*., 2008).

1.8 Drug Therapy

Recent results in drug development involve the direct inhibition of HIF-1 and other transcription factors involved in the up-regulation of glycolysis during hypoxia and/or low glucose conditions. Another potential area of drug therapy is the alteration of enzymes involved in the glycolytic pathway that are targeted by HIF-1 through gene regulation. Research on hexokinase type II has identified an agent, 2-deoxyglucose, which binds to and inhibits the enzyme reducing its accessibility to glucose. This results in a decrease in ATP production, shutting down cellular functions and resulting in apoptosis. It has been suggested that further advancement in drug therapy could aim to target the inhibition of ATP production

through other components of glycolysis and oxidative phosphorylation (Geschwind *et al*., 2002).

1.8 ADP-dependent Glucokinase

1.8.1 Cloning and Characterisation

ADP-dependent glucokinase (ADP-GK) was first characterised in the archaeon *Pyrococcus furiosus* as a key enzyme in a modified Embden-Meyerhof pathway. The enzyme's physical properties resembled eukaryotic hexokinases, but experiments clearly showed that ADP-GK belonged to a novel family of hexose kinases when compared to other glucokinase and glycolytic enzymes. ADP-GK has a Km value of 0.033 mM for ADP, and a Km value of 0.73 mM for glucose indicating a high affinity for both compounds. ADP-GK was shown to phosphorylate glucose to glucose-6-phosphate using ADP. The utilisation of ADP instead of ATP has been hypothesised to be important in times of starvation when ATP levels are low, and elevated ADP levels ensure adequate phosphorylation of glucose used for entry into glycolysis and subsequent ATP generation (Kengen, 1995).

ADP-GK was recently cloned and characterised from the mouse, confirming that this novel glycolytic enzyme was also present in eukaryotic species. The ADP-GK gene has been mapped to mouse chromosome 9. The recombinant mouse ADP-GK (rmADP-GK) protein has a molecular mass of 51.5 kDa with an apparent Km of 96 μM for glucose and 0.28 mM for ADP. A high specificity for D-glucose was exhibited, as well as inhibition at high concentrations by its substrate and product AMP. The rmADP-GK protein activity differed substantially from ATP-utilising hexokinases and showed no inhibition by its product glucose-6-phosphate. The rmADP-GK protein was also shown to utilize CDP and GDP, two products present during extreme hypoxic and anoxic conditions, suggesting that the enzyme may have an important role in maintaining ATP production during times of cellular stress (Ronimus and Morgan, 2004).

1.8.2 Potential Significance

Sequencing of the human genome verified the presence of an ADP-GK gene located on chromosome 15, with 4 possible alternative promoters and a premessenger coding RNA sequence comprising of 7 exons. Gene expression experiments have revealed a high level of expression throughout a number of mammalian tissues including lymphatic, epithelial, muscular and endocrine organs. It has been suggested that ADP-GK may have an important role in cellular adaptation to low glucose and/or hypoxic conditions. Therefore ADP-GK activity may represent important cellular processes involved in cell survival during disease states such as cancer, heart attack, stroke and sepsis, as well as normal physiological processes such as embryonic development and maintenance of stem cells (Ronimus and Morgan, 2004).

Low glucose and/or hypoxic conditions often arise during disease states such as cancer. Adaptation to these changes is vital for cellular survival and often requires the alteration of various pathways to meet the metabolic demand. One alteration is the switch from aerobic to anaerobic glycolysis. ADP-GK catalyses the first step in glycolysis utilising ADP instead of ATP as its substrate for phosphorylation, therefore conserving cellular ATP levels. This conservation may be important when glycolytic processes become anaerobic and ATP production is substantially reduced. It has been hypothesised that preferential utilisation of ADP-GK instead of ATP-dependent hexokinases may provide advantages for growth and metastasis for cancerous and diseased cells over normal healthy cells (Ronimus and Morgan, 2004).

1.8.3 Regulation of ADP-GK gene expression

Promoter analysis of hexokinase II has shown the presence of hypoxia response elements (HREs) and binding sites for HIF transcription factors (Semenza *et al*., 1994). It has been demonstrated that the ADP-GK promoter does not contain a HRE and therefore it is likely that HIF-1 does not have a direct role in ADP-GK regulation. It is possible however that AMPK is a regulator of ADP-GK activity, as AMPK is up-regulated during hypoxia and the production of AMP by ADP-GK is observed during glucose phosphorylation. The role of AMPK within the cell is to conserve cellular ATP levels during low oxygen conditions when

oxidative phosphorylation is switched to anaerobic glycolysis. Therefore it could be essential for cell survival to activate ADP-GK to ensure the conservation of ATP. It is also possible that AMPK phosphorylates ADP-GK on exposure to hypoxia and this may result in changes in the AMP/ATP ratios (Laderoute, 2006).

1.8.4 Drug Therapy

It has been suggested that ADP-GK could provide a new target for drug therapies for cancer and tissue recovery (Ronimus and Morgan, 2004). Firstly, if ADP-GK is up-regulated during hypoxia and/or low glucose conditions, its removal or down-regulation may provide a means of therapy, even in the presence of hypoxia. Secondly, during heart attacks and strokes the up-regulation of ADP-GK may promote adaptation to changes in the cellular environment, potentially avoiding permanent damage to surrounding tissue. Drug therapies could be developed to target ADP-GK after or during the onset of heart attacks and strokes promoting cell survival, recovery and reducing the overall effects of disease. Finally, due to the functional similarities between hexokinase type II and ADP-GK it is possible that similar agents used to inhibit hexokinase type II could also be used on ADP-GK.

1.9 Research aims

Human ADP-dependent glucokinase is a recently indentified enzyme. Little is known about its cellular roles and regulation of expression of the human ADP-GK gene has not previously been studied. The research objectives of this project addressed this by using RT-qPCR and promoter analysis to identify factors affecting gene expression. Obtaining information on the regulation of hADP-GK will, in the future, help with identifying the possible role of hADP-GK in terms of glycolysis, and other physiological processes.

Specific aims of the project:

- To investigate the regulation of human ADP-GK in response to changes in glucose concentration
- To identify the sub-cellular localisation of human ADP-GK
- To identify possible transcription factor recognition elements within the human ADP-GK promoter

Chapter Two: Materials and Methods

2.1 Materials

2.1.1 Cell culture

Opti-MEM, α-MEM, RPMI Medium 1640 media, fetal calf serum (FCS), penicillin/streptomycin (penstrep) (100x) mix and TrypLE™ Express were obtained from Invitrogen Corporation, CA, USA. Dimethyl sulfoxide (DMSO) was purchased from Sigma-Aldrich, St Louis, MO, USA. Seventy-five cm^2 flasks were supplied by Nunc™, Roskilde, Denmark. Tissue culture 145 x 20 mm dishes were obtained from Greiner Bio-one GmbH, Frichenhausen, Germany. SiHa and the HCT116 ADP-GK over-expressing cell line were provided by Professor Bill Wilson, Auckland Cancer Society Research Centre, School of Medical Sciences, Auckland University, Auckland, NZ.

2.1.2 DNA manipulations

Oligo nucleotide primers for PCR and lysozyme were obtained from Sigma-Aldrich, St Louis, MO, USA. Trizol®, 10x reaction buffer for faststart PCR, Purelink™ HiPure Midikit Kit, pCMV SPORT-βGal and 1 kb plus DNA ladder (1.0 µg/µL) were acquired from Invitrogen Corporation, CA, USA**.** iScript™ cDNA synthesis kit was supplied by Bio-Rad Laboratories, CA, USA. Absolute SYBR capillary mix was obtained from Thermo Fisher Scientific, ABgene House, Surrey, UK. Faststart *Taq* polymerase, low EEO agarose and dNTP mix [10 mM] were purchased from Roche Applied Science, Mannheim, Germany. Restriction endonucleases and buffers were obtained from New England Biolabs, MA, USA and Roche, Mount Wellington, NZ. pGL3-Basic vector, pGEM®-T Vector and ligation system, Wizard® SV Gel and PCR clean-up system and luciferase assay reagent were obtained from Promega Corporation, USA. *E. coli* XL-1 Blue strain was obtained from Stratagene, CA, USA. Optikinase™ and T4 polynucleotide kinase were supplied by usb, Cleveland, Ohio, USA.

2.1.3 Protein manipulations

Monoclonal IgG2 antibody against ADP-dependent glucokinase was obtained from Abnova, Taipei, Taiwan. Rabbit secondary anti-mouse IgG antibody conjugated to horseradish peroxidase, rabbit primary anti-Protein Disulfide Isomerase (PDI) IgG antibody, tubulin (104K4800) monoclonal antibody and N,N,N',N'-Tetramethylenediamine (TEMED) were purchased from Sigma-Aldrich, St Louis, MO, USA. The following antibodies were obtained from Abcam, Cambridge, MA, USA: Rabbit polyclonal (primary antibodies) to Prohibitin and pan Cadherin. Fluorescein-5-isothiocyanate (FITC)-conjugated AffiniPure goat anti-mouse IgG and Tetramethyl Rhodamine Isothiocyanate (TRITC)-conjugated AffiniPure goat anti-rabbit IgG secondary antibodies were supplied by Jackson Immuno Research Laboratories, PA, USA. Sp1 (PEP-2) rabbit polyclonal IgG, Sp3 (D-20) rabbit polyclonal IgG and GR (E-20) rabbit polyclonal IgG antibodies were obtained from Santa Cruz Biotechnology, Santa Cruz, USA. BM chemiluminescence blotting substrate A and B, and positively charged nylon membrane were acquired from Roche Applied Sciences, Mannheim, Germany. Bio-Rad protein assay and precision plus dual colour protein standards were purchased from Bio-Rad Laboratories, CA, USA. Complete™ mini EDTA-free protease inhibitor tablets were obtained from Roche Molecular Biochemicals, IN, USA. Bovine serum albumin (BSA) was supplied by New England Biolabs, MA, USA. ProLong® Gold antifade reagent with 4',6-diamidino-2-phenylindole (DAPI) was obtained from Invitrogen Corporation, CA, USA. FuGene 6 transfection reagent was provided by Roche Diagnostics Corperation, IN, USA. Ninety-six well clear flat bottom microplates and 96 well white flat bottom microplates were obtained from Greiner Bio-one, Germany. Lab-Tek II chamber slides were purchased from Nalge Nunc International, IL, USA.

2.1.4 General laboratory materials

Aseptic pipette tips, 1.5 mL micro-centrifuge tubes, and PCR tubes were purchased from Axygen Union City, CA, USA. Triton X-100, sodium dodecyl sulphate (SDS), ammonium persulfate (APS), NaCl, Coomassie brilliant blue and glucose were obtained from Merck, Darmstadt, Germany. LB broth (10 g SELECT peptone 140, 5 g SELECT yeast extract, 5 g sodium chloride per litre) was supplied by Invitrogen Corporation, CA, USA.

All reagents and chemicals were of analytical grade.

2.2 Methods

2.2.1 Cell culture

All handling of cells was carried out using a laminar air flow hood under aseptic conditions. Opti-MEM, α-MEM, and RPMI Medium 1640 glucose-free media were filter sterilized, stored at 4ºC and warmed to 37ºC prior to use. Initial starting cells were obtained from liquid nitrogen stores, centrifuged briefly to remove DMSO and re-suspended in media prior to use. HeLa cells were grown in Opti-MEM with 2% FCS and 1% penstrep at 37ºC in a 5% CO_2 incubator. SiHa and HCT116 cell lines were grown in α-MEM with 4% FCS and 1x penstrep at 37ºC in a 5% CO_2 incubator. HCT116 cells were cultured in the presence of 3 µM puromycin. After growth was obtained in respective media, cells were transferred to flasks containing RPMI 1640 glucose-free medium supplemented with 4% FCS and 1x penstrep. Cells were treated with or without glucose, and incubated in 5% CO_2 at 37ºC in a humidified atmosphere. Cells were grown in 10 mL of media in 75 cm^2 flasks (T75) for RNA extraction and 15 mL of media in 145 x 20 mm round plates for protein extraction.

Cells were passaged using TrypLE™ Express according to manufacturers' instructions after the removal of spent media. After application of the trypsin solution, cells were dislodged from the bottom of the flask with a slight tapping pressure administered to the side of the flask. Cells were then re-suspended in fresh medium and transferred to new flasks for further growth. Cells were passaged approximately every three days depending on the confluence of each flask. Prior to the first passage, cells were removed to maintain cell stocks. Cells were re-suspended in 2 mL of FCS and 100 µL of DMSO, and aliquoted into 1 mL cryovials.

2.2.2 RNA and cDNA preparation

RNA extraction from cultured cells was carried out using TRizol® Reagent. After removal of media from culture flasks, 0.7 mL of TRizol® Reagent was applied to each T75 flask and incubated at room temperature for 5 minutes. Cells were then dislodged from the bottom of the flask by scraping and transferred to a 1.5 mL microcentrifuge tube, where 200 µL of chloroform was added by vigorous shaking, followed by incubation at room temperature for 3 minutes. The samples were then centrifuged at 4ºC for 15 minutes at 11,000 x g. After

centrifugation, the samples were separated into three phases: an upper layer consisting of a colourless aqueous phase, a middle layer, and a lower layer consisting of a red phenol-chloroform phase. The upper colourless layer was transferred to a new 1.5 mL microcentrifuge tube without disturbing the middle layer as it contained unwanted proteins and mixed with 0.5 mL of isopropanol to allow the precipitation of the RNA. After incubation at room temperature for 10 minutes, samples were centrifuged at 4ºC for 10-30 minutes at 11,000 x g. The centrifugation step resulted in the precipitated RNA forming a pellet on the bottom of the tube, supernatant was removed and the pellet was re-suspended in 1 mL of 75% DEPC-ethanol (0.01% diethlpyrocarbonate treated water with 75% absolute ethanol). Samples were then vortexed for 5-10 seconds and centrifuged for 5 minutes at 6000 x g. After the removal of the supernatant, the RNA pellet was left to air dry for an hour at room temperature, until all traces of ethanol had been evaporated. The pellet was then re-suspended in DEPC-treated water and incubated at 55ºC for 10 minutes. RNA quantities were measured by absorbance at 260 and 280 nm using the Nanodrop spectrophotometer (Nanodrop Technologies). RNA samples were expected to have a ratio of approximately 2 at $A_{260/280}$ (Wilfinger *et al.*, 1997).

iScript™ cDNA synthesis kit for Reverse Transcription PCR (RT-PCR) was used for first-strand cDNA synthesis. The iScript reverse transcriptase has greater sensitivity than other enzymes because it is RNase H+ compared with RNase H- enzymes, and is a modified Moloney Murine Leukemia Virus (MMVL)-derived transcriptase which is optimised for reliable cDNA synthesis from RNA over a wide range of input. Oligo (dT) primers were used to synthesise cDNA from total RNA, which was carried out in a PCR laminar flow cabinet. cDNA quantities were measured by absorbance at 260 nm using the Nanodrop spectrophotometer (Nanodrop Technologies). Tables 2.1 and 2.2 present the components and reaction protocol respectively used to synthesis cDNA.

Components	Volume per Reaction
5x iScript reaction mix	4 µL
iScript reverse transcriptase (1 U/µL)	1 µL
Nuclease-free water	To 20 µL
RNA template (100 fg to 1 µg total RNA)	*
Total volume	20 µL

Table 2.1 Reaction setup for cDNA synthesis using iScript™

*Amount dependent on RNA concentration

Reaction mixture was incubated as follows:
5 minutes at 25ºC
30 minutes at 42ºC
5 minutes at 85ºC
Hold at 4ºC (optional)

Table 2.2 Reaction protocol for cDNA synthesis using iScript™

2.2.3 Polymerase chain reaction

The method of polymerase chain reaction (PCR) enables short, specific DNA sequences to be amplified through a process of thermal cycling, involving a thermostable polymerase and specific pairs of primers. PCR was used to amplify sequences of the ADP-dependent glucokinase coding region to check product specificity, and promoter region to be used directly for cloning. These reactions were carried out using Faststart *Taq* (*Thermophilus aquaticus*) DNA polymerase.

2.2.3.1 Amplification of coding regions

PCR reactions were carried out in 0.2 mL PCR tubes with a total reaction volume of 50 µL. Thirty microlitres of sterile water, 5 µL of reaction buffer (500 mM Tris-HCl, pH 8.3, 100 mM KCl, 50 mM $(NH_4)_2SO_4$) (Invitrogen), 2.5 µL of 20 mM Mg^{2+}, 5.0 µL of 3.0 mM dNTP mix, 2.5 µL of forward and reverse primers, each at a concentration of 100 ng/µL, 0.5 µL of Faststart *Taq* DNA polymerase (1.0 U/µL), and 2 µL of cDNA template (1.35 µg/µL) were

added to the PCR tube. Each tube was mixed gently by vortex and pulse centrifuged to allow the collection of the contents in the tube bottom. Table 2.3 presents the PCR scheme carried out using the PTC-200 PCR machine, Biolab Scientific LTD.

2.2.3.2 Amplification of promoter regions

PCR reactions were carried out in 0.2 mL PCR tubes with a total reaction volume of 50.0 µL. Twenty three microlitres of sterile water, 5.0 µL of 10x PCR reaction buffer (500 mM Tris-HCl, pH 8.3, 100 mM KCl, 50 mM $(NH_4)_2SO_4$) (Invitrogen), 2.5 µL of 25 mM Mg^{2+}, 5.0 µL of 3 mM dNTP mix, 5.0 µL forward and reverse primer, each at a concentration of 50 ng/µL, 2.5 µL of Faststart *Taq* DNA polymerase (1.0 U/µL) and 2.0 µL of template DNA (100 ng/uL) were added to each PCR tube. Each tube was mixed gently by vortex and pulse-centrifuged to allow collection of the contents in the tube bottom. Table 2.3 illustrates the PCR program carried out using the PTC-200, Biolab Scientific LTD.

95ºC 5.0 min				Initial denaturing
	95ºC	30 sec		Denaturing
	Primer dependent	30 sec	45x cycles	Annealing
	72ºC	30 sec		Extension
72ºC 7.0 min				Final extension

Table 2.3 PCR scheme for hADP-GK coding and promoter region amplification

All PCR products were measured by absorbance at 260 and 280 nm using the Nanodrop spectrophotometer (Nanodrop Technologies). DNA samples were expected to have a ratio of approximately 1.8 at $A_{260/280}$ (Wilfinger *et al*., 1997).

2.2.4 Agarose gel electrophoresis

Agarose gel electrophoresis is a technique that can be used to analyse PCR products. After completion of PCR, 10 µL of each reaction was mixed with 2 µL of DNA loading dye (40% w/v sucrose, 0.25% bromophenol blue) and loaded onto a 1% agarose gel (0.6 g agarose dissolved in 60 mL of 1x TAE) with 1 µL of ethidium bromide (0.5 µg/mL) to allow the separation of PCR products. Once dissolved, the agarose was allowed to cool to ~55ºC and then poured into the electrophoresis apparatus equipped with a 10 well comb, and left for 20-30 minutes to allow solidification. The comb was then removed and 1x TAE was poured over the gel. Each sample was then loaded onto the gel along with a 1 kb plus DNA ladder (1.0 µg/µL) to allow the determination of DNA fragment size. Electrophoresis was carried out at 100 volts for one hour until the dye front was approximately three quarters of the way down the agarose gel. Ethidium bromide is an intercalating agent that binds strongly with DNA and can be used to visualise DNA as it fluoresces orange under UV light. A Gel Doc™ (BioRad) was used to visualise the DNA bands and photographs of the gel were taken for further analysis or as a permanent record.

2.2.5 Real-time PCR

Real-time PCR is a method of polymerase chain reaction that involves the detection of PCR products during the exponential phase of amplification at each cycle. Unlike conventional PCR which only allows detection at the end of the reaction, real-time PCR allows amplification and detection to occur at the same time for each reaction cycle. Real-time PCR was used to analyse the relative quantification of the ADP-GK coding region before and after glucose treatments.

After the extraction of RNA from cultured cell lines and first strand cDNA synthesis, serial dilutions of cDNA in water were carried out at 1:10, 1:100, 1:1000 and 1:10,000 for the production of standard curves using real-time PCR. Seven point five microlitres of PCR mastermix containing 5.0 µL of Absolute mastermix, 0.5 µL each of the forward and reverse primers, at a concentration of 100 µg/µL for ADP-GK 644 and 50 µg/µL for β-actin 202, and 1.5 µL of sterile water was added to each well of the 96-well plate with 2.5 µL of cDNA template to a total volume of 10 µL per reaction. All reactions were carried out in triplicate.

The following PCR scheme was used for real-time PCR using the Roche LC480, Roche, Mount Wellington, NZ.

Target ºC	Acquisition Mode	Hold mm:ss	Ramp Rate ºC/s	Acquisitions Per ºC
Program Name: Denature **Cycles**: 1				
95	None	15:00	4.4	-
Program Name: Amplification **Cycles:** 40				
95	None	00:10	4.4	-
61	None	00:10	2.2	-
72	None	00:16	4.4	-
85	Single	00:01	4.4	-
Program Name: Melt **Cycles:** 1				
95	None	00:01	4.4	-
65	None	00:15	2.2	-
95	Continuous	-	-	5
Program Name: Cool **Cycles:** 1				
40	None	00:30	1.5	-

Table 2.4 RT-PCR reaction scheme

2.2.6 Restriction endonuclease digests

Restriction endonuclease digests were used to prepare PCR products and vectors for ligation, to verify PCR and primer specificity, and to characterise the pGL3-Basic vector after cloning. The components of the enzyme digests are listed below in Table 2.7.

Component	Concentration	Volume (µL)
Buffer 4	10x	2
Enzyme	10 U/µL	1
Plasmid from rapid boil	-	5
Sterile water	-	Up to 20 µL total volume

Table 2.5 Components of the restriction endonuclease digests

The reaction was incubated at 37ºC for 1 hour and then samples were loaded onto a 1% agarose gel in 1x TAE for analysis by gel electrophoresis.

2.2.7 Cloning hADP-GK promoter fragments

2.2.7.1 Preparation of heat shock competent E.coli cells

Escherichia coli (E. coli) XL-1 Blue competent cells were prepared using a $CaCl_2$ method. Fifty millilitres of LB broth was inoculated with 1 mL of overnight culture and grown to an optical density (O.D.) of approximately 0.5 at A_{600}. The cells were then collected by centrifugation at 1000 x g for 10 minutes. The supernatant was removed and 50 mL of ice-cold 50 mM $CaCl_2$ was used to re-suspend the pellet followed by an incubation period of 20 minutes on ice. Centrifugation was repeated and the pellet was re-suspended in 2 mL of ice-cold 50 mM $CaCl_2$ followed by incubation on ice for 2 hours. Glycerol stocks were prepared using the competent *E. coli* XL-1 Blue cells by mixing 500 µL of sterile 40% glycerol with 500 µL of overnight culture (5 mL of broth plus 5 µL of ampicillin (100 mg/mL)).

2.2.7.2 Cloning PCR products into pGEM®-T vector

The pGEM®-T Vector Systems kit was used to clone the hADP-GK promoter region from PCR products. This vector was used initially during cloning to ensure that the ends of the hADP-GK promoter fragments contained the required restriction endonuclease cut sites for correct ligation into the pGL3-Basic vector. The pGEM®-T Vector Systems kit uses a convenient method for cloning PCR products. The vector is prepared by restriction digest with *Eco* RV followed by the addition of 3´ terminal thymidines to each end of the cut vector. The addition of the 3´ T overhangs ensures that the vector does not re-ligate and allows the insertion of PCR products which have characteristic deoxyadenosine ends formed by some thermostable polymerases during PCR. Table 2.6 lists the components of the pGEM®-T cloning protocol. A diagram of the pGEM®-T vector can be found in the Appendix one.

Component	**Concentration**	**Volume (µL)**
Rapid ligation buffer	2x	5
pGEM®-T vector	50 ng/µL	1
PCR product	2.5 – 250 ng	0.5
T4 DNA ligase	3 U/µL	1
Sterile water	-	Up to 10 µL total volume

Table 2.6 Components of the pGEM®-T cloning protocol

After mixing, the samples were left at room temperature for 1 hour and then used for the transformation of *E. coli* XL-1 Blue cells.

2.2.7.3 Transformation of competent XL-1 Blue strain

Five microlitres of ligation mixture was mixed with 100 µL of competent *E. coli* cells and incubated on ice for 20 minutes. The cells were then heat shocked for one and a half minutes at 42ºC and then incubated on ice for 5 minutes. Nine hundred microlitres of room-temperature LB broth was added to the heat shocked cells and incubated at 37ºC with shaking for one and a half hours. Cells were then collected by centrifugation at 5000 x g for 5

minutes. Eight hundred microlitres of supernatant was removed and the remaining 100 µL of supernatant was used to re-suspend the pellet of cells. The cell suspension was then plated out onto LB plates containing ampicillin (100 mg/mL) with 20 µL of 24 mg/mL isopropyl-beta-D-thiogalactopyranoside (IPTG) and 50 µL of 20 mg/mL 5-Bromo-4-Chloro-3-Indolyl-BD-Galactopyranoside (X-gal) pipetted and spread on the agar surface for blue/white selection. Ampicillin was used for antibiotic selection of positive transformed cells.

2.2.7.4 Cloning PCR products into the pGL3-Basic Vector

The pGL3-Basic vector was used for hADP-GK promoter analysis because its luciferase reporter gene can be used to monitor the activity of gene promoters using transfections of eukaryotic cells followed by luciferase assays. The pGL3-Basic vector and hADP-GK promoter fragments cut from pGEM®-T vector were ligated using a 3:1 insert to vector ratio. Table 2.6 lists the components of the ligation. Appendix one illustrates the pGL3-Basic vector.

Components	**Concentration**	**Volume (µL)**
Promoter fragment (746 bp)	~100 ng/µL	6.6
Vector (4818 bp**)**	50 ng/µL	1.4
Ligase	1 U/µL	1
Ligase buffer (5x)	-	4
Sterile water	-	Up to 20 µL total volume

Table 2.7 Reaction components of the ligation protocol for pGL3-Basic vector

After the addition of all components the reaction mixture was incubated at 4ºC overnight before transformation. Ten microlitres of ligation mixture was mixed with 100 µL of competent *E. coli* XL-1 Blue cells and plated on LB plates containing 100 mg/mL ampicillin and incubated at 37ºC overnight. Ampicillin was used for antibiotic selection of positive transformants. Positive colonies were picked and grown overnight at 37ºC in 5 mL LB broths containing 5 µL of ampicillin (100 mg/mL). The rapid boil and medium-scale plasmid

preparation methods were used to isolate plasmids from overnight cultures; refer to following Sections 2.2.8 and 2.2.9.

2.2.8 Rapid boil plasmid isolation

The rapid boil plasmid preparation is a quick and inexpensive method for isolating plasmid for confirmation of cloning. This technique was used to isolate plasmid so that the hADP-GK promoter insert could be removed by restriction endonuclease digest and then re-cloned into the pGL3-Basic vector for further analysis. Positive transformants (white colonies) were chosen from the LB plates, grown overnight at 37ºC, and placed into 5 mL LB broths containing 100 mg/mL of ampicillin. One point five millilitres of overnight culture was collected by centrifugation at 12,000 x g for 1 minute. The supernatant was removed and the cells were re-suspended in 350 µL of STET (5% triton X-100, 8% sucrose, 50 mM Na_2EDTA pH 8, 50 mM Tris.HCl, pH 8, milli-Q (MQ) water to 100 mL) buffer. Twenty-five microlitres of freshly prepared lysozyme (10 mg/mL) was added to each sample and boiled for exactly 40 seconds. Immediate centrifugation followed for 10 minutes at 12,000 x g. The pellet was then removed using a toothpick and 400 µL of room temperature isopropanol was added and samples were incubated at -20ºC for 20-30 minutes to allow the precipitation of DNA. The samples were then centrifuged at 12,000 x g for 5 minutes. Supernatant was removed and the DNA pellet was re-suspended in ice-cold 95% ethanol. A final centrifuge step at 12,000 x g for 1 minute was carried out followed by the removal of the supernatant. The pellet was then left to air dry at room temperature until all the residual ethanol had been removed by evaporation. The DNA was then dissolved in 50 µL of TE buffer and stored at 4ºC until further use.

2.2.9 Medium-scale plasmid isolation

Medium-scale plasmid DNA preparation was carried out to produce high quality plasmid DNA for the transfection of mammalian cell lines. One hundred millilitres of LB broth containing 1 mL of ampicillin (100 mg/mL) was inoculated with 5 mL of fresh 50 mL overnight culture of transformed *E. coli* XL-1 Blue cells and grown overnight at 37ºC with gentle shaking. The Qiagen Plasmid Midi Kit was used to isolate plasmid DNA according to manufacturers' instructions. The protocol is based on a modified alkaline lysis procedure,

which is followed by the binding of plasmid DNA to a patented Qiagen anion-exchange resin which yields transfection grade DNA.

2.2.10 DNA sequencing

Direct DNA sequencing was carried out in the Allan Wilson Centre genome sequencing service (Massey University) by Ms Lorraine Berry. For DNA sequencing, 3.2 pmol of primer and plasmid DNA (200 ng) were supplied to a total volume of 15 µL in sterile water. The BigDye™ Terminator Version 3.1 Ready Reaction sequencing kit (Applied Biosystems Inc., Foster City, CA, USA) and the ABI3730 Genetic Analyzer were used to carry out the DNA sequencing.

2.2.11 Transfection of mammalian cells for reporter gene assays

Transfections were carried out using HeLa cells which were seeded in 12 well tissue culture plates in 1 mL of Opti-MEM media 24 hours prior to each transfection. An optimal cell density of approximately 70 -80% confluence was required for each transfection. The pGL3-Basic vector containing the hADP-GK promoter insert (pGL3B-hADP-GKprom plasmid) used for transfection was quantified by measuring absorbance at 260 nm using the Nanodrop® ND-100 spectrophotometer (Nanodrop) and subsequently diluted in TE to a concentration of 0.5 µg/µL. pCMV SPORT β-gal (β-Galactosidase vector) was used as a control at a concentration of 0.25 µg/µL. FuGENE®6 was used to transiently transfect, according to manufacturers' instructions, HeLa cells with the pCMV SPORT β-gal and pGL3B-hADP-GKprom plasmid at a total concentration of 0.75 µg/µL with a ratio of 3:1 of FuGENE®6 per µg of total plasmid DNA.

The transfections were carried out in triplicate. Cells were first washed twice with PBS and then harvested using 100 µL of cell lysis buffer (25 mM Tris-HCl, pH 7.8, 2 mM 1,2-disminocyclohexane-N,N,N',N-tetraacetic acid (CDTA), 2 mM dithiothreitol, 10% glycerol and 5% v/v triton X-100) 48 hours after transfection. The cell lysates were then used for β-galactosidase and luciferase assays for analysis of promoter activity.

2.2.12 β-Galactosidase Assay

To correct for variations associated with transfection efficiency, integrity of plasmid and cell density, the plasmid pCMV SPORT-β-gal was used as an internal control. Each transfection was harvested after 48 hours using cell lysis buffer. Five microlitres of the lysate was added to 100 µL of β-galactosidase assay buffer (60 mM NaH_2PO_4, 40 mM Na_2HPO_2, 10 mM KCl, 1 mM $MgCl_2$) and 50 µL of ONPG buffer (o-nitrophenyl 1-β-D- galactopyranoside, 2 mg/mL in 60 mM NaH_2PO_4, 40 mM Na_2PO_2) in a 96 well clear bottomed microtitre plate. The samples were then incubated for 10-30 minutes at 37ºC until a faint yellow colour was observed. Fifty microlitres of 1 M Na_2CO_3 was then added to all samples to stop the reaction. The absorbance of each sample was measured at a wavelength of 405 nm with the 96 well plate reader (anthos reader HT2 type 12 500, anthos labtech instruments, Salzburg, Austria). Five microlitres of cell lysis buffer was used as a blank.

2.2.13 Calculations for luciferase activity

To ensure that variations in plasmid integrity, transfection efficiency and cell density were kept to a minimum, a number of controls were carried out. Every transient transfection was carried out in triplicate, and each experiment was repeated three times on separate occasions. Excel was used to analyse the data produced from both the β-galactosidase and luciferase assays. The standard error was calculated for each triplicate, and was then used to test significance via a paired student *t*-test. The p-value calculated by the paired student *t*-test indicates the similarity between the samples. The data sets are significantly different from each other when the p-value is below 0.05, with a 95% confidence interval. Table 2.8, 2.9 and 2.10 show the processing of the data sets obtained from the β-galactosidase and luciferase assays, as well as the calculated normalised luciferase activities.

	Absorbance 405 nm			
Triplicates	**1**	**2**	**3**	**Average**
β-gal	βa	βb	βc	
Cell lysis blank	Ba	Bb	Bc	AvgB
Corrected β-gal	βa – AvgB = cβa	βb – AvgB = cβb	βc – AvgB = cβc	AvgCβ1

Table 2.8 β-galactosidase assay data

Corrected β-galactosidase activities were calculated by subtracting the average β-gal activity in the blank (cell lysis buffer) read at 405 nm. Each β-galactosidase assay was measured in triplicate.

	Luciferase Maxima			
Triplicates	**1**	**2**	**3**	**Average**
Luciferase	La	Lb	Lc	
Cell lysis blank	LBa	LBb	LBc	AvgLB
Corrected Luciferase	La – AvgLB = cLa	Lb – AvgLB = cLb	Lc – AvgLB = cLc	AvgCL1

Table 2.9 Luciferase assay data

Luciferase activity was corrected by subtracting the average blank luciferase activity (cell lysis buffer). Luciferase activity was measured as actual photons were released during the reaction using the 96 well plate reader FLUOstar galaxy equipped with a chemiluminescence detection system. Each luciferase assay was measured in triplicate.

	Luciferase Maxima			
Triplicates	**1**	**2**	**3**	**Average**
Corrected β gal	AvgCβ1	AvgCβ2	AvgCβ3	
Correct luciferase	AvgCL1	AvgCL2	AvgCL3	
Normalised Luciferase	AvgCL1/AvgCβ1	AvgCL2/AvgCβ2	AvgCL3/AvgCβ3	AvgNL

Table 2.10 Normalised luciferase activities

The normalised luciferase activities for each transient transfection were calculated by dividing the corrected luciferase activity values by the corrected β-galactosidase activity values. Each transient transfection was carried out in triplicate on the same day (a, b and c) and then repeated in triplicate on three separate occasions (1, 2 and 3). Then values were averaged prior to normalisation.

2.2.14 Whole cell extracts for western blot analysis and EMSA

HeLa, HCT116 and SiHa cell lines were cultured to approximately 80% confluence in 145 x 20 mm round tissue culture plates. Prior to harvesting the cells were washed twice with PBS (0.14 M NaCl, 10 mM Na_2HPO_4, 2.7 mM KCl, 1.8 mM KH_2PO_4; pH 7.2-7.4) to remove any excess media retained on the plate. One millilitre of TEN buffer (40 mM Tris-HCl; pH7.4, 0.15 M NaCl, 1 mM EDTA) was added to each plate and then the cells were removed by scraping and collected in a 1.5 mL microcentrifuge tubes. The cells were then pelleted by centrifugation at 4ºC for 5 minutes at 12,000 x g. The supernatant was discarded and the pellet was re-suspended in 100 µL of extraction buffer (40 mM N-[2-hydroxyethyl]piperazine-N'-[2-ethane sulfonic acid] (HEPES); pH 7.9, 1 mM dithiothreitol, 0.4 M KCl, 10% glycerol and protease inhibitor cocktail) and subjected to three cycles of freeze-thawing in liquid nitrogen to disrupt cell membranes. Samples were centrifuged again at 4ºC for 15 minutes at 12,000 x g to remove cell debris. The supernatant was aliquoted into 20 µL volumes, snap frozen with liquid nitrogen and stored at -80ºC.

2.2.15 Protein quantification

Quantification of total protein extracts was carried out using a Bradford assay and/or absorbance at 260 nm using the Nanodrop spectrophotometer (Nanodrop Technologies). The Bio-Rad protein assay was used to determine protein concentrations according to the manufactures' directions. This assay used Coomassie-brilliant blue G-250 dye to carry out the Bradford assay. A range of bovine serum albumin (BSA) from 0.2-5.0 µg was used to construct a protein standard curve. Each standard sample was measured in duplicate. The SiHa, HCT116 and HeLa protein samples were diluted 1:20 in water, and added in triplicate along with each BSA standard to 180 µL of 1:5 diluted Bio-Rad protein reagent in water. A 96 well clear bottom microplate was used with total sample volumes of 200 µL. All samples were left at room temperature for 5 minutes to allow a blue colour to develop before being measured at an absorbance of 595 nm using the 96 well plate reader (anthos reader HT2 type 12 500, anthos labtech instruments, Salzburg, Austria).

2.2.16 SDS-PAGE

The technique of sodium dodecylsulphate polyacrylamide gel electrophoresis (SDS-PAGE) was used to visualise and determine the molecular weight of hADP-GK from whole cell extracts according to the method established by (Laemmli, 1970). A 10% polyacrylamide resolving gel and a 4% polyacrylamide stacking gel were used to prepare protein denaturing gels for SDS-PAGE (Ornstien, 1964). All samples were denatured using 5x treatment buffer (0.06 M Tris-HCl; pH 6.8, 5 % β mercaptoethanol, 5% w/v SDS, 0.001% w/v bromophenol blue, 25% glycerol) by heating in a boiling waterbath for 2-5 minutes. Samples including 10 µL of molecular weight standard (precision plus dual colour standards) for size determination were separated by electrophoresis on the 10% polyacrylamide gel using the mini-protean 3 system (Bio-Rad) for 1 hour at 120 V.

2.2.17 Staining of protein gels

After SDS-PAGE, Coomassie-blue solution (2.5 mM Coomassie-brilliant blue (R-250) 10% acetic acid, 50% methanol) was used to stain protein gels to allow the visualisation of protein bands. Protein gels were incubated at room temperature for 5 minutes in Coomassie-blue solution with gentle shaking and then submerged in destain solution (6% v/v acetic acid, 15% v/v methanol) at room temperature with gentle shaking. Destain solution was changed 3-5 times over a 1-2 hour period and then left overnight to allow the removal of excess Coomassie-blue solution.

2.2.18 Western Blotting

After separation by SDS-PAGE, proteins were transferred to a positively charged nylon membrane using the same mini-protean 3 system (Bio-Rad). The transfer was carried out in cold transfer buffer (25 mM Tris, 192 mM glycine; pH 8.3) at 450 mA for 1-1.5 hours. Upon completion of transfer, the nylon membrane was blocked in 5% skim milk diluted in TBST (50 mM Tris-HCl; pH 7.5, 0.15 M NaCl, 1 mL/L of Tween-20) for two hours at room temperature. Primary and secondary antibodies were diluted in 0.5% v/v blocking solution (2.5% skim milk in TBST) prior to each incubation step. Primary antibody was incubated with the membrane overnight at 4 ºC with gentle shaking. TBST was used to wash the excess antibody off the membrane in four 10 minute wash cycles. The membrane was then

incubated in secondary antibody for 45 minutes at room temperature, and then washed with TBST in three 15 minute wash steps. BM chemiluminescence blotting substrate (POD) was used for chemiluminescence detection following manufactures' instructions. The detection of the protein bands was carried out on X-ray film using a dark room and an X-ray film processor. The molecular weight of the protein was determined using fluorescent paint (Polymark, natural glow fabric paint) to mark the position of each molecular weight standard on the gel.

2.2.19 Immunofluorescence

Immunofluorescence microscopy was used to visualise cellular localisation of proteins within cultured cell lines. Cells were cultured overnight in Lab-Tek II chamber slides (Nalge Nunc International) in 1 mL of media. Medium was then removed and cells were washed twice with 1 mL of PBS (40 mM Tris-HCl; pH 7.4, 0.15 NaCl, 1 mM EDTA) and fixed to the chamber slides using 1 mL of 4% paraformaldehyde incubated at room temperature for 20 minutes. The fixing solution was then washed from the cells by PBS in five 10 minute wash steps. Cells were stored at this point in 0.1% azide at 4 ºC until required or used immediately.

The cells were then permeabilised by treating with 0.1% SDS (10%) in blocking buffer (1% BSA in PBS) at room temperature for 15 minutes with gentle shaking, followed by incubation in blocking buffer for 45 minutes at room temperature. Primary and secondary antibodies were made to the appropriate dilution in blocking buffer prior to incubation. The cells were incubated in primary antibodies overnight at 4ºC, followed by five 10 minute washes with cold PBS. The secondary antibodies were then applied to the cells in each chamber and kept in the dark for an incubation period of 1 hour at room temperature. The slides were kept in the dark from this point as much as possible. The chambers were removed from the slides, and 20 µL of mounting solution containing DAPI was applied to the middle of each chamber well. The slide was covered with a coverslip and sealed with nail polish to prevent dehydration of cells. Detection of protein cellular localisation was carried out using fluorescence microscopy (Olympus fluorescent microscope) at 100x magnification

with oil immersion. The filters used included U-MWU2 Ultraviolet excitation (wideband), U-MWIBA2 Blue excitation (wideband) and U-MWIG2 Green excitation (wideband).

2.2.20 ^{32}P- labelling of oligonucleotides

Oligonucleotides labelled with ^{32}P were used as probes for electrophoretic mobility shift assays (EMSA). The 5´ end of each oligonucleotide was labelled with γ^{32}P [ATP]. A 10% polyacrylamide gel was used to purify the labelled oligonucleotides. The following reaction mixture was used to for labelling: 1.5 µL of optikinase™ (10 U/µL), 1 µL of single stranded (forward) oligonucleotide (100 ng), 2.5 µL of 10x optikinase reaction buffer (500 mM Tris-HCl; pH 7.5, 50 mM dithiothreitol, 100 mM $MgCl_2$), 5 µL of γ^{32}P [ATP] with a total volume of 25 µL. The reaction mixture was incubated at 37ºC for 40 minutes and then placed in a waterbath and incubated at 65ºC for 10 minutes to terminate the reaction. A second oligonucleotide mixture containing 600 ng (6x) of reverse single stranded oligonucleotide, and 50 mM KCl was added to the reaction mixture to a total volume of 50 µL. The samples were then boiled at 95ºC for five minutes and left to cool slowly for an hour to allow the annealing of the two strands to occur.

After annealing, 50 µL of gel shift buffer (GSB) was added to each sample and the entire 100 µL reaction was then loaded onto a 10% polyacrylamide gel (37 cm long; 4 mm spacers) in 1 x TBE (0.89 M boric acid, 0.89 M Tris, 0.02 mM EDTA; pH 8). Electrophoresis was carried out at 30 W (~1500 V) for 1-1.5 hours until the bromophenol blue dye was approximately 20 cm from the bottom of the gel. After electrophoresis, the gel was covered with glad wrap and was exposed using X-ray film administered for approximately one minute. The X-ray film was then used to map the double-stranded oligonucleotides labelled with ^{32}P to the gel and the bands were cut from the gel and eluted in 200-400 µL of 50 mM KCl. The gel slices were incubated at 37 ºC overnight to allow the elution of the labelled oligonucleotides to occur. The supernatant was then removed after the samples were vortexed and centrifuged at 12,000 g for 5 minutes. To ensure that oligonucleotides were correctly labelled with ^{32}P, each oligonucleotide was analysed by scintillation counting.

2.2.21 Electrophoretic mobility shift assay (EMSA)

Each EMSA reaction contained the following components: 50 % v/v of gel shift buffer (GSB), 1 µL of poly dI.dC (1 µg/µL in 50mM $MgCl_2$), 10-20 µg of protein and 0.5 ng of ^{32}P labelled oligonucleotide with a total volume of 20 µL. Double-stranded competitor or antibodies were also added to the reaction mixture if required for the experiment, a list of antibodies can be found in Section 2.1.3. All components except the labelled oligonucleotide were incubated on ice for 10 minutes. Following this, 1 µL of ^{32}P labelled oligonucleotide was added to each sample and incubated at room temperature for 15 minutes. Ten microlitres of the reaction mixture was then loaded onto a 4% non-denaturing polyacrylamide gel (BRL V15.17 apparatus with 0.75 mm spacers) submerged in 0.25 mM TBE buffer. Electrophoresis was carried out at 200 V for approximately 80 minutes. After completion of gel electrophoresis, the gel was spread onto DE-81 paper and dried using a gel drier (model 583, Bio-Rad). The gel was then placed in a radioactive safe cassette and exposed to X-ray film for 5-20 hours at -80°C. The X-ray film was then developed in a dark room using an X-ray film processor.

Chapter 3: The analysis of human ADP-dependent glucokinase expression at the transcriptional level

3.1 Introduction

The exact metabolic role of human ADP-dependent glucokinase (hADP-GK) is not known. An examination of gene regulation at the transcriptional level can provide insights into environmental and cellular factors which may affect gene expression. As ADP-GK is thought to be involved in glycolysis, as an alternative enzyme in the phosphorylation of glucose to glucose-6-phosphate, the response to glucose concentration was evaluated at the transcription level. Changes in glucose concentration have been shown experimentally to regulate the genes of other metabolic enzymes including hexokinase and pyruvate kinase, two of the regulatory enzymes in the pathway of glycolysis (Won *et al*., 2009). The transcriptional activity of hADP-GK was investigated in response to alterations in extracellular glucose concentration to better understand its role in glycolysis and tumour metabolism. This was carried out using mammalian cell lines in tissue-culture and mRNA for hADP-GK was measured using kinetic or quantitative PCR (qPCR) after reverse transcription.

Kinetic PCR is a relatively new method which involves the detection of PCR products during the exponential phase (Figure 3.1) of amplification in each reaction cycle. This means that amplification and detection can occur at the same time, allowing the collection of data for every cycle of the reaction. The PCR product is detected by the instrument through the use of fluorescent dyes that intercalate with the DNA or bind in the major groove. The amount of fluorescence is proportional to the amount of target, and the measurement from each cycle can be used to form a plotted standard curve for analysis. This method is highly specific, sensitive and requires very small amounts of sample for successful amplification. Relative quantification using kinetic or qPCR is an analysis method that measures the change in expression levels of a target mRNA to that of a reference. Changes in mRNA levels are determined by comparing the steady-state mRNA over a number of samples, and by expressing the amounts of mRNA in relation to the reference RNA. The reference RNA is termed an “endogenous control”, which is a house-keeping gene that normally remains consistently expressed. The mRNA is converted to cDNA by reverse transcription (RT) for

quantification by qPCR. Collectively this method is known as RT-qPCR. To obtain optimal results, normalisation is carried out to reduce intra- and inter-assay variations, thus controlling experimental error.

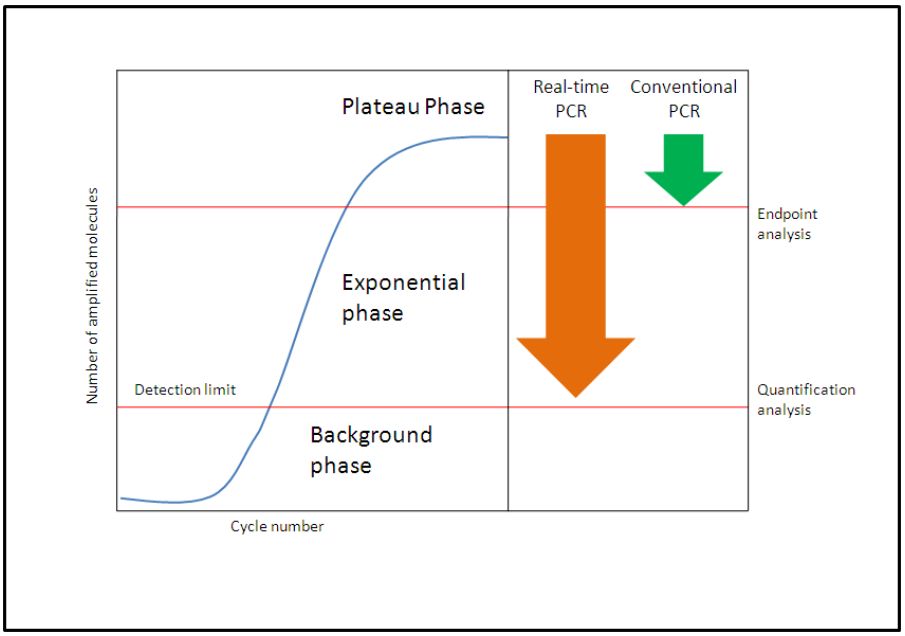

Figure 3.1 Differences between Real-time PCR and conventional PCR methods, adapted from (Lightcycler® 480 Real-time PCR Application Manual, 2009).

Real-time PCR incorporates both the exponential phase and plateau phase in its analysis via melting curves and quantification, while conventional PCR methods can only be used for endpoint analysis.

This chapter describes how an RT-qPCR assay was designed for real-time PCR using the Roche Lighcycler® 480 which enabled the detection of ADP-dependent glucokinase gene expression using relative quantification. This method was then used to analyse changes in gene expression in response to changes in glucose concentration in the medium during cell culture.

3.2 Assay design

3.2.1 Primer design and amplification of ADP-GK coding region using conventional PCR

Forward and reverse primer pairs (644, 202) were designed to flank intron/exon boundaries of the ADP-GK (Figure 3.2) and β-actin coding regions, respectively. This strategy was chosen to eliminate the possibility of genomic DNA (gDNA) contamination. The ADP-GK (644) primer pair was expected to produce a 181 base pair (bp) product upon amplification, in comparison to 102,531,392 bp of gDNA. β-actin was used as a reference gene (internal control) for real-time PCR since it is constitutively expressed in all cell lines. The forward and reverse primer pair for β-actin (202) was expected to produce a 202 bp product. The sequences for both pairs of primers are listed in Table 3.1.

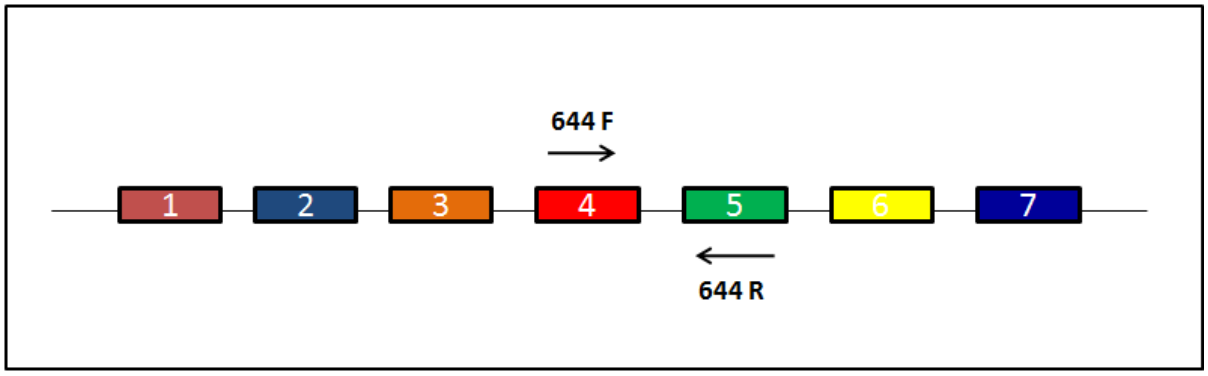

Figure 3.2 Intron and exon regions of hADP-GK coding region with 644 primer binding sites

Forward and reverse 644 primer pair bind across exons 4 and 5 to produce amplicons spanning an intron/exon boundary to eliminate genomic contamination during PCR. hADP-GK coding region includes 7 exons with a total length of 2539 bp.

cDNA Target	Accession #	Primer Pair	Sequence (5´→3´)
ADP-GK	NM 031284.4	Forward 644 Reverse 644	GTTCCACCAGAGTCATTGC GCTGAAACTCCTCCAGGCTA
β-actin	NM 001101	Forward 202 Reverse 202	CCTTCTACAATGAGCTGCG CCGGAGTCCATCACGA

Table 3.1 Primer sequences

Forward and reverse primer sequences (644, 202) were designed across an intron/exon boundary of the coding region of the human ADP-dependent glucokinase gene and β-actin respectively using the Lightcycler® 480 primer design software.

95ºC for 5 min		
95ºC for 30 sec	45x cycles	Denaturing
58ºC for 30 sec		Annealing
72ºC for 30 sec		Extension
72ºC for 7 min		Final Extension

Two microlitres of first strand cDNA template at various dilutions was added to the PCR master mix containing 2.5 µL (100 ng/µL) of forward and reverse primer 644 or 2.5 µL (50 ng/µL) of forward and reverse primer 202, 5.0 µL of 10x PCR reaction buffer (500 mM Tris-HCl, pH 8.3, 100 mM KCl, 50 mM $(NH_4)_2SO_4$), 2.5 µL of 25 mM Mg^{2+}, 5.0 µL of 3 mM dNTPs, 0.5 µL of Faststart *Taq* polymerase (5U/µL) (Roche), and 48.0 µL of sterile water for a total volume of 50.0 µL.

Table 3.2 PCR protocol for hADP-GK coding region amplification

PCR reaction protocol and master mix used for the amplification of the human ADP-GK coding region.

PCR optimisation was carried out using a range of annealing temperatures from 56-60ºC to optimise the amplification of the coding regions of the human ADP-GK and β-actin genes. The annealing temperature of 58ºC with a Mg^{2+} concentration of 25 mM was the most successful (Figure 3.3) when applied to the reaction described in Table 3.2, giving a discrete product for both ADP-GK and β-actin with no formation of primer dimers.

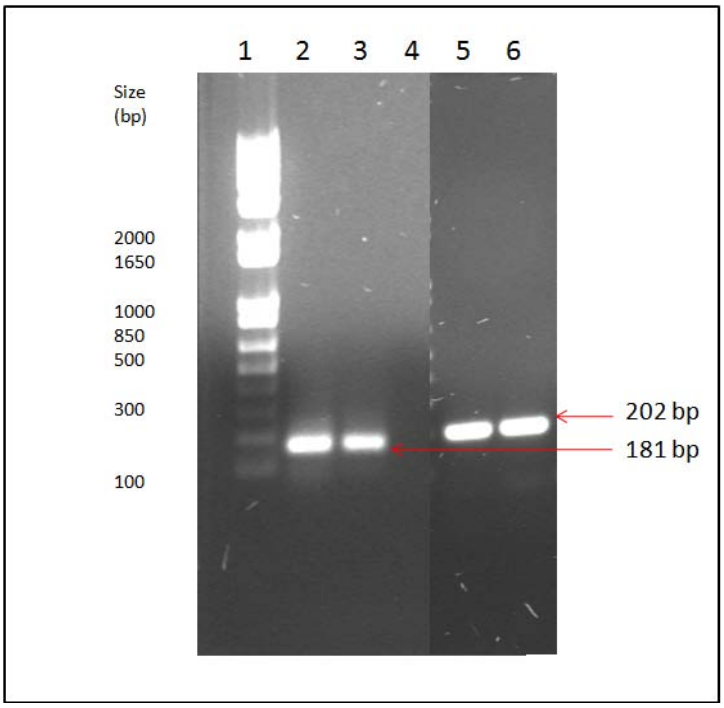

Figure 3.3 Visualisation of primer specificity and product amplification

A 1% agarose gel in 1x TAE buffer was used to separate 15 µL samples of PCR reaction by electrophoresis for approximately an hour at 100 volts. One µL of ethidium bromide (0.5 µg/mL) was added to the agarose gel to allow the visualisation of DNA under UV light. Lane one contains 10 µL of a 1 kb ladder used to estimate the molecular size of the DNA bands. The molecular sizes are indicated on the left hand side of the figure in base pairs (bp).

Lane one: Ten microlitres of 1 kb plus ladder (1.0 µg/µL); **Lane two:** Fifteen microlitres of undiluted cDNA PCR product (ADP-GK, 644); **Lane three:** Fifteen microlitres 1:10 diluted cDNA PCR product (ADP-GK, 644); **Lane four:** NTC; **Lane five:** Fifteen microlitres 1:10 diluted cDNA PCR product (β-actin, 202); **Lane six:** Fifteen microlitres undiluted cDNA PCR product (β-actin, 202).

3.2.2 Restriction endonuclease digest

To confirm that the designed primers had amplified specific sequences of the human ADP-GK coding region, restriction endonuclease digests were performed. Five microlitres (10%) of PCR sample was digested with 1.0 µL of restriction endonuclease *Fok* I (8-10 U/µL), as outlined in Section 2.2.8. *Fok* I was expected to produce two bands of approximately 40 bp and 141 bp (Figure 3.4). A 1 kb plus ladder was used to estimate the size of the bands. Figure 3.5 shows the result of the restriction endonuclease digest by gel electrophoresis. The digest successfully produced the 141 bp band, while the 40 bp band was too small to be visualised, indicating that the primer pair was amplifying a specific sequence of the human ADP-GK gene.

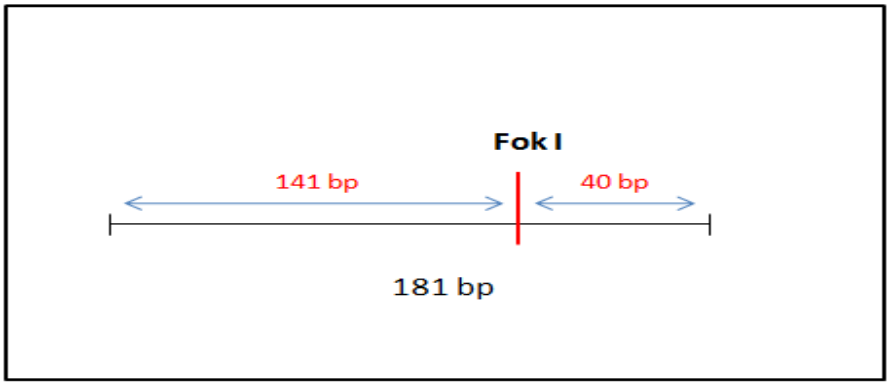

Figure 3.4 Schematic representation of the restriction digest carried out on the hADP-GK coding region sequence

Fok I restriction enzyme site when cut produces a 141 bp product and a 40 bp product from the 181 bp amplicons. These products can be visualised on an agarose gel by the process of gel electrophoresis.

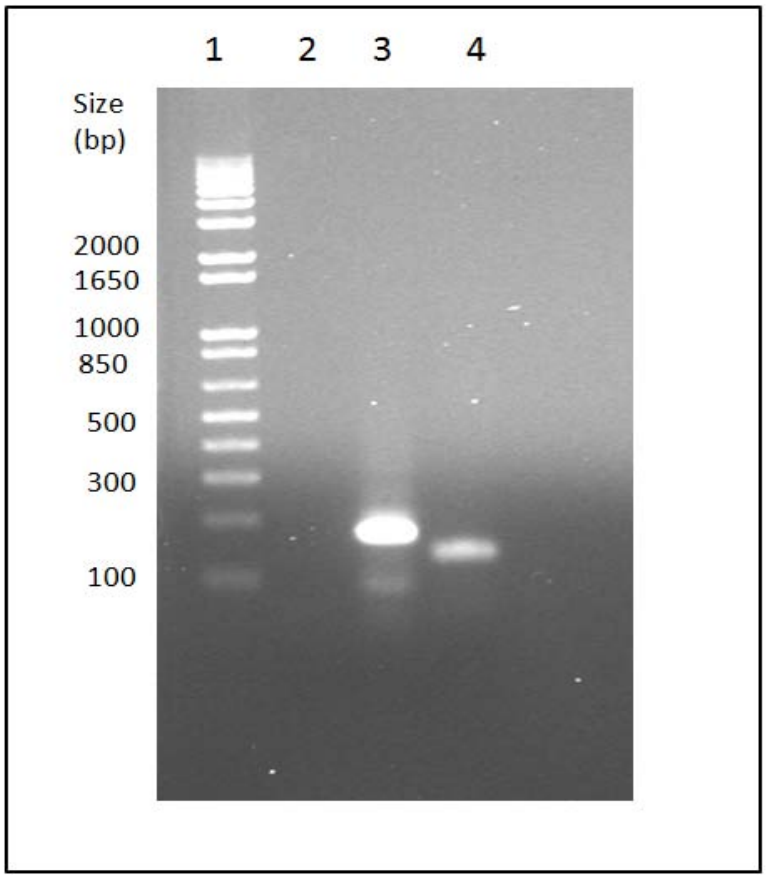

Figure 3.5 Digestion of hADP-GK coding sequence products generated by 644 primer pair.

Digested and undigested samples were separated on a 1% agarose gel in 1x TAE buffer for approximately an hour at 100 volts. One microlitre (0.5 µg/mL) of ethidium bromide was added to the agarose gel allow the visualisation of the bands. Molecular size markers were used to determine the size of the band and these are labelled on the 1 kb plus ladder in base pairs (bp).

Lane one: Ten microlitres of 1 kb plus ladder (1.0 µg/µL); **Lane two:** NTC; **Lane three:** Fifteen microlitres of uncut PCR product; **Lane four:** Fifteen microlitres of PCR product cut with *Fok* I.

3.2.3 DNA sequencing

To further confirm the specificity of the primers designed to amplify sequences of the human ADP-GK coding region, direct DNA sequencing was carried out. The sequencing reaction used the forward and reverse primer pair (644) for the 181 bp product. Sequencing was carried out by Lorraine Berry (Allan Wilson Centre Genome Sequencing Service). The sequencing chromatogram for the forward primer showed that the primer pair (644) was specifically amplifying the coding region of hADP-GK during PCR; however the reverse primer did not sufficiently sequence the coding region. The chromatograph for the forward primer can be found in Appendix 2. Direct DNA sequencing was not carried out for the β-actin coding region as primers had been used previously and verified.

3.2.4 Real-time PCR optimisation and amplification efficiency

Real-time PCR experiments were carried out on the LightCycler® 480 System (Roche). Amplification of cDNA prepared from RNA isolated from SiHa cells was carried out using the conditions presented in Section 2.2.2. cDNA concentrations were determined by absorbance at 260 nm using the Nanodrop spectrophotometer (Nanodrop Technologies), and serial dilutions were carried out for standard curve preparation. Triplicate samples resulted in identical sigmoid curves for amplification, with the reactions reaching a plateau stage as saturation was approached. Single peak melting curves (Tm ~87 for ADP-GK, Tm ~90 for β-actin) were obtained indicating that no primer-dimers or non-specific amplicons were produced from the template samples (Figure 3.6). Non-template controls (NTC) containing water blanks were analysed alongside the ADP-GK and β-actin samples for each experiment. Ten microlitre samples of PCR products were analysed by gel electrophoresis after real-time PCR to check for single product amplification. Bands with a size of 181 bp were expected and can be visualised on the agarose gel (Figure 3.7). All NTC samples were product free indicating that amplification seen from target and reference samples were not due to contamination.

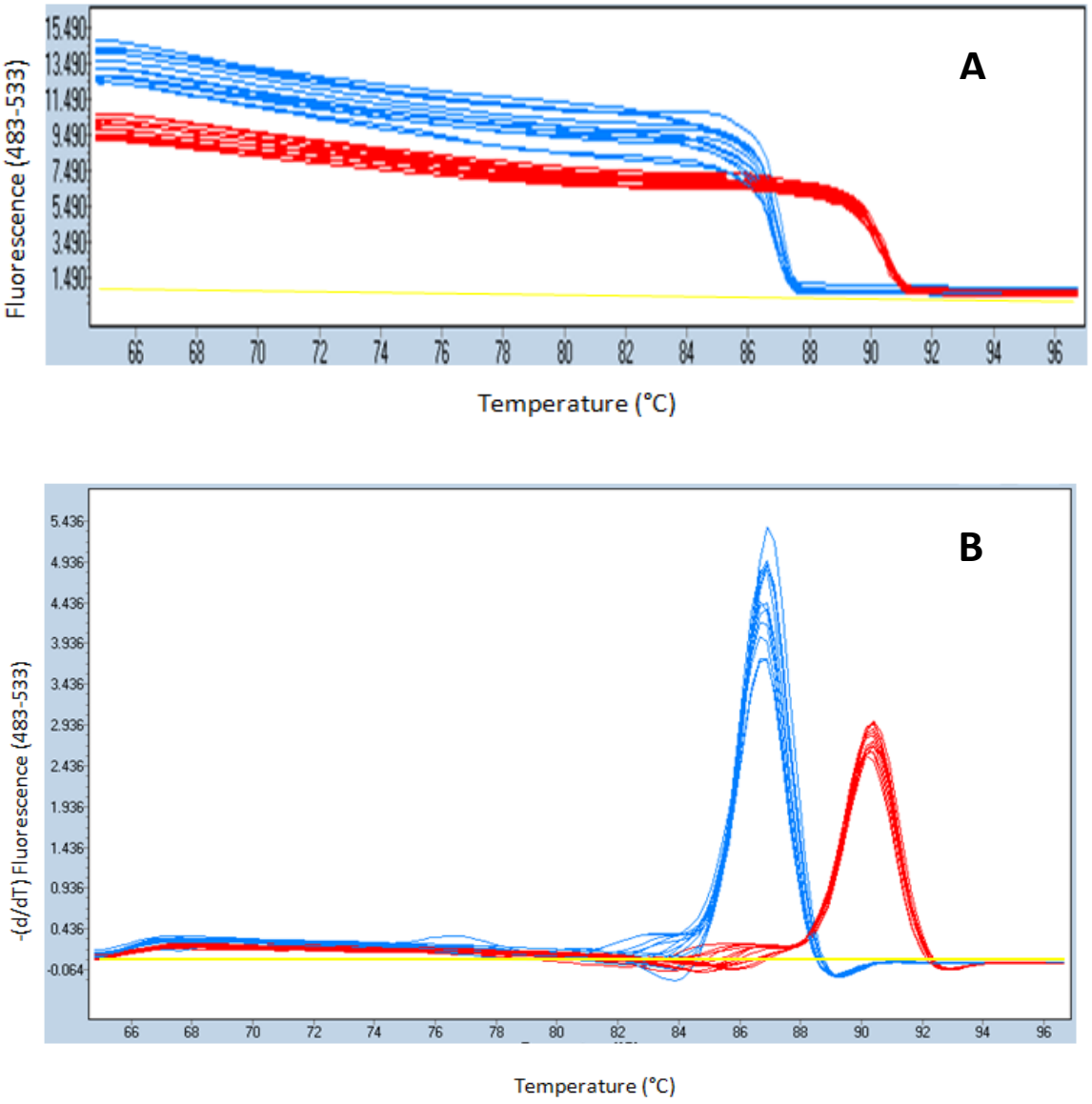

Figure 3.6 Melting peaks and curves showing primer specificity for hADP-GK and β-actin targets

Amplification melting curves generated by the Lightcycler® 480 analysis software are presented in graph A. Amplification melting peaks are presented in graph B. ADP-GK 644 PCR products are shown in blue (Tm~87), and β-actin 202 reference PCR products are shown in red (Tm~90), while the NTC is shown in yellow.

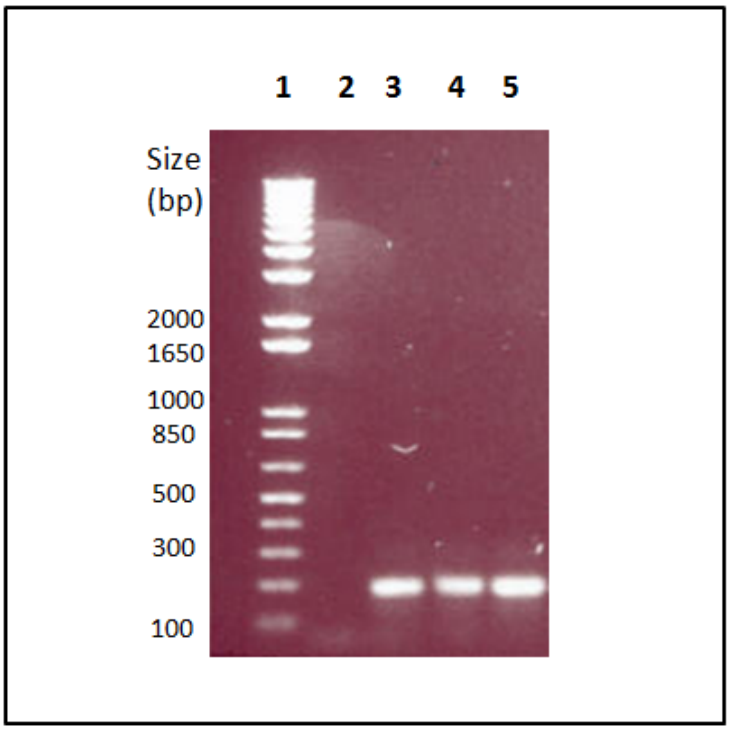

Figure 3.7 Visualisation of hADP-GK PCR products after real-time PCR

Ten microliter samples of PCR products were separated on a 1% agarose gel in 1x TAE buffer at 100 volts for approximately 1 hour. The agarose gel contained 1 µL (0.5 µg/mL) of ethidium bromide for the visualisation of bands under UV light. A 1 kb plus ladder was used to determine the size of the amplicons, with molecular sizes indicated on the left hand side of the gel in base pairs (bp).

Lane one: Ten microlitres of 1 kb plus ladder (1.0 µg/µL); **Lane two:** NTC; **Lane Three, Four and Five:** Ten microlitres of 1:10 diluted ADP-GK PCR product in triplicate.

Before relative quantification was used to analyse the expression of hADP-GK, amplification efficiencies were determined for both ADP-GK and β-actin primer pairs. A series of dilutions called relative standards were prepared by making serial dilutions of the cDNA template (1:10), and amplification curves were constructed using the Lightcycler® 480 analysis software. By using the cDNA template to construct the amplification curves, the PCR efficiencies were more likely to be the same as the test samples during experiments representing different glucose concentrations. Each relative standard was determined in

triplicate and each standard curve contained at least three or four different concentrations to ensure that results were statistically valid.

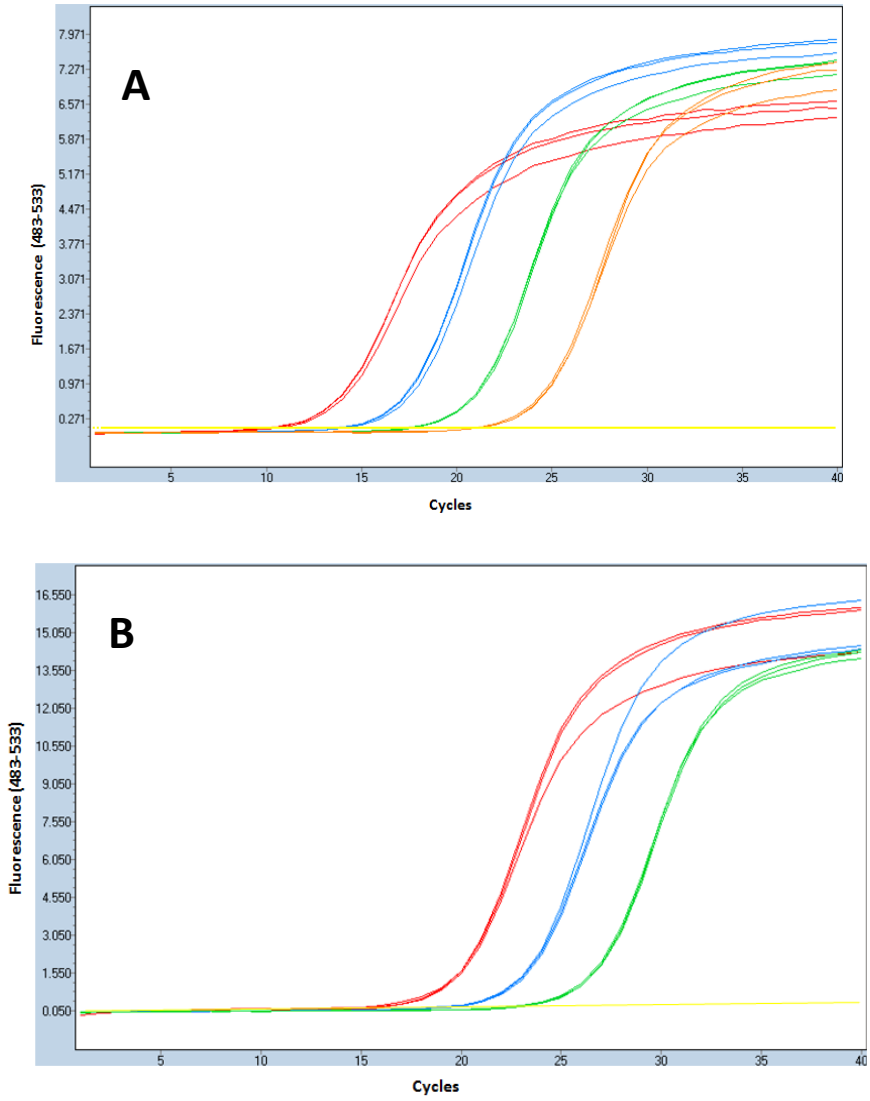

Figure 3.8 PCR amplification efficiency determination of β-actin and hADP-GK cDNA

Amplification curves for β-actin are shown in graph A and ADP-GK in graph B. The serial 1:10 dilutions are shown by the colours red, blue, green and orange which depict the decreasing cDNA concentration respectively. The NTC is shown in yellow for both amplicons.

The hADP-GK standard curve had only three points when compared to the four points obtained for β-actin. This was due to the difficulty of amplifying cDNA at very dilute concentrations (1:10,000, orange amplification curve Figure 3.8 A), indicating lower levels of hADP-GK transcripts. Both target and reference samples were used to prepare standard curves for subsequent relative quantification analysis. All relative standard samples were amplified as described in Section 2.2.5. Figure 3.8 illustrates the amplification curves for the reference 202 β-actin and target 644 hADP-GK transcripts respectively. Melting curves and peaks showed single peak amplification with the expected Tm (Figure 3.6).

3.3 Results

3.3.1 Standard curve analysis of amplification efficiencies

Amplification efficiencies (E) for the analysis of gene expression using relative quantification should have a value of approximately 2. This number is considered the "perfect" amplification efficiency and ensures that the cDNA produced from cellular RNA is representative of the mRNA population in each sample (Bustin *et al.*, 2009). To construct the standard curves, the log concentration was plotted against the average of the quantification points (Cq) for each of the triplicate samples. The slope of the standard curve should have an approximate value of -3.32 when the amplification efficiency is 2, which indicates that the amount of template is doubling with each cycle of PCR (Hoffmann, 2009). The value of the slope was used in Equation 1.1 to calculate the amplification efficiency for each sample. Figure 3.9 and 3.10 illustrate the standard curves constructed for both β-actin and ADP-GK targets, respectively. PCR amplification efficiencies are summarised in Table 3.3.

Equation 1.1

$$E = 10^{-1/slope}$$

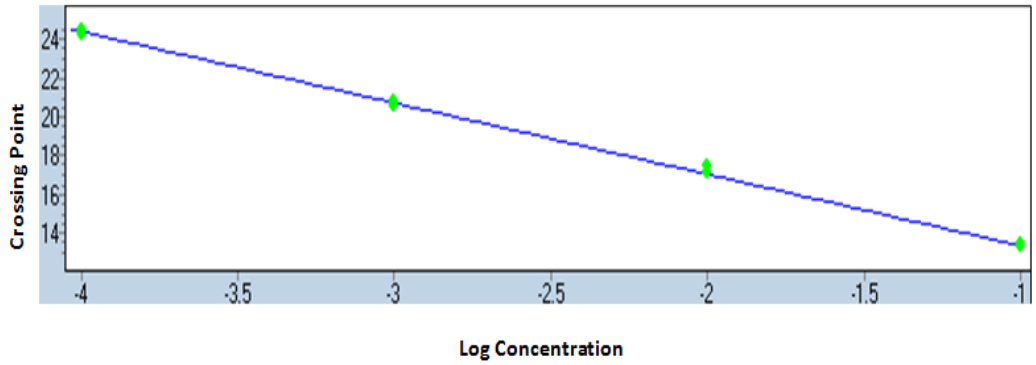

Figure 3.9 β-actin standard curve for the analysis of amplification efficiency

One to ten serially diluted cDNA prepared from RNA isolated from SiHa cultured cells. The standard curve was constructed with triplicate samples amplified using the 202 β-actin primer pair. The standard error had a value of 0.0203 with a slope of -3.66 and regression coefficient of 0.9971.

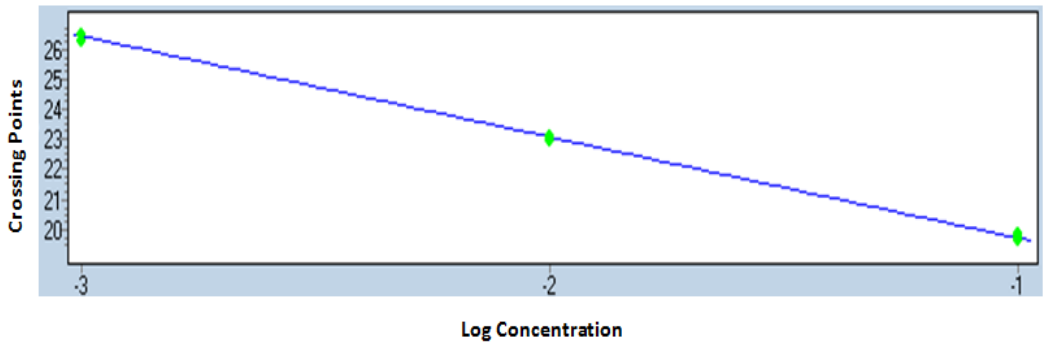

Figure 3.10 hADP-GK standard curve for the analysis of amplification efficiency

One to ten serially diluted cDNA prepared from RNA extracted from SiHa cultured cells. The standard curve was constructed using triplicate samples amplified using the 644 ADP-GK primer pair. The standard error has a value of 0.0179 with a slope of -3.36 and regression coefficient of 0.9796.

cDNA target	Standard curve parameters			
	Efficiency	**Error**	**Slope**	**R^2**
ADP-GK	1.988	0.0179	-3.36	0.9796
β-actin	1.877	0.0203	-3.66	0.9971

Table 3.3 Standard curve parameters

Each standard curve was chosen based on an efficiency value of 2 ±10%, and a slope value between -3.1 and -3.6. These parameters ensure that the PCR assay is precise, reproducible and that PCR products are doubling upon each cycle, indicating amplification efficiency. The linear range of each standard curve should span at least three orders of magnitude, and the range of values should span the interval of each sample being quantified. The range of ADP-GK standard curve includes three point values instead of four, due to the inconsistency of triplicate amplification at more diluted concentrations (Bustin *et al*., 2009).

3.3.2 Gene expression analysis using relative quantification

After determining PCR amplification efficiencies by analysis of standard curves, cDNA samples were measured using the Lightcycler® 480 for both 644 ADP-GK and 202 β-actin targets to assess the variability of intra- and inter-assay measurements. SiHa cells grown in normal tissue culture glucose concentrations of 4.6 mM were screened for differences over a 24 hour time period. cDNA samples were diluted 1:100 to ensure that Cq values fell within the range of the standard curves, and to eliminate high Cq values over 35, which are an indication of potential contamination often resulting in larger intra- and inter-assay differences. Table 3.4 and 3.5 display the intra- and inter-assay variability's, respectively.

Run #	644 ADP-GK			202 β-actin		
	Mean Cq	**Stdev.**	**CV%**	**Mean Cq**	**Stdev.**	**CV%**
1	30.79	0.10	0.03	24.63	0.28	0.32
2	31.05	0.55	0.98	24.25	0.21	0.17
3	30.29	0.18	0.10	24.66	0.08	0.02

Table 3.4 Intra-assay differences for real-time PCR

Stdev. = Standard deviation, CV% = coefficient of variance, n=3

cDNA target	Mean Cq	Stdev.	CV%
644 ADP-GK	30.71	0.39	0.49
202 β-actin	24.51	0.23	0.21

Table 3.5 Inter-assay differences for real-time PCR

Stdev. = Standard deviation, CV% = coefficient of variance, n=3

Relative quantification analysis uses the efficiencies determined from each standard curve with a mathematically calibrated method which is outlined in Equation 1.2. This method assumes that each sample containing the same target cDNA will have the same template concentration at identical crossing points. The model uses a calibrator sample to compare with unknown samples using the crossing points (Cq values) and the amplification efficiencies (E). The calibrator is a sample that is typically an untreated control and should represent even ratios of target versus reference. The target sample is the gene of interest, while the reference is the internally controlled gene which remains the same throughout treatment. The calibrator is used to normalise the target and reference samples within each assay while providing consistency between several triplicate assays, thereby minimising intra- and inter-assay variation (Bustin *et al*., 2009, Ovstebo *et al*., 2003).

Equation 1.2

$$\text{Normalized ratio} = \frac{(E_{ref})^{Cq\ sample}}{(E_{target})^{Cq\ sample}} \div \frac{(E_{ref})^{Cq\ calibrator}}{(E_{target})^{Cq\ calibrator}}$$

3.3.2.1 The regulation of ADP-GK transcription by glucose concentration

Relative quantification analysis was used to investigate the effect of glucose concentration on the expression of hADP-GK at the transcriptional level. Cultured SiHa cell lines were incubated for 6, 24 and 48 hours, whilst treated with various glucose concentrations (0, 0.25, 0.50, 0.75, 1.0, 5.0 & 10.0 mM). RNA was extracted from each cell sample and used to produce cDNA via first-strand cDNA synthesis (Section 2.2.2). The cDNA obtained from each treated sample was measured for the target ADP-GK and house-keeping gene β-actin with the Lightcycler® 480 using the designed real-time PCR assay (Section 2.2.5). To ensure that the PCR assay was reproducible and accurate each sample was measured in triplicate to account for intra-assay differences. Inter-assay differences were addressed by conducting triplicate experiments for each of the three time points and including a calibrator sample in each assay. SiHa cultured cells grown in a glucose concentration of 4.6 mM (normal tissue culture concentration) was used as the calibrator sample in every experiment.

Normalised target to reference ratios were determined using Equation 1.2 and are displayed in Table 3.6. The "coefficient of variance" (CV) for the normalised ratios should be between 0.12% and 3% which shows minimal variation between samples, higher CV values are expected for samples that are more diluted. CV values for 6, 24 and 48 hour ratios still show low variation in inter-assay experiments. Normalised ratios were used to construct the column graph depicted in Figure 3.11. For all three time periods the 5 mM samples have similar ratios to the 4.6 mM control, all other concentrations deviating from the normal tissue culture glucose concentration show slightly reduced quantities of transcript determined by a ratio value below 1.

Nomalised Ratios	**Glucose concentration (mM)**							
	4.6 Control	**10.0**	**5 .0**	**1.0**	**0.75**	**0.50**	**0.25**	**0.00**
48 hours (CV %)	1.00	0.82±0.21 (8.04%)	0.98±0.11 (2.02%)	0.64±0.20 (7.91%)	0.72±0.11 (2.47%)	0.51±0.14 (5.46%)	0.62±0.09 (1.64%)	0.58±0.20 (14.62%)
24 hours (CV %)	1.00	0.45±0.17 (11.10%)	0.93±0.16 (3.43%)	0.73±0.11 (2.98%)	0.57±0.22 (11.78%)	0.35±0.22 (6.32%)	0.45±0.11 (4.90%)	0.74±0.21 (7.52%)
6 hours (CV %)	1.00	0.76±0.09 (2.41%)	0.92±0.14 (2.92%)	0.71±0.21 (6.09%)	0.50±0.09 (3.14%)	0.61±0.11 (3.43%)	0.57±0.13 (5.21%)	0.56±0.06 (1.16%)

Table 3.6 Relative transcript ratios after 48, 24 and 6 hour time periods

Stdev. = Standard deviation, CV% = coefficient of variance

Statistical analysis using Minitab® statistical software package was carried out to determine if any normalised target to reference ratios were significantly different. ANOVA analysis compared each of the time periods and glucose concentration. A significant difference with a P value of 0.006 was observed for the 5 mM glucose concentrations for each time period compared to the other glucose concentrations. Comparisons within each glucose concentration revealed the ratio for 24 hour 10 mM glucose concentration was significantly different with a P value of 0.003 when compared to the 48 and 6 hour ratios for the same concentration of glucose. However there was no significant difference across the rest of the glucose concentrations within in each time period. The significant difference observed for the 5 mM ratios compared with other glucose concentrations suggests that when glucose concentration is altered from the normal glucose level used in tissue culture medium, the

expression of hADP-GK gene is decreased. The differences observed however were very small and some of the values obtained had CV values higher than would normally be expected. Therefore, no definite conclusion can be made about the effect of glucose concentration on expression of hADP-GK.

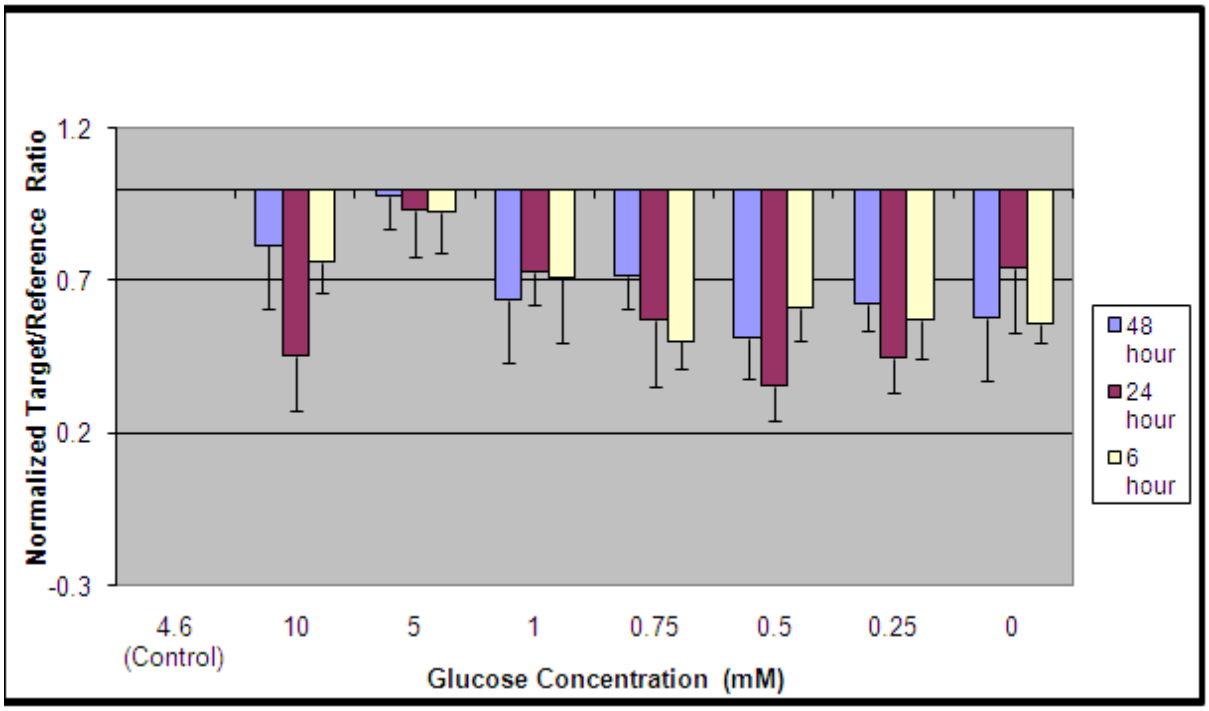

Figure 3.11 Column graph showing the relationship between glucose concentration and hADP-GK gene expression

mRNA pooled from SiHa cultured cells treated with a range of glucose concentrations for various time periods were measured by RT-qPCR. Each bar is representative of 3 individually pooled experiments that included triplicate samples. Forty-eight hours is depicted in blue, 24 hours is depicted in purple, and 6 hours is depicted in yellow. The 4.6 mM control sample was set at a ratio of 1. Normalised ratios were determined by the Cq values of the reference and target, which were then normalised to the calibrator (control). Errors bars show the standard deviation.

3.4 Discussion

3.4.1 Chapter Summary

The aim of this study was to investigate the effect of glucose concentration on the expression of human ADP-GK at the transcriptional level using RT-qPCR. Understanding the regulation of hADP-GK at the transcriptional level may provide insights into the metabolic role of the enzyme, and the advantages of utilising an ADP-dependent enzyme rather than an ATP-dependent enzyme, such as hexokinase. An RT-qPCR assay was designed for the Roche Lightcycler® 480 to allow the relative quantification of ADP-GK coding region transcripts, which were compared to a house keeping gene (β-actin) that was constitutively expressed across all cell lines. The expression of the ADP-GK coding region during treatment could be visualised using the Lightcycler® 480 software by mathematically constructing a ratio of target to reference crossing points (Cq), and normalising to a calibrator (control) sample which had a set ratio of 1.

Primers were designed flanking intron/exon boundaries of the hADP-GK and β-actin coding regions, which ensured the absence of genomic DNA contamination during PCR. RNA was extracted from cultured SiHa cells, and then used to synthesise first strand cDNA. Conventional PCR was carried out to ensure that amplification of products occurred using the designed primers and first strand cDNA. Primer specificity was confirmed by restriction endonuclease digests and DNA sequencing. The primers were then used to develop an RT-qPCR assay that could be used to monitor transcripts of the hADP-GK and β-actin coding regions. Standard curves were constructed to test amplification efficiencies of both the target ADP-GK and reference β-actin cDNA which lay within 90% of the "perfect amplification efficiency" of 2 and had slopes between -3.1 and -3.6. The standard curves were then used for relative quantification to assess the effects of glucose concentration on the expression of the ADP-GK coding region.

SiHa cultured cells were treated with a range of glucose concentrations spanning the normal blood glucose concentration, as well as high and low glucose concentrations which were hypothesised to have the most effect on hADP-GK gene expression. Three time periods of 6, 24 and 48 hours were chosen to represent short-term and long-term exposure to changes in glucose concentration within the environment. Twelve hour experiments were omitted from the range of time points due to the difficulty of carrying out the experiments within that time period. Each experiment was carried out in triplicate on separate occasions, with every sample measured in triplicate to minimise intra- and inter-assay differences. Most of the Cq value variations were low with CV values between 0 and 3%; however some CV values were greater than 3 % but less than 15 %.

Relative quantification was used for the analysis of gene expression by comparing the relative amounts of reference transcripts to ADP-GK transcripts for each glucose concentration. A ratio of 1 was set for the normalisation control which represented normal tissue-culture media glucose concentration at 4.6 mM. The concentration of glucose in tissue-culture media closely resembles the concentration of glucose in the blood. If a ratio above 1 was obtained then the number of target transcripts is greater than the number of reference transcripts, indicating an increase in expression of the target gene compared to the reference gene. If a ratio below 1 was obtained during analysis, then the number of target transcripts is smaller than the number of reference transcripts, indicating that the expression of the target gene is lower than that of the reference gene.

3.4.2 Effect of glucose concentration on ADP-GK transcription

For the RT-qPCR experiments conducted, the results showed that the expression of hADP-GK gene was lower than the expression of the β-actin reference gene. This is represented by the ADP-GK: β-actin ratios below the normalised ratio of 1. The samples from cells grown in 5 mM glucose concentrations for each time point have ratios that are close to the normalised ratio of 1, which is to be expected because the concentration of glucose is relatively similar at 4.6 mM and 5.0 mM. Any glucose concentration below 5 mM resulted in a decreased target to reference ratio representing a decrease in hADP-GK gene expression. Many factors during cell culture can affect the proliferation and metabolism of the cell lines

being investigated. It is important to monitor the temperature, pH and pO_2, as well as measuring the carbon sources available and by-products produced (Genzel *et al*., 2004). To further verify the results of this experiment, the concentration of glucose should be measured before and after each time period to determine the relative utilisation of glucose and to determine the actual initial glucose concentration. This is important as FCS which is supplemented to all cells for adequate growth contains a small amount of glucose and all media contains glutamine which can also be used by cells for energy requirements. These factors may contribute to the differences seen with in triplicate experiments and across time periods.

Glucose concentrations above 5.0 mM also show a decrease in the number of transcripts for hADP-GK compared to β-actin, indicating that high glucose concentrations may inhibit hADP-GK gene expression. Glucose concentrations above 10 mM are defined as diabetic conditions, and it has been shown that high concentrations of glucose in cell culture have pathogenic effects on cell proliferation through inhibition of signal transduction pathways, e.g. protein kinase C (PKC) (Cosio and Wilmer, 1995). At glucose concentrations of 0.25 mM and 0 mM no further decreases in ADP-GK gene expression were observed, suggesting that once the glucose concentration deviates from 4.6 mM the expression of hADP-GK gene is reduced. This could be due to impaired cellular function when glucose availability is reduced, however changes in the expression of the reference gene would also be observed and this was not the case. It is therefore possible that the changes in hADP-GK gene expression are caused by alterations in transcription factors responsible for the activation of the hADP-GK promoter that rely on the presence of glucose to be functional. Carbohydrate response element-binding protein (ChREBP) is a transcription factor that is glucose responsive. Changes in glucose concentration result in the activation of ChREBP and its translocation from the cytosol to the nucleus to allow the activation of glycolytic enzymes (Herman and Kahn, 2006). It is therefore possible that the transcription factors that are responsible for the activation of hADP-GK may be glucose-responsive or require normal physiological glucose concentrations for optimal activity.

The results showed very little difference between the three time periods of 6, 24 and 48 hours in terms of target to reference ratios for each glucose concentration and no consistent trends were observed as indicated by the ANOVA statistical analysis. The only difference between the three time periods was the ratio for the samples prepared from cells grown in 10 mM glucose concentrations for the 24 hour time period, which was significantly larger than that of the 48 and 6 hour ratios. It is possible that 10 mM concentrations of glucose have a more pronounced effect on ADP-GK gene expression at 24 hours, but inhibition of ADP-GK gene expression by high glucose concentrations would most likely be seen during early hours of exposure rather than after 24 hours when the glucose concentration is likely to become reduced as it is utilised by the cells. It is likely that the result was not indicative of a true trend and most likely due to variations in inter-assay experiments, which is clearly represented by the CV value of 11.10%. However, all ratios had CV values <15% which are in agreement with CVs measured in other experimental studies (Ovstebo *et al.*, 2003) indicating that intra- and inter-assay variation was controlled and kept to a minimum. Higher CV values can be associated with more dilute cDNA samples as a result of reduced transcript levels and the limit of sensitivity of the assay.

The data presented in this chapter showed that hADP-GK gene expression was not up-regulated by low glucose concentrations as hypothesised, and that the deviation in glucose concentration from the normal tissue culture glucose concentration of 4.6 mM resulted in a small two fold decrease in the expression of hADP-GK gene at the transcriptional level. There were no significant differences between the three different treatment exposure times of 6, 24 and 48 hours as indicated by the statistical ANOVA tests. High glucose concentrations also resulted in inhibition of ADP-GK gene expression. To verify the results shown in this experiment a second reference gene such as Glyceraldehyde 3-phosphate dehydrogenase (GAPDH) would be required. It is also possible that different splice variants may change with alterations in glucose concentration and exhibit tissue specific expression with multiple protein species (Lu *et al*., 2001). It is possible that hADP-GK does not respond to glucose concentration and that ADP-GK is regulated differently to the hexokinase type II enzyme which is up-regulated during low glucose conditions (Marin-Hernandez *et al.*, 2006, Rempel *et al*., 1996).

Chapter 4: Cloning of the putative promoter of ADP-dependent glucokinase

4.1 Introduction

The expression of a gene within a eukaryotic cell is highly dependent on its promoter's activity, which is in turn dependent on the transcription factors that bind to and induce activation. Each promoter has a number of binding elements which allow interactions to occur between the promoter and specific transcription factors, and depending on the environmental status of the cell, transcription factor binding may be altered in relation to the needs of the cell. Previous to this experiment, no research on the hADP-GK promoter or cognate transcription factors had been carried out and it is still unclear where the promoter for the hADP-GK is located. The RT-qPCR experiments showed only minor changes in hADP-GK gene expression at the transcriptional level when glucose concentrations were altered from the normal tissue culture glucose concentration. Previous work (Hole, 2009) suggested major changes in tissue-specific regulation of hADP-GK at the protein level. An understanding of the transcriptional regulation of hADP-GK may provide insights into its biological function and its tissue-specific expression pattern. As a first step towards characterising the hADP-GK promoter, sequence comparisons and transcription factor binding sites were investigated *in silico* prior to the cloning of the putative promoter into a reporter-gene vector for analysis of promoter activity.

4.2 Promoter homology

The hADP-GK promoter sequence was analysed using the GCG version 11.1 (Accelrys Inc., San Diego, CA) software package which is able to align DNA sequences to compare sequence similarity and identify potential restriction endonuclease cutting sites. A comparison between the human and mouse ADP-GK promoter sequence was carried out using the Bestfit application. The result showed a 66.8 % identity between the two sequences indicating that the ADP-GK promoter sequence is conserved between the two species. The alignment of the two sequences can be found in Appendix 4.1. An alignment was also performed using Bestfit between the human ADP-GK promoter sequence and the human hexokinase type II sequence to analyse similarity. Hexokinase type II was chosen for sequence comparison because this glycolytic enzyme is up-regulated by hypoxia and glucose

concentration in tumours. It has been postulated that hADP-GK would also be up-regulated by the same environmental factors (Ronimus and Morgan, 2004). The results of the alignment showed only 40% similarity between the two sequences and the alignment can also be found in Appendix 4.2. This indicates that the two promoter sequences are not very similar and therefore could be regulated by different pathways, even though it has been suggested that the two enzymes carry out the same function in glycolysis.

Further investigation into the homology of the ADP-GK promoter was carried out by submitting the promoter sequence into the Basic Local Alignment Search Tool using nucleotides (BLASTN) to investigate homology between different species. BLASTN calculates sequence similarity between sets of nucleotide or protein sequences. The BLASTN results showed sequence similarity across a number of species including chimpanzee, Rhesus monkey, marmoset, mouse, rat and cow. The search revealed that the promoter sequence had 97% identity with a region of the orang-utan genome. These results indicate that the ADP-GK promoter sequence is likely to be conserved across mammals and the transcription factor binding elements within the promoter sequence are therefore likely to be important in the regulation of the expression of ADP-GK. The results from the BLASTN analysis can be found in Appendix 5.

4.3 Identification of potential promoter elements

To investigate potential transcription factors that may have important roles in hADP-GK gene expression, cognate binding sites were identified using the AliBaba2 program which uses the binding sites collected in the TRANSFAC® database to predict possible transcription factor binding sites on uncharacterised DNA (Garbe, 2002). Figure 4.1 illustrates four putative transcription factor binding elements on the hADP-GK promoter sequence that were chosen for further investigation. These include specificity factor 1 (Sp1), glucocorticoid receptor (GR) and a cAMP responsive element (CRE). The entire promoter sequence with predicted transcription factor binding sites can be found in Appendix 3. Figure 4.2 illustrates the positioning of the four putative transcription binding elements on the 746 bp promoter construct chosen for further analysis. As the transcription start point (tsp) of hADP-GK has

not been determined, the upstream sequence is numbered relative to the ATG start codon at +1.

Figure 4.1 Predicted transcription factor elements

Four transcription factor elements chosen from the homology comparisons between mouse and human ADP-GK promoter sequences, include GR1 (A), GR2 (B), CRE1 (C) and Sp1 (D). Oligonucleotides were designed across each transcription factor element and were approximately 30 bases long. Accession number for promoter sequence NT 010194.

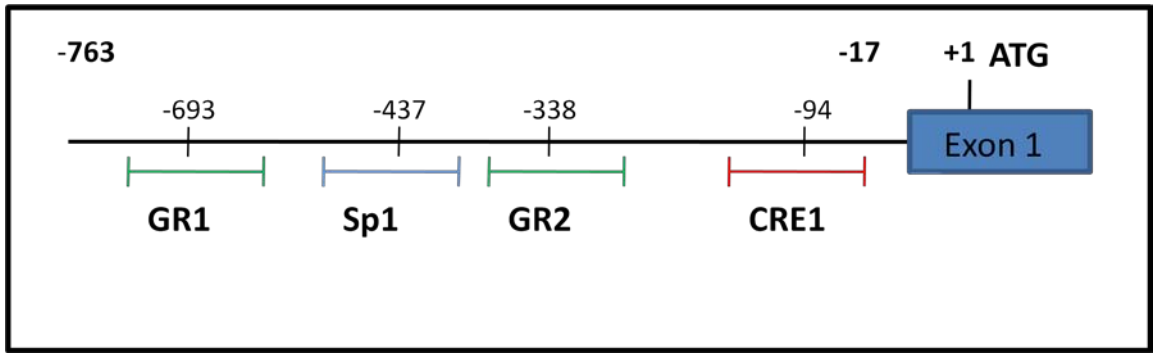

Figure 4.2 The positioning of putative transcription factor binding elements on the hADP-GK putative promoter relative to the ATG start codon in exon 1

The positions of four transcription factor binding sites chosen from homology comparisons between the human and mouse promoter regions shown on the 746 bp promoter construct. Green represents the two glucocorticoid receptor elements (GR1 and GR2). Blue represents the specificity factor 1 (Sp1) element and red represents the cAMP response element (CRE1). Primers were designed to flank either side of the transcription factor binding sites.

4.4 Cloning the hADP-GK promoter

4.4.1 Primer design and amplification of ADP-GK promoter using conventional PCR

Forward and reverse primers (R1, F1, F2, and F3) were designed to produce three different constructs of the hADP-GK promoter relative to the ATG start codon in exon 1 by amplification using conventional PCR. The R1/ F1 primer pair was expected to produce a promoter product of 746 bp, the R1/F2 primer pair was expected to produce a promoter product of 1,323 bp, and finally the R1/F3 primer pair was expected to produce a promoter product of 2,362 bp (Figure 4.3). Numbering of bp is relative to the ATG start codon at +1. Restriction endonuclease sites were added to the 5´ end of each primer to enable cloning into the multiple cloning site of the pGL3-Basic vector to be used as a reporter gene vector. Forward primers (F1, F2, and F3) had a *Sac* I site included at the 5´ end and the reverse primer (R3) had an *Xho* I site included at the 5´ end. Neither site occurred within the promoter sequence to be amplified. All primer sequences are listed in Table 4.1.

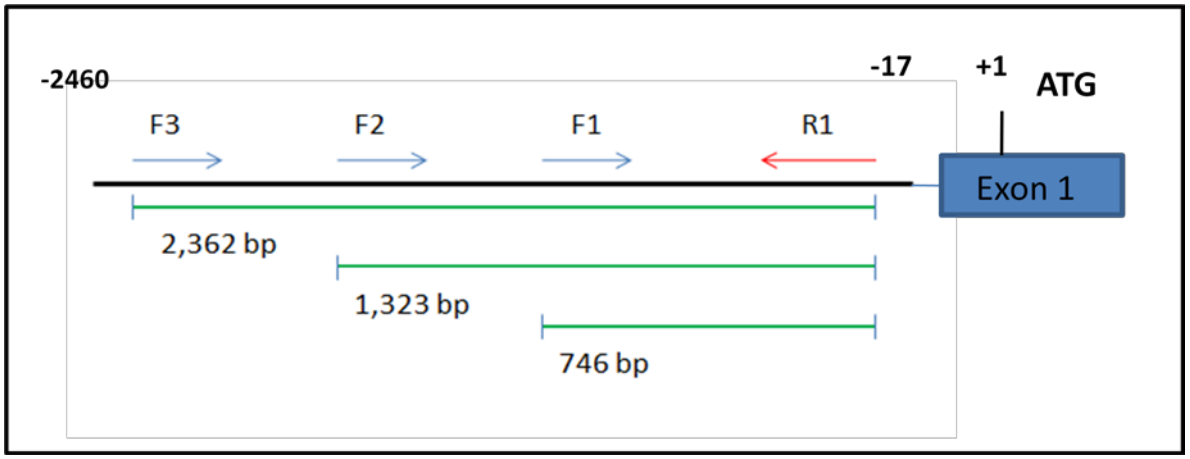

Figure 4.3 hADP-GK promoter constructs relative to the ATG start codon in exon 1

Four primers (R1, F1, F2, and F3) were designed across the hADP-GK promoter upstream from the ATG of exon 1 to produce three different sized constructs by conventional PCR for cloning. Promoter constructs are depicted in green. The hADP-GK upstream sequence is shown in black, with the forward primers in blue and reverse primer in red.

Primer	**Primer sequence 5´→ 3´**
R1	cgcg CTCGAG TCCTGCGCGAACCAACTCCTTTCCTA
F1	ccgg GAGCTC TTCTCAACCCAGGTCCATAACTCTCG
F2	ccgg GAGCTC CCTGACAGCTGAGGGTTGTGAGAAGA
F3	ccgg GAGCTC GCCATGTCTGGAAGCAATTTGGGTGG

Table 4.1 Promoter primer sequences

Forward and reverse primer sequences (R1, F1, F2, and F3) were designed across the putative hADP-GK promoter. Restriction endonuclease binding sites are underlined at the 5´ end of each primer. All forward primers have a *Sac* I restriction site, and the reverse has an *Xho* I restriction site.

PCR optimization was carried out using a range of annealing temperatures from 56-60°C to optimise the amplification of all three promoter products from gDNA. Various polymerase enzymes were used to produce high quality PCR products and to minimise non-specific PCR products. An annealing temperature of 56ºC with a Mg^{2+} concentration of 25 mM was successful (Figure 4.4) when applied to the reaction described in Table 4.2, giving discrete bands for primer pairs F1/R1 and F2/R1. Some non-specific bands were visualised in lane 4 along with the correct PCR product. These bands were removed when more specific polymerase enzymes were used and all PCR products were verified by restriction endonuclease digest and DNA sequencing. Further optimisation of F3/R1 was unsuccessful in producing the 2,362 bp promoter product and only non-specific bands were amplified (lane 5). PCR products were quantified by spectrophotometry using the Nanodrop spectrophotometer (Nanodrop Technologies).

95ºC for 5 min		
95ºC for 30 sec	45x cycles	Denaturing
56ºC for 30 sec		Annealing
72ºC for 30 sec		Extension
72ºC for 7 min		Final Extension

Two microlitres of genomic DNA template was added to the PCR master mix containing 2.5 µL (100 ng/µL) of forward (F1, F2, F3) and reverse (R1) primers, 5.0 µL of 10x PCR reaction buffer (500 mM Tris-HCl, pH 8.3, 100 mM KCl, 50 mM $(NH_4)_2SO_4$), 2.5 µL of 25 mM Mg^{2+}, 5.0 µL of 3 mM dNTPs, 0.5 µL of Faststart *Taq* polymerase (5 U/µL) (Roche), and 48 µL of sterile water for a total volume of 50.0 µL.

Table 4.2 PCR protocol for amplification of hADP-GK promoter regions

PCR reaction protocol and master mix ingredients used for the amplification of two human ADP-GK promoter regions.

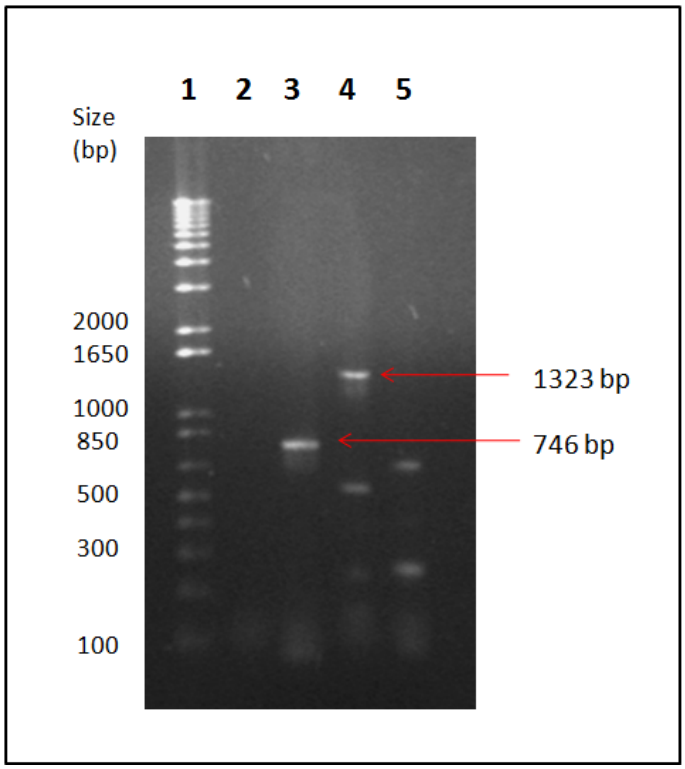

Figure 4.4 Visualisation of promoter product amplification and primer specificity for cloning

Gel electrophoresis using a 1% agarose gel in 1x TAE buffer was carried out to separate 15 µL PCR samples for approximately an hour at 100 volts. One microlitre of ethidium bromide (0.5 µg/mL) was added to the agarose gel to allow the visualisation of DNA under UV light. Lane one contains a 1 kb ladder used to estimate the molecular size of the PCR products. The molecular sizes are indicated on the left hand side of the figure shown in base pairs (bp).

Lane one: Ten microlitres of 1 kb plus ladder (1 µg/µL); **Lane two:** Non-template control (NTC); **Lane 3:** Fifteen microlitres (30%) of undiluted promoter PCR product (F1); **Lane four:** Fifteen microlitres (30%) of undiluted promoter PCR product (F2); **Lane five:** Fifteen microlitres (30%) of undiluted promoter PCR product (F3).

4.3.2 Restriction endonuclease digest

To ensure that the designed primers had specifically amplified regions of the hADP-GK promoter, restriction endonuclease digests were carried out. Five microlitres (10%) of PCR product was digested with 1.0 µL of restriction endonuclease *Kpn* I or *Bst* BI (8-10 U/µL) as outlined in Section 2.2.6. *Bst* BI was used to digest the F1 product and was expected to produce two bands sized 340 bp and 406 bp (Figure 4.5). *Kpn* I was used to digest the F2 product and was expected to produce two bands sized 467 bp and 856 bp (Figure 4.5). Figure 4.6 shows the results of the restriction endonuclease digests visualised by gel electrophoresis. A 1 kb ladder was used to determine the sizes of the digested PCR products. The digests successfully produced the expected bands, indicating that the PCR products were specifically amplified from the hADP-GK promoter with the designed primers.

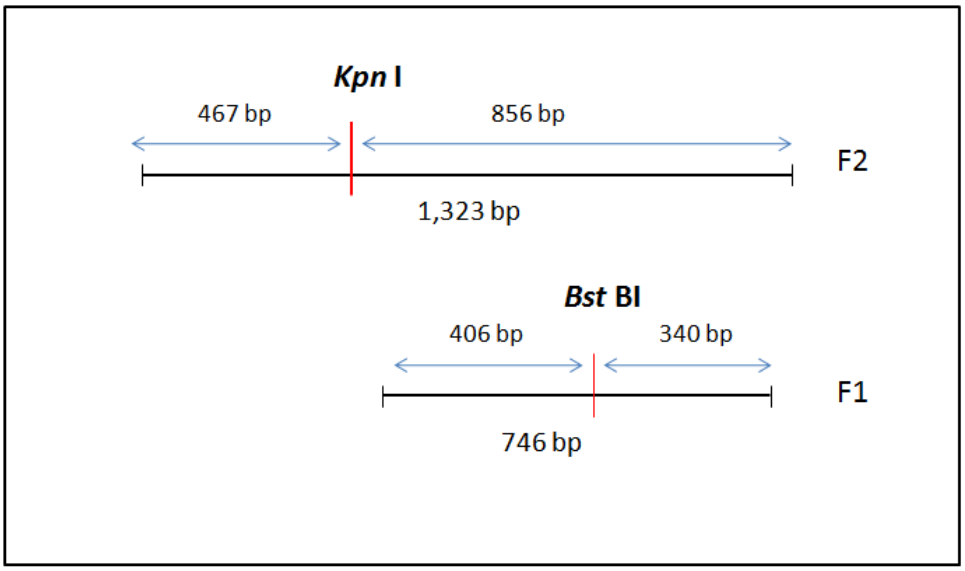

Figure 4.5 Schematic representation of the restriction digest carried out on the hADP-GK promoter constructs F1 and F2

Kpn I and *Bst* BI restriction enzyme sites when cut produce the specific sized products illustrated above. These products can be visualised on an agarose gel by gel electrophoresis.

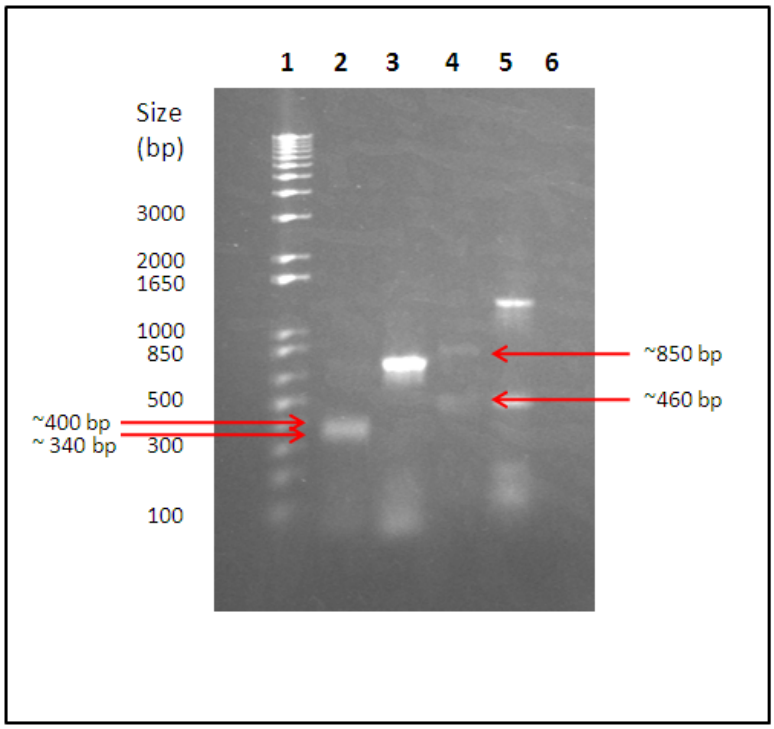

Figure 4.6 Digestion of hADP-GK promoter constructs F1 and F2

Digested and undigested samples were separated on a 1 % agarose gel in 1x TAE buffer by gel electrophoresis at 100 volts for approximately 1 hour. One microlitre of ethidium bromide (0.5 µg/mL) was added to the agarose gel prior to electrophoresis to allow the visualisation of the bands under UV light. Molecular size markers were used to determine the size of each band and the sizes are indicated on the left hand side of the gel in base pairs (bp).

Lane one: 10 µL of 1 kb plus ladder (1 µg/µL); **Lane two:** 15 µL of F1 promoter product digested with *Bst* BI; **Lane three:** 15 µL of uncut F1 promoter product; **Lane four:** 15 µL of F2 promoter product digested with *Kpn* I; **Lane five:** 15 µL of uncut F2 promoter product; **Lane six:** NTC

4.3.4 Cloning and transformation strategy

Initial cloning of the hADP-GK promoter constructs was carried out using the pGEM®-T Systems kit as described in Section 2.2.7.2. Due to the 3´ A ends that are attached by *Taq* polymerase during conventional PCR, the promoter constructs were able to be ligated into the pGEM®-T vector. *E. coli* XL-1 Blue competent cells were transformed using heat shock

treatment as described in Section 2.2.7.1. Cells were then plated on LB/AMP plates with IPTG and X-gal for selection of transformants. The rapid boil method outlined in Section 2.2.8 was used to isolate plasmids from positive colonies. This vector was used initially to facilitate restriction endonuclease digestion that was required for ligation into the pGL3-Basic vector used for promoter analysis. Promoter sequences were removed from the pGEM®-T vector by restriction endonuclease digests using *Sac* I and *Xho* I enzymes.

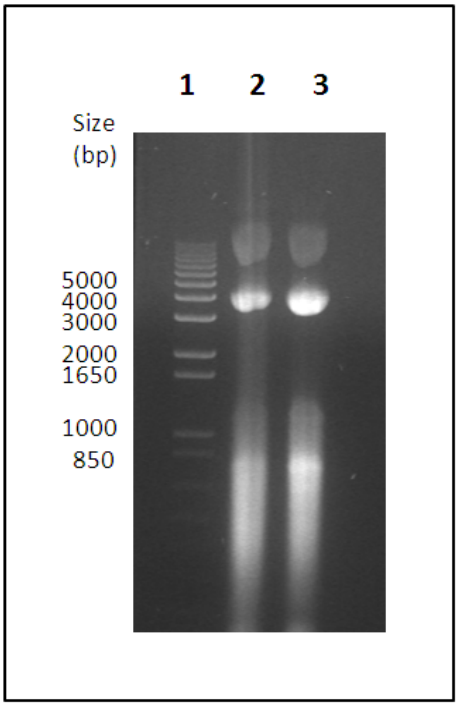

Figure 4.7 pGL3-Basic plasmid isolated from a transformed colony

Positive colonies were chosen from antibiotic treated plates and used for the isolation of the pGL3-Basic vector containing the hADP-GK promoter inserts by rapid boil treatment after overnight culture in 5 ml broths. A 1% agarose gel in 1x TAE buffer was used to visualise the plasmid by electrophoresis for approximately an hour at 100 volts. One microlitre of ethidium bromide (0.5 µg/ mL) was added to the agarose gel for the visualisation of the bands under UV light.

Lane one: Ten microlitres of 1 kb plus ladder (1.0 µg/µL); **Lane two and three:** Fifteen microlitres of purified pGL3-Basic plasmid containing insert.

The hADP-GK putative promoter constructs were then ligated into the pGL3-Basic vector at a 3:1 insert: vector ratio with T4 DNA ligase. pGL3-Basic vector was also cut with *Sac* I and *Xho* I and treated with thermosensitive alkaline phosphatase to facilitate ligation of the promoter constructs into the vector. *E. coli* XL-1 Blue competent cells were mixed with ligated plasmid/construct and transformed using LB-AMP plates as described in Section 2.2.7.4. The rapid boil method was used to isolate plasmids from positive colonies. Gel electrophoresis was used to check the stability of the plasmid after isolation by rapid boil preparation (Figure 4.7). RNA bands can be seen around 850 bp; this is due to the rapid boil method producing crude plasmid and the absence of RNase of digests after the plasmid preparation.

4.3.5 Cloning and transformation confirmation

To ensure that cloning of the hADP-GK promoter constructs into the pGL3-Basic vector was successful, digestion with restriction endonucleases was carried out. *Bst* BI and *Kpn* I restriction enzymes were used to cut the F1 and F2 constructs, respectively. If cloning was successful then linear bands would result from the restriction endonuclease digests when compared to an uncut vector control. The linear band around 5000 bp produced as a result of the *Bst* BI digest for the F1 promoter construct indicates that the F1 construct was inserted in the vector (Figure 4.8). An equivalent experiment was carried out for the F2 promoter construct, however it did not appear to be ligated into the pGL3-Basic vector as upon digestion with *Kpn* I restriction endonuclease, the two linear fragments of 5641 bp and 500 bp that were expected were not observed. Full excision of the insert from the pGL3-Basic was not carried out as the restriction endonuclease enzymes used prior to ligation required different enzymatic conditions and was therefore omitted due to time constraints.

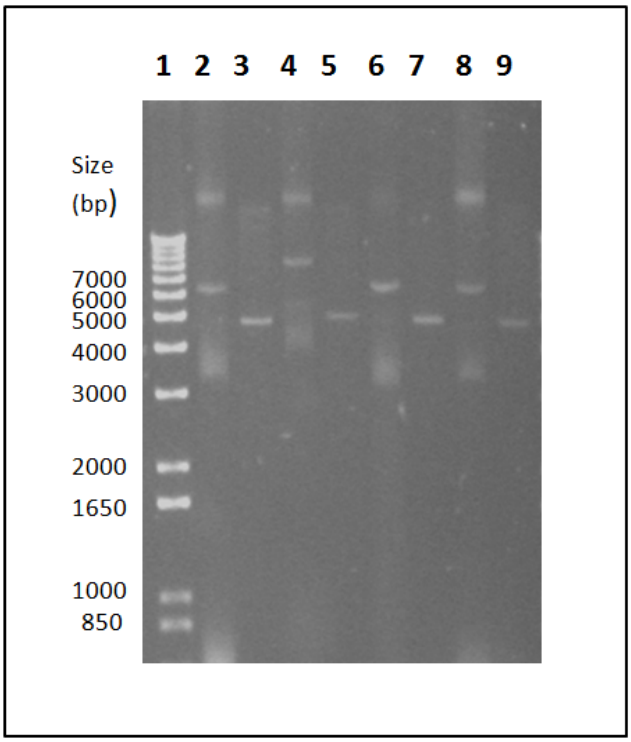

Figure 4.8 Restriction endonuclease digest for confirmation of cloning strategy

A 1% agarose gel in 1x TAE buffer was used to separate 10 µL of *Bst* BI digested and undigested plasmid by electrophoresis for approximately an hour at 100 volts. One microlitre of ethidium bromide (0.5 µg/mL) was added to the agarose gel to allow the visualisation of the bands under UV light. Molecular size markers were used to determine the sizes of the bands and these are labelled on the 1 kb plus ladder in base pairs (bp)

Lane one: Ten microlitres of 1 kb plus ladder (1 µg/µL); **Lanes two, four, six and eight:** Ten microlitres of uncut pGL3-Basic vector; **Lanes three, five, seven and nine:** Ten microlitres of *Bst* BI cut pGL3-Basic vector isolated from positive clones from antibiotic selection plates.

To further confirm the cloning of the F1 and F2 promoter constructs into the pGL3-Basic vector after selection of positive colonies from antibiotic plates, PCR using plasmid specific RV primer 3 and GL primer 2 was carried out using the reaction protocol described in Table 4.2. These primers flank the multiple cloning site of the pGL3-Basic vector, which should include the ligated inserts F1 and F2. The sequences of the RV primer 3 and GL primer 2 are shown in Table 4.3. The PCR reactions were then separated by gel electrophoresis to visualise the F1 and F2 inserts (Figure 4.9). The gel electrophoresis showed that the F1

promoter construct had been successfully inserted into the pGL3-Basic vector with the presence of the 746 bp product verified by the ~700 bp PCR produced insert in lane 5. The bands are slightly larger due to the addition of the multiple cloning sites. The F2 promoter construct had unfortunately not been cloned, as indicated by the absence of a band around 1,323 bp. The higher mobility band around 200 bp represents the multiple cloning site, which is the only part of the plasmid that can be amplified during PCR (lanes 2 and 3). Further PCR reactions were carried out on a number of positive colonies picked from antibiotic selection plates for the F1 promoter construct. Further cloning attempts were unsuccessful for the F2 promoter construct. It was possible the incorrect band was excised during gel purification of the F2 product.

Primer	**Primer sequence 5´→3´**
RV primer 3	CTAGCAAAATAGGCTGTCCC
GL primer 2	CTTTATGTTTTTGGCGTCTTCCA

Table 4.3 RV primer 3 and GL primer 2 sequences

RV primer 3 and GL primer 2 flank the multiple cloning site of the pGL3-Basic vector. The primers were used to verify the presence of the hADP-GK putative promoter inserts within the reporter gene plasmid prior to carrying out activity assays.

Finally, direct DNA sequencing was carried out on pGL3-Basic vector that had been selected from a positive colony and shown to include the 746 bp insert by restriction endonuclease digestion and PCR. Direct DNA sequencing was carried out to ensure that the cloned inserts were in fact the correct constructs required for analysis of the hADP-GK promoter and that no alteration to the promoter sequence had occurred during PCR cloning or transformation. RV primer 3 and GL primer 2 were used in the sequencing reaction. The results of the DNA sequencing reaction showed the presence of the F1 promoter construct within the pGL3-Basic vector without any base changes to the sequence. The results of the DNA sequencing can be found in Appendix 2.

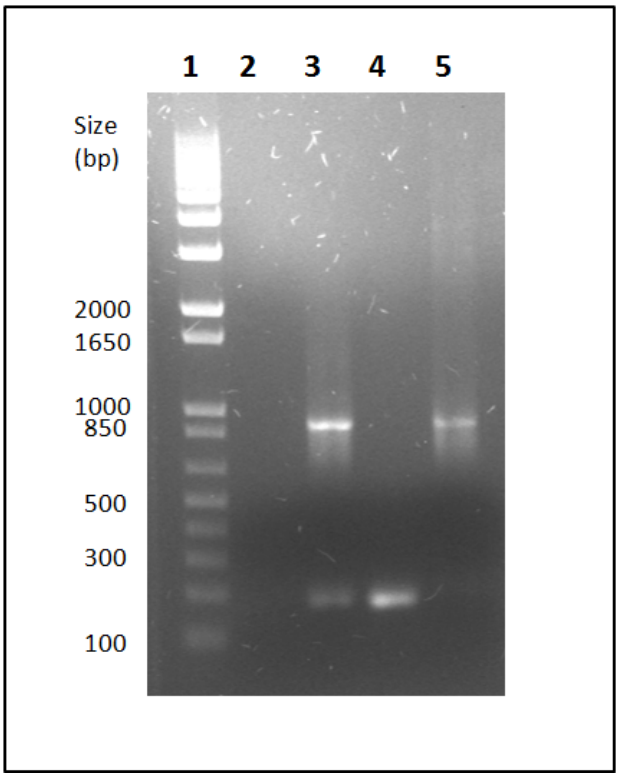

Figure 4.9 PCR products obtained from pGL3-Basic vector using RV primer 3 and GL primer 2

One positive colony, from antibiotic selection plates, for each promoter construct F1 and F2 were selected for PCR. Fifteen microlitres of each PCR reaction was loaded onto a 1% agarose gel in 1x TAE and electrophoresis at 100 volts was carried out for approximately one hour. One microlitre of ethidium bromide (0.5 µg/mL) was added to the agarose gel for the visualisation of the bands under UV light. A 1 kb plus ladder was used to determine the molecular sizes of each band and are labelled on the left hand side of the gel in base pairs (bp).

Lane one: Ten microlitres of 1 kb plus ladder (1.0 µg/µL); **Lane two:** NTC; **Lane three:** F1 colony; **Lane four:** F2 colony; **Lane five:** PCR positive control (700 bp)

4.5 Discussion

Human ADP-dependent glucokinase (hADP-GK) is a relatively novel enzyme, and prior to this study no information on the promoter of hADP-GK had been obtained. Analysis of the promoter regions is an important step in understanding the role of hADP-GK in the metabolism of glucose, as wells as elucidating its role in overall cell function during normal and disease states. In this chapter the initial analysis of the promoter region included homology comparison between species and between glucose phosphorylating enzymes, identification of potential transcription factor binding sites, and the cloning of the promoter into a reporter gene vector for further analysis.

Comparison of the hADP-GK promoter with the promoter region from mouse ADP-GK (mADP-GK) showed that 67% of the sequence was conserved between the two species using the GCG version 11.1 (Accelrys Inc., San Diego, CA) program. A large region of similarity was observed close to a potential tsp of the hADP-GK gene (2458, Appendix 4.1). The NCBI BLASTN tool was used to compare similarity of the hADP-GK promoter across the mammalian genome and the results showed that the promoter region was conserved across a number of species with the highest similarity found across a small range of primates. The conservation of the promoter region was indicative that the transcription factor elements within the region maybe important for gene regulation and identifying these conserved transcription factor binding sites is an important first step in elucidating the role of ADP-GK within these mammalian species. Further alignments between the primate and human promoter sequences to investigate transcription factor binding site conservation could provide more information. Further comparison of the hADP-GK promoter region with that of the hexokinase type II promoter showed only partial similarity (40%) with no significant pattern of alignment using the GCG version 11.1 program (Appendix 4.2). No significant alignment was shown between the hADP-GK and hexokinase type II promoter regions when submitted to BLAST (NCBI).

The TRANSFAC database was used by the AliBaba 2 program to identify potential transcription factor binding sites within the hADP-GK promoter sequence. The hADP-GK and mADP-GK were compared to identify if any of the potential transcription factor elements were conserved between the two sequences. A small number of elements were conserved between the two promoters and these included a small number of Sp1 elements, as well as a cAMP-reponse element (CRE), two glucocorticoid receptor (GR) elements and a GATA box. The hexokinase type II promoter and hADP-GK were also checked for transcription factor element conservation, the GATA 1 box was shown to be conserved along with a small number of Sp1 elements. Hexokinase type II has been shown to have a CRE element within its promoter (Osawa *et al*., 1996). The CRE element was shown to sit just in front of the transcription start point, which is also predicted by the AliBaba 2 program for the hADP-GK promoter (Lee and Pedersen, 2003). There was no sequence similarity, however, between the CRE element in the hexokinase type II and ADP-GK promoter region examined.

Forward and reverse primers were designed across the hADP-GK promoter to allow the amplification of products containing the conserved transcription factor binding elements. A 746 bp product was successfully amplified and cloned into a pGL3-Basic vector containing a reporter gene. Two other constructs 1,323 bp and 2,362 bp long were not successfully amplified or cloned. The 746 bp construct contained a number of conserved transcription factor binding sites close to the putative transcription start point (tsp) and was therefore used for further analysis of promoter activity and transcription factor binding proteins.

Chapter 5: Promoter activity and transcription factor binding elements

5.1 Introduction

Transcription factors are important for promoter activity and interact with the promoter region by binding to their cognate sequences on the DNA. The identification of transcription factor binding sites using homology comparisons and sequence databases revealed the possible importance of the promoter region closest to the ATG start codon in exon 1. This region is known as the core promoter region and was hypothesised to contain the transcription start point (tsp). This chapter describes how luciferase assays and electrophoretic mobility shift assays (EMSA) were used to investigate the activity of the putative promoter region and the potential transcription factor proteins which may be important for the regulation of hADP-GK.

5.2 hADP-GK promoter activity

Once the -746hADP-GK promoter construct had been successfully cloned into the pGL3-Basic vector and confirmed by DNA sequencing, transient transfections were carried out in HeLa cells to determine whether the promoter construct was active. The pGL3-B-hADP-GKprom plasmid was co-transfected with a control plasmid pCMV SPORT β-gal to normalise transfection efficiency and cell number variation. Harvesting of the transfected cells was carried out after 48 hours, and cell lysates were used for luciferase and β-galactosidase assays. Section 2.2.13 and Table 2.10 outline the method for the calculation of normalised luciferase activity. Table 5.1 shows the data for the luciferase and β-galactosidase assays for the pGL3-B-hADP-GKprom vector and the pGL3-Basic vector control. Figure 5.1 illustrates the results of repeated normalised luciferase assays.

	Normalised Luciferase				
Triplicates	**1**	**2**	**3**	**Average**	**Std dev**
pGL3-Basic Control	10.67	473.16	1.43	161.75	207.604
pGL3-B-hADP-GKprom	165,514.80	388,484.30	419,358	324,452.40	105958.4

Table 5.1 Luciferase and β-galactosidase data

The normalised luciferase activities for each transfection were calculated by the dividing the corrected luciferase activity value by the corrected β-galactosidase activity value. Each transfection was carried out in triplicate on the same day, and each experiment was repeated on three separate occasions. Values were averaged prior to normalisation. Normalised luciferase activities were averaged and the standard deviations calculated.

The luciferase assay results showed that the 746 bp promoter construct was sufficient to drive the reporter gene to produce substantial amounts of luciferin compared to the no insert pGL3-Basic control (Figure 5.1). A paired student *t*-test with one tailed distribution was used to test the significance of the normalised luciferase activity values of the pGL3-B-hADP-GKprom vector compared with the no insert pGL3-Basic control. A p-value of 0.03 was obtained indicating that the two data sets are significantly different with a greater than 95% confidence interval.

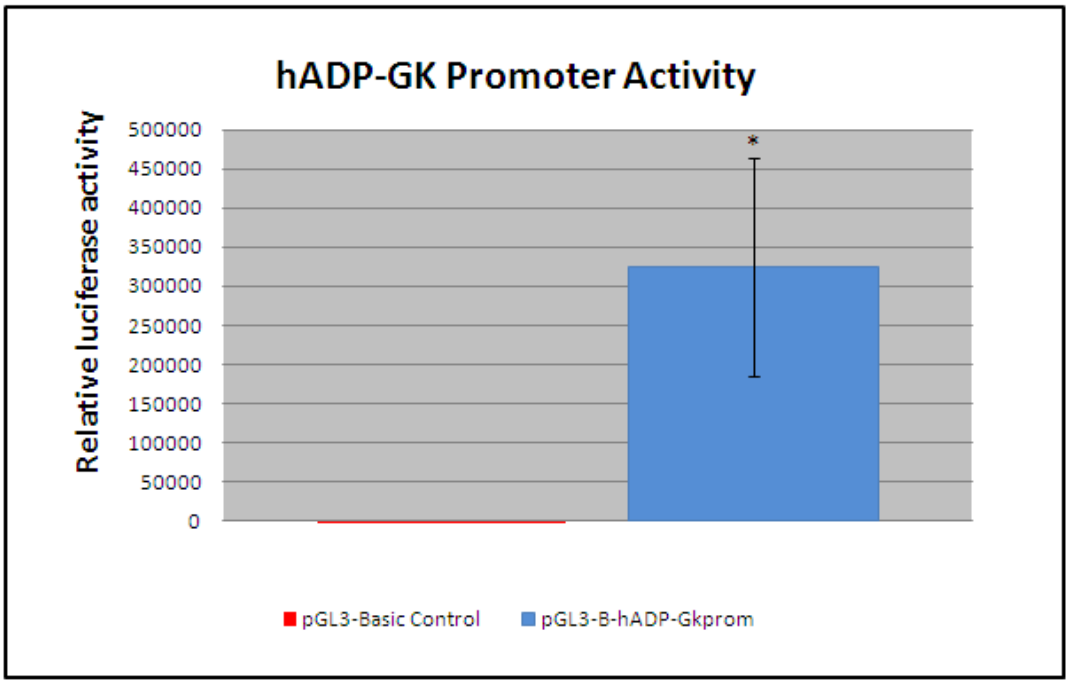

Figure 5.1 Normalised luciferase assays

HeLa cells were transfected with 0.5 µg of pGL3-B-hADP-GKprom plasmid along with 0.25 µg of pCMV SPORT β-gal plasmid as described in Section 2.2.11-2.2.13. A pGL3-Basic vector without an insert was used as a negative control to show that luciferase production was not possible without a promoter construct. The results are an average of three experiments carried out in triplicate. The standard deviation is represented by the error bar and the asterix indicates a significant difference between the control plasmid and pGL3-B-hADP-GKprom within less than 5% chance the data set is similar to the control or >95% confidence that the two sets are different.

5.3 Promoter element and transcription factor identification

5.3.1 Labelling of oligonucleotides with ^{32}P

To identify potential transcription factor binding sites, small oligonucleotides were designed to represent elements located in the hADP-GK promoter region. Table 5.2 displays the sequences of the oligonucleotides. The oligonucleotides were labelled with $\gamma^{32}P$ [ATP] and purified using polyacrylamide gel electrophoresis. After purification the incorporation of $\gamma^{32}P$ [ATP] into each oligonucleotide was measured by scintillation counting to ensure sufficient labelling had occurred. Figure 5.2 illustrates the ^{32}P-oligonucleotides within the polyacrylamide gel prior to excision, and Table 5.3 displays the results of the scintillation count carried out.

Promoter Element	**Primer Pair**	**Sequence (5´→3´)**
Glucocorticoid receptor (GR1)	Forward	GTTTGTTAAAGGGAACAGCGCCCCCAAAAG
	Reverse	CTTTTGGGGGCGCTGTTCCCTTTAACAAAC
Glucocorticoid receptor (GR2)	Forward	CCGCTTCTTCACAATCTGTCCGTTTCGTT
	Reverse	AACGAAACGGACAGATTGTGAAGAAGCGG
cAMP response element (CRE)	Forward	GCACCCTTGTGACGTAGCGCTTGTGTCGAC
	Reverse	GTCGACACAAGCGCTACGTCACAAGGGTGC
Specificity factor 1 (Sp1)	Forward	CAAATGAGGGGACACGGGCGGAGGGAGGG
	Reverse	ATCCCTCCCTCCGCCCGTGTCCCCTCATTTG

Table 5.2 Oligonucleotide sequences for EMSA

Forward and reverse oligonucleotide sequences were designed across potential transcription factor binding sites located on the hADP-GK promoter region.

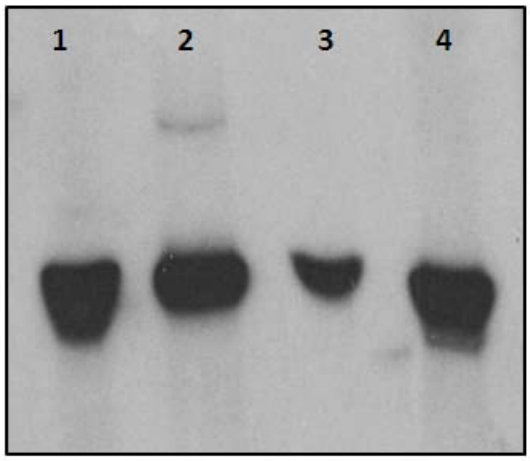

Figure 5.2 Sequencing gel for labelled oligonucleotide purification

One hundred microlitres of each ^{32}P-oligonucleotide was loaded onto a 10% acrylamide gel in 1x TBE and separated by gel electrophoresis at 30 W (1500 V) for approximately 1 hour until the bromophenol blue dye front had reached ~20 cm from the bottom of the gel. After electrophoresis the gel was exposed to X-ray film for approximately one minute to enable the visualisation of the bands within the gel. The bands were then cut from the gel and eluted using 50 mM KCl.

Lane one: Sp1 ^{32}P-oligonucleotide; **Lane two:** CRE1 ^{32}P-oligonucleotide; **Lane three:** GR2 ^{32}P-oligonucleotide; **Lane four:** GR1 ^{32}P-oligonucleotide

^{32}P-oligonucleotide	**Scintillation count (cpm) / µl**	
	Read 1	**Read 2**
GR1	27064	27083
GR2	1381	1383
CRE1	33445	33315
Sp1	26811	26429
Blank	7	6

Table 5.3 Scintillation counts for ^{32}P-oligonucleotides after labelling

After gel purification, each ^{32}P-oligonucleotide was checked for sufficient labelling by scintillation counting. Reads between 10,000-15,000 cpm indicate sufficient labelling.

5.3.2 Glucocorticoid receptor promoter elements (GR1 and GR2)

Two potential glucocorticoid receptor elements were identified in the promoter region of hADP-GK. Both elements were also found in the mouse promoter region indicating that these regions could be functionally conserved. The scintillation count revealed that the GR2 ^{32}P-oligonucleotide had not been sufficiently labelled with only a read of ~1300 counts per minute (cpm), so the GR2 oligonucleotide was not used for further EMSA assays. To determine if GR did in fact bind to the glucocorticoid receptor element present within the hADP-GK promoter, competitor assays and antibody supershift experiments were carried out. EMSA titration assays were initially carried out using HeLa and SiHa whole cell extracts to determine an appropriate amount of extract to use for each assay. Figure 5.3 presents the EMSA gels for the GR1 ^{32}P-oligonucleotide using both HeLa (A) and SiHa (B) cell extracts. In the absence of whole cell extract no bands can be visualised and unbound oligonucleotide can be seen at the bottom of the gel (lane one).

The EMSA titration assays showed that proteins from both whole cell extracts were able to bind to the GR1 ^{32}P-oligonucleotide as indicated by the bands visualised in Figure 5.3. From the titration assays it could be deduced that 20 µg of protein extract was sufficient to ensure the interaction between protein and DNA was visible and could be used for further EMSA experiments. The same binding patterns were observed for both HeLa and SiHa cell extracts with only minor differences in band intensity between the two gels, therefore HeLa whole cell extracts were used for all subsequent assays.

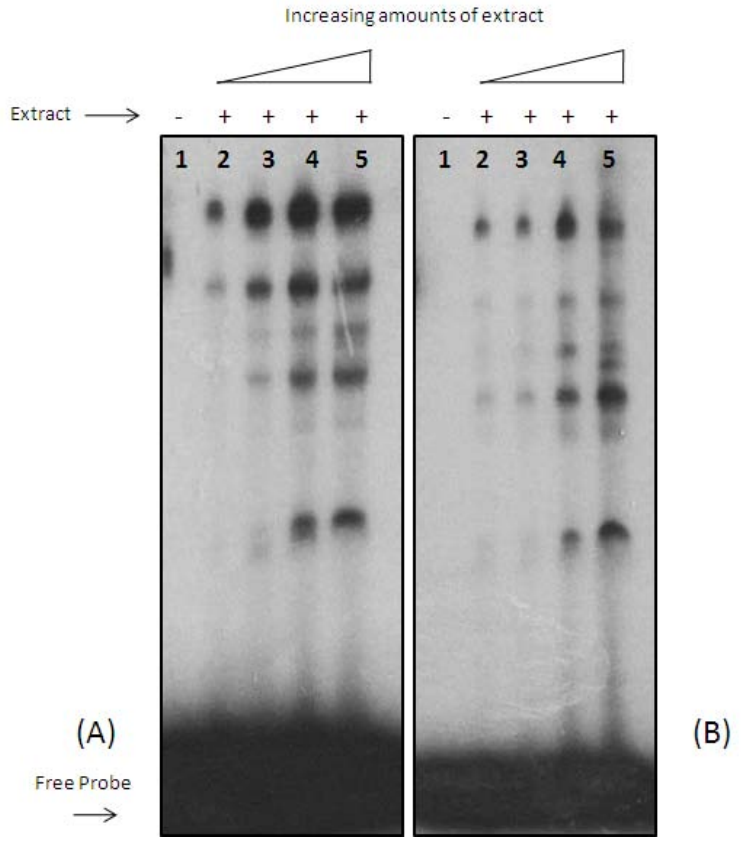

Figure 5.3 EMSA titration assays with GR1 ^{32}P oligonucleotide

Approximately 0.5 ng of GR1 ^{32}P-oligonucleotide was added to increasing amounts (0, 10, 20, 40, 80 µg) of HeLa (A) and SiHa (B) whole cell extracts with a total volume of 20µL in each EMSA reaction. Half of the reaction volume was loaded onto the gel. The gel was transferred and dried onto DE-81 paper. The gel was then exposed to X-ray film for 18 hours at -80°C. The unbound oligonucleotide can be visualised at the bottom of the gel.

Lane one: Free probe only; **Lane two, three, four and five:** HeLa (A) and SiHa (B) whole cell extracts.

To test whether the GR1 ^{32}P-oligonucleotide was representative of a glucocorticoid receptor element in the hADP-GK promoter region, competitor assays using homologous, specific non-homologous GR oligonucleotides and non-specific non-homologous oligonucleotides were carried out. Unlabeled, double-stranded oligonucleotides are often used in EMSA as competitors to determine the specificity of protein-DNA interactions. When a specific competitor is added to the EMSA reaction a decrease in band intensity is observed if there is

an interaction between the binding protein from the whole cell extract and the unlabelled competitor. A non-specific (NS) competitor will show no or very little change in band intensity of the shifted band. A specific non-homologous GR competitor (GRE) was used to determine if the GR1 ^{32}P-oligonucleotide contained a true glucocorticoid receptor element. This non-homologous competitor was obtained from the tyrosine amino transferase promoter sequence in rat. A homologous GR competitor (GR1) and non-specific non-homologous competitor (NS) were also used as controls for the competitor assay. The non-homologous competitor (NS) sequence was obtained from the topoisomerase IIα promoter sequence (Magan, 2009). Table 5.4 presents the sequences of the competitor oligonucleotides.

Competitor oligonucleotide		**Sequence 5´→3´**
GRE	Forward	TCGACTGTACAGGATGTTCTAGCTACT
	Reverse	AGTAGCTAGAACATCCTGTACAGTCGA
NS	Forward	CGAGTCAGGGATTGGCTGGTCGTCGCTTC
	Reverse	CTTCTTTAGCCCGCCCCAAGCAGCAGACG
Sp1 WT	Forward	CTGCTTCGGGCGGGCTAAAG
	Reverse	CTTTAGCCCGCCCGAAGCAG
Sp1 MT	Forward	CTGCTTCGTGCGTGCTAAAG
	Reverse	CTTTAGCACGCACGAAGCAG

Table 5.4 Competitor oligonucleotide sequences

Double-stranded oligonucleotide sequences used for competitor assays with GR1, Sp1 and CRE ^{32}P-labelled oligonucleotides.

Figure 5.4 shows the competitor assay using the GR1 ^{32}P-oligonucleotide with increasing amounts of double-stranded competitors. The absence of cell extract in lane one results in the absence of visible shifted bands, and free unbound oligonucleotide can be visualised at the bottom of the gel. Lane two contains no competitor and represents the "normal" amount of protein binding to the GR1 ^{32}P-oligonucleotide. This lane was used as a control to compare with the competitor reactions. Lanes 3, 4 and 5 contain the specific non-homologous competitor (GRE), and the band intensity patterns in Figure 5.4 show very little change in

intensity indicating that no competition between the labelled and unlabeled oligonucleotide for protein binding has occurred.

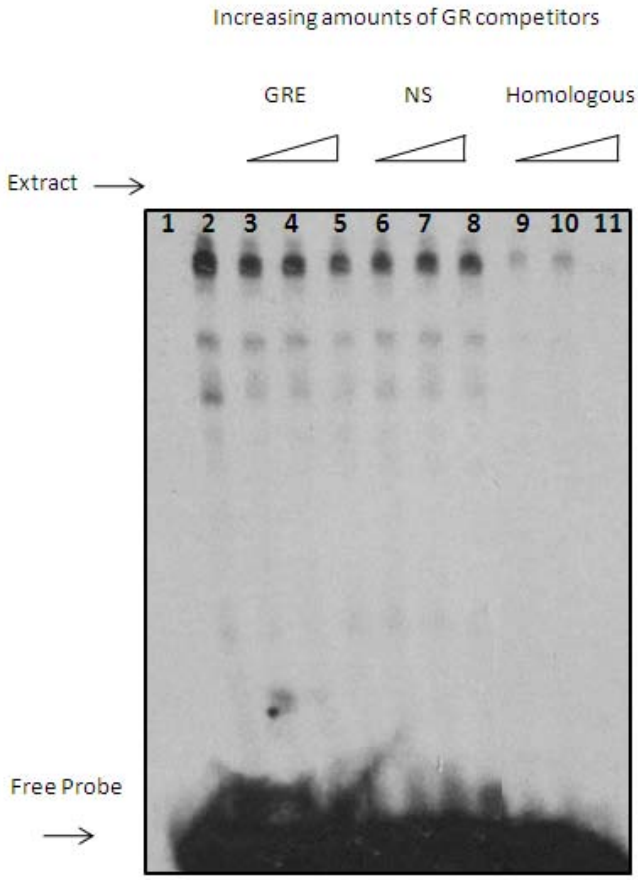

Figure 5.4 EMSA using GR oligonucleotide competitors

Twenty micrograms of HeLa whole cell extract was added to increasing amounts of unlabelled GR double-stranded competitor (5, 50, 100 ng) along with 0.5 ng of GR1 ^{32}P-oligonucleotide with a total volume of 20 µL for each EMSA reaction. Half of the reaction was loaded onto the gel. The gel was transferred and dried onto DE-81 paper before exposure to X-ray film for 18 hours at -80°C. NS, non-specific competitor.

Lane one: Free probe only; **Lane two:** Extract only; **Lanes three, four and five:** Extract and non-homologous GR competitor; **Lanes six, seven and eight:** Extract and NS competitor; **Lanes nine, ten and eleven:** Homologous GR1 competitor.

Lanes 6, 7 and 8 in Figure 5.4 contain the non-specific competitor (NS) which showed some reduction in band intensity in lane 6, but this was likely caused by a loading inconsistency rather than competitive interaction between the oligonucleotides and extract protein as higher amounts of non-specific competitor did not reduce band intensity (lanes 7 and 8). Lanes 9, 10 and 11 contain the homologous competitor (GR1) which showed a marked reduction in band intensity which was specific for the GR1 ^{32}P-oligonucleotide. These lanes were used as positive controls for competitive interactions.

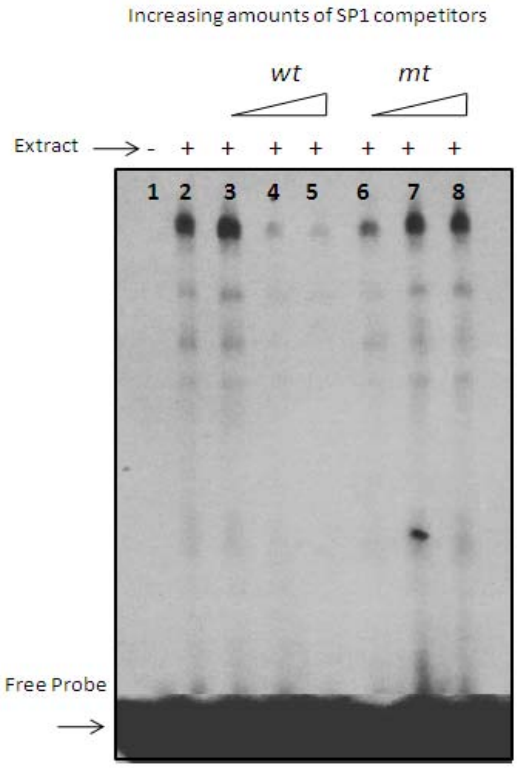

Figure 5.5 EMSA using Sp1 oligonucleotide competitors

Twenty micrograms of HeLa whole cell extract was added to increasing amounts of unlabelled Sp1*wt* or Sp1*mt* double-stranded competitor (5, 50, 100 ng) along with 0.5 ng of GR1 ^{32}P-oligonucleotide with a total volume of 20 µL for each EMSA reaction. Half of each reaction was loaded onto the gel. The gel was transferred and dried on DE-81 paper and exposed to X-ray film for 18 hours at -80°C.

Lane one: Free probe only; **Lane two**: Extract only; **Lanes three, four and five:** Extract and Sp1*wt* competitor; **Lanes six, seven and eight:** Extract and Sp1*mt* competitor.

The results for the competitor assay using homologous and non-homologous GR competitors indicated that the promoter element was not likely to be a glucocorticoid receptor element. To further elucidate what protein could be binding to the element, competitor assays using Sp1 wild-type (Sp1*wt*) and Sp1 mutant (Sp1*mt*) unlabelled oligonucleotides were carried out. The sequences of the two Sp1 competitor oligonucleotides are listed in Table 5.4. Sp1*wt* and Sp1*mt* competitor sequences were obtained from the topoisomerase IIα promoter sequence (Magan, 2009).

Figure 5.5 shows the competitor assay using Sp1*wt* and Sp1*mt* oligonucleotides with the GR1 ^{32}P-oligonucleotide and HeLa whole cell extract. Lane 1 contained no shifted bands and was representative of unbound labelled oligonucleotide at the bottom of the gel. Lane 2 did not contain competitor and represented the "normal" amount of protein binding to the DNA. This lane was used as a control to compare with the competitor reactions. Lanes 3, 4 and 5 contained Sp1*wt* double-stranded competitor in increasing amounts. There was a large reduction in band intensity in lanes 4 and 5 indicating that the unlabelled oligonucleotide had competed for the binding of protein. Lanes 6, 7 and 8 contained the Sp1*mt* double-stranded oligonucleotide. There was a small reduction in band intensity in lane 6, but because lanes 7 and 8 do not exhibit the same reduction this result was likely due to loading inconsistencies. The competitor assay indicated that the promoter element may be an Sp1 element, rather than a GR element.

To further investigate if the element could be a Sp1 binding element, antibody supershift assays were carried out. The addition of an antibody, which is antigen specific, to an EMSA reaction allows the identification of proteins that form specific interactions with DNA. When the antibody binds to the protein-DNA complex, the original band that is seen is moved to a lower mobility (supershift) because the entire complex of antibody, protein and DNA is much larger than just the transcription factor-DNA complex. In other cases the addition of an antibody can cause a reduction in band intensity as it inhibits the binding of protein to the DNA by obstructing the DNA binding site. Sp1 and Sp3 antibodies were used for antibody supershifts due to the large number of Sp1 sites predicted by the AliBaba 2 program spanning the hADP-GK promoter region. Sp3 antibody was used to verify if the Sp1 binding sites

were specific, however, Sp3 and Sp1 often bind at the same sites as they are both members of the Sp family of transcription regulators and recognise similar cognate DNA elements.

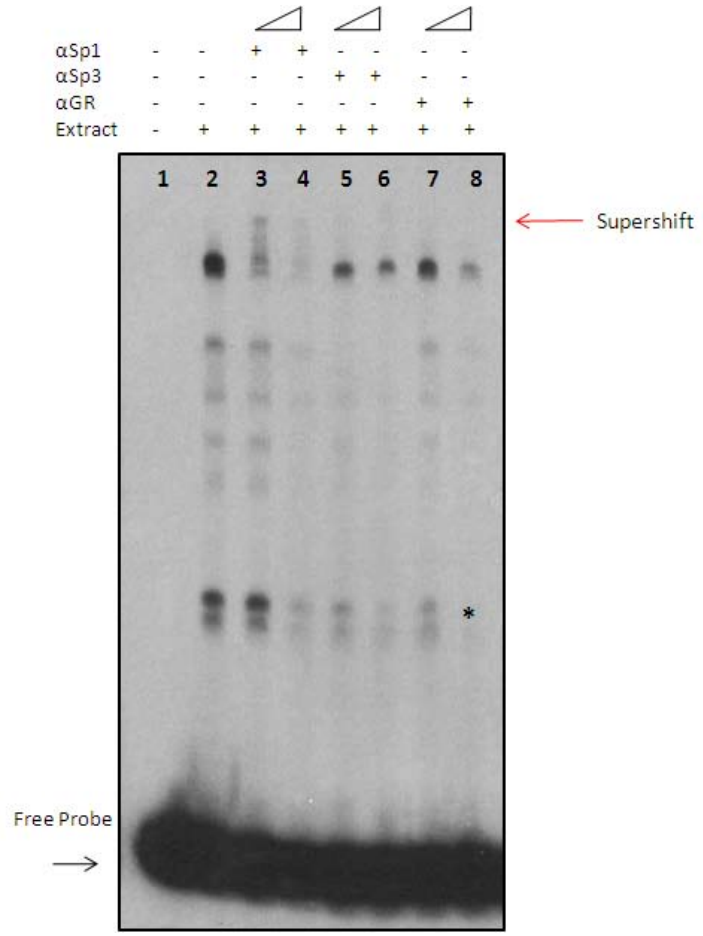

Figure 5.6 Antibody supershifts to verify Sp1 element identification

Twenty micrograms of HeLa whole cell extract was added to Sp1, Sp3 or GR antibody (0.2 µg and 0.4 µg), along with approximately 0.5 ng of GR1 ^{32}P-oligonucleotide with a total volume of 25 µL for each EMSA reaction. Ten microlitres of the reaction volume was loaded onto the gel. The gel was transferred and dried onto DE-81 paper before exposure to film for 18 hours at -80°C. Unbound oligonucleotide is visualised at the bottom of the gel. The asterix represents non-specific interactions.

Lane one: Free probe only; **Lane two:** Extract only; **Lanes three and four:** Extract and Sp1 antibody; **Lanes five and six:** Extract and Sp3 antibody; **Lanes seven and eight:** Extract and GR antibody.

Figure 5.6 illustrates the antibody supershift assays using Sp1, Sp3 and GR antibodies with the GR ^{32}P-oligonucleotide and HeLa whole cell extracts. Lane 1 is representative of unbound labelled oligonucleotide at the bottom of the gel. Lane 2 contained no antibody and represented the "normal" binding patterns of protein to DNA; this lane was used as a control to compare with the various antibody reactions. Lane 3 and 4 contained Sp1 antibody and it was observed that Sp1 caused a supershift to occur, as well as a reduction in band intensity. This indicated that the promoter element thought to be a glucocorticoid receptor was possibly an Sp1 element. Lanes 5 and 6 contained Sp3 antibody which resulted in a small reduction in band intensity when compared to the control in lane 2 but no obvious supershift. Lanes 7 and 8 contained a GR antibody which also resulted in a small decrease in band intensity. There were some higher mobility bands (as indicated by the *) seen in Figure 5.6. These bands were reduced with higher concentrations of Sp3 and GR antibody and were likely to be non-specific interactions between smaller proteins and DNA or interactions between oligonucleotides, as these bands were not seen in the previous figures.

5.3.3 cAMP response element (CRE)

The results from the AliBaba2 program indicated a potential CRE element located on the hADP-GK promoter. Promoter comparisons between the human and mouse ADP-GK promoter showed that this region was conserved and therefore may have potential functional significance. To investigate the CRE element, antibody supershift and competitor EMSA's were carried out subsequent to titration assays which were carried out using HeLa (A) and SiHa (B) whole cell extracts (Figure 5.7). The titration assays provided an indication of how much protein extract to use for further assays.

In Figure 5.7 lane 1 contained probe only. Lanes 2, 3, 4 and 5 shows the binding of protein to the CRE ^{32}P-oligonucleotide in increasing amounts, with the binding patterns between HeLa and SiHa extracts approximately the same with only minor differences in intensity. The results shown in Figure 5.7 suggest more than one protein complex can form on the hADP-GK CRE element. The protein binding at the element could be either different multimers (i.e. monomeric or dimeric cAMP binding protein (CREB)) or CREB forming complexes with other regulatory transcription factors. Subsequent antibody supershifts and competitor assays

were carried using HeLa whole cell extracts. From the titration assay it was deduced that 20 µg of whole cell extract was sufficient to show the interactions between protein and DNA, and was therefore used in further EMSA reactions.

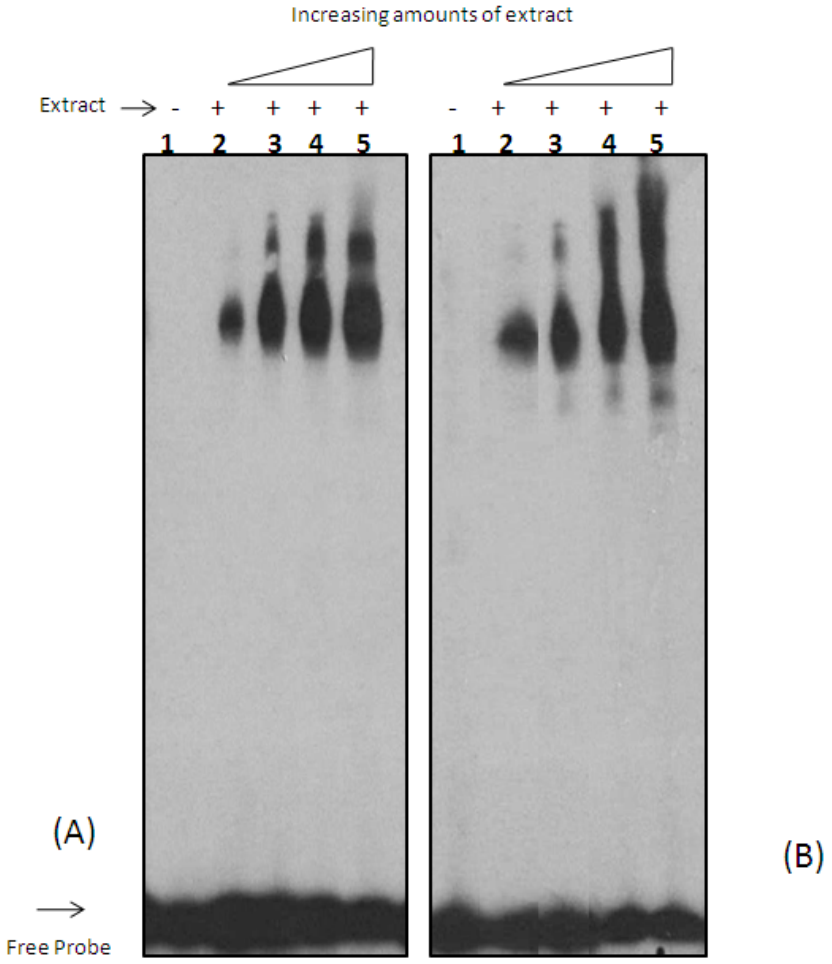

Figure 5.7 EMSA titration assays with CRE ^{32}P-oligonulceotide

Approximately 0.5 ng of CRE ^{32}P-oligonucleotide was added to increasing amounts (0, 10, 20, 40, 80 µg) of HeLa (A) and SiHa (B) whole cell extracts with a total volume of 20 µL in each EMSA reaction. Half of the reaction volume was loaded onto the gel. The gel was transferred and dried onto DE-81 paper. The gel was then exposed to X-ray film for 5 hours at -80°C. The unbound oligonucleotide can be visualised at the bottom of the gel.

Lane one: Free probe only; **Lane two, three, four and five:** HeLa (A) and SiHa (B) whole cell extracts.

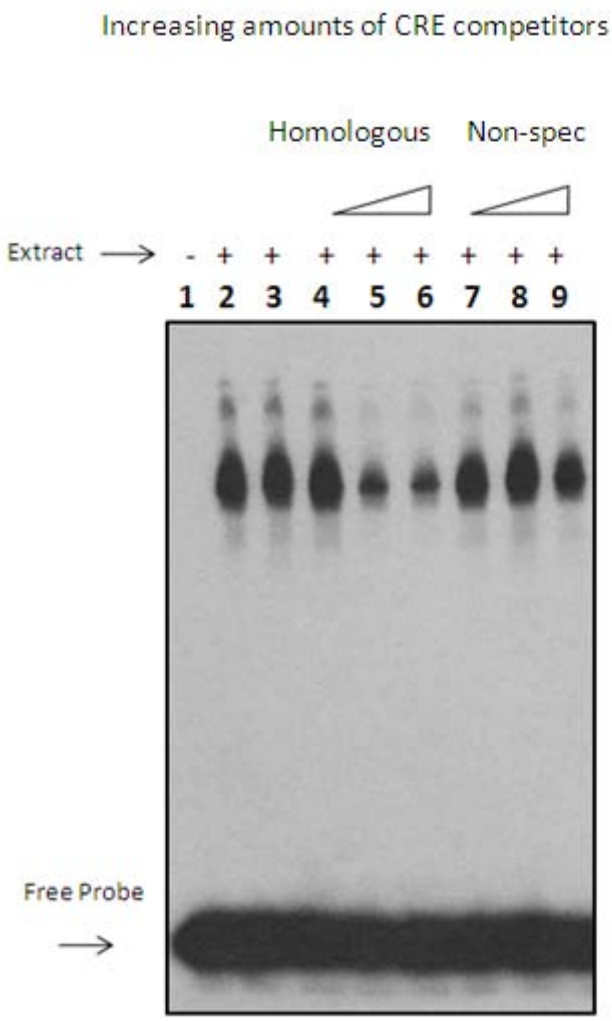

Figure 5.8 EMSA competitor assay using unlabelled CRE oligonucleotides

Twenty micrograms of HeLa extract was added to increasing amounts of unlabelled homologous and non-specific double-stranded competitors (5, 50, 100 ng) along with approximately 0.5 ng of CRE ^{32}P-labelled oligonucleotide with a total volume of 20 µL for each EMSA reaction. Half of the reaction volume was loaded onto the gel. The gel was transferred and dried on DE-81 paper and exposed to X-ray film for 6 hours at -80ºC.

Lane one: Free probe only; **Lane two and three:** Extract only; **Lanes four, five & six:** Extract and homologous CRE competitor; **Lanes seven, eight & nine:** Extract and non-specific competitor

To verify the interactions observed between the potential CRE element and protein from the whole cell extract, competitor assays using the homologous unlabelled CRE oligonucleotide (Table 5.2), and a non-specific (NS) unlabelled oligonucleotide were carried out (Table 5.4). Figure 5.8 presents the results of the CRE competitor assay. Lane 1 contained free probe only and the unbound oligonucleotide can be visualised at the bottom of the gel. Lanes 2 and 3 contained no unlabelled double-stranded competitor and represented the "normal" protein-DNA complexes. Lanes 4, 5 and 6 contained increasing amounts of homologous CRE unlabelled oligonucleotide. Theses lanes showed a marked reduction in band intensity which was to be expected with a homologous oligonucleotide. Lanes 7, 8 and 9 contained increasing amounts of a non-specific unlabelled oligonucleotide. No reduction in band intensity was observed with the non-specific competitor indicating that the protein binding to the CRE element was likely to be specific.

Sp1 elements flank both sides of the CRE element, so to determine if the putative CRE element was real and not an Sp1 element, Sp1 competitor and antibody supershift assays were carried out using the CRE ^{32}P-oligonucleotide and HeLa whole cell extracts. Wildtype (*wt*) and mutant (*mt*) Sp1 double-stranded oligonucleotides were used for the competitor assays. The sequences of these can be found in Table 4.5. Sp1 and Sp3 antibodies were used for the antibody supershift assays. Figure 5.9 and 5.10 present the Sp1 *wt*/*mt* competitor and Sp1/Sp3 antibody supershift assays, respectively.

Lane 1 in Figure 5.9 contained free-probe only and represented a negative control for protein-DNA interactions. The unbound oligonucleotide can be visualised at the bottom of the gel. Lane 2 contained no competitor and represented "normal" protein-DNA interactions. Lanes 3, 4 and 5 contained the Sp1*wt* double-stranded competitor and lanes 6, 7 and 8 contained the Sp1*mt* double-stranded competitor. There was no reduction in band intensity for any of the competitor reactions, indicating that the protein binding to the CRE element was not Sp1 or does not interact with Sp1 protein. These results can be verified by comparing the results illustrated in Figure 5.8 that show definite competitive reactions between the homologous competitor (lanes 3, 4 and 5) and CRE ^{32}P-oligonucleotide.

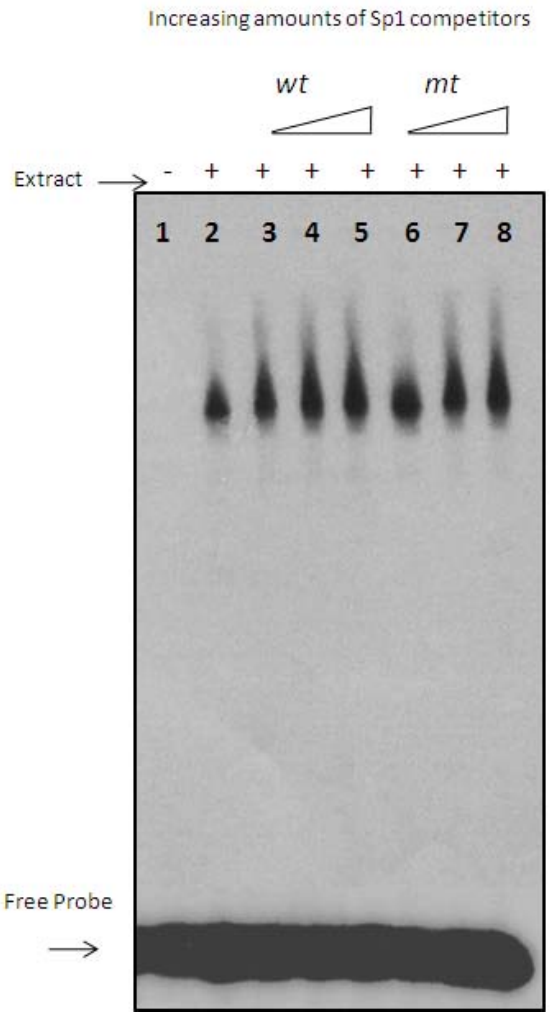

Figure 5.9 EMSA competitor assay using Sp1*wt* and Sp1*mt* unlabelled oligonucleotides

Approximately 0.5 ng of CRE ^{32}P-oligonucleotide was added to 20 µg of HeLa whole cell extract and increasing amounts of Sp1wt/Sp1*mt* unlabelled oligonucleotide (5, 50, 100 ng) with a total volume of 20 µL for each EMSA reaction. Half of the reaction volume was loaded onto the gel. The gel was transferred and dried on DE-81 paper and exposed to X-ray film for 5 hours at -80ºC.

Lane one: Free probe only; **Lane two:** Extract only; **Lanes three, four and five:** Extract and Sp1*wt* competitor; **Lanes six, seven and eight:** Extract and Sp1*mt* competitor.

.

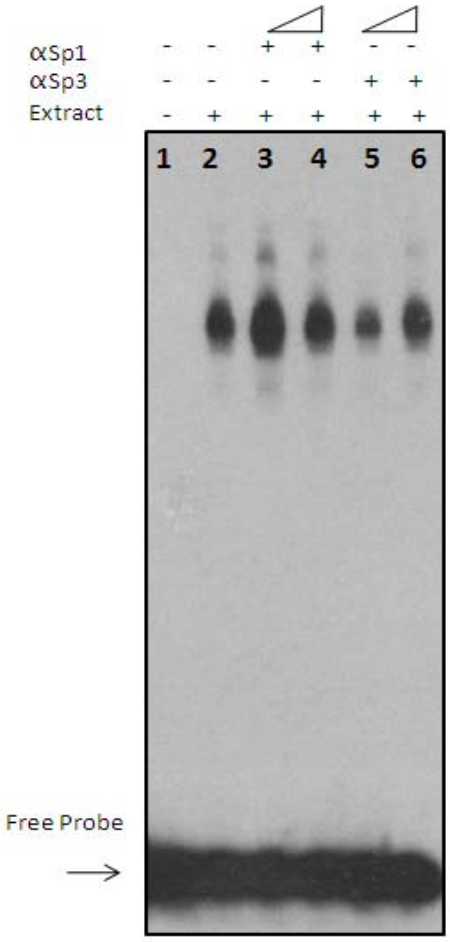

Figure 5.10 Sp1 and Sp3 antibody supershift with CRE ^{32}P-oligonucleotide

Twenty micrograms of HeLa whole cell extract was added to two different amounts of Sp1 and Sp3 antibodies (0.2 µg and 0.4 µg) along with 0.5 ng of CRE ^{32}P-oligonucleotide with a total volume of 25 µL. Ten microlitres of each reaction was loaded on the gel. The gel was transferred and dried onto De-81 paper and exposed on X-ray film for 5 hours at -80ºC.

Lane one: Free probe only; **Lane two:** Extract only; **Lanes three and four:** Extract and Sp1 antibody; **Lanes five and six:** Extract and Sp3 antibody.

Lane 1 in Figure 5.10 contained free-probe only, while lane 2 represented the HeLa whole cell extract control. Lane 3 and 4 contained the Sp1 antibody, and lane 5 and 6 contained the Sp3 antibody. No obvious supershifts occurred for either Sp1 or Sp3 antibodies. There was a small reduction in band intensity in lane 5 which may be a loading error. The results depicted in Figure 5.10 verified that the CRE ^{32}P- oligonucleotide was not likely to contain an Sp1 site.

5.3.4 Specificity factor 1 promoter element (Sp1)

The AliBaba 2 program predicted a number of Sp1 elements within the hADP-GK promoter close to the putative transcription start point (tsp). A small proportion of these Sp1 elements were shown to be conserved in the mouse promoter upon homology comparisons (Section 4.2). One of these conserved Sp1 promoter elements close to the putative tsp was chosen for further analysis using EMSA. To determine if this region contained a putative Sp1 element, antibody supershifts with Sp1 and Sp3 antibodies, and competitor assays using Sp1 *wt* and *mt* double-stranded oligonucleotides were used along with the Sp1 ^{32}P-labelled oligonucleotide. Initially titration assays were performed, as described previously, to determine if protein was able to bind to the Sp1 ^{32}P-oligonucleotide and optimise the amount of whole cell extract required to obtain sufficient interactions between protein and DNA. Figure 5.11 presents the EMSA titration gels for the Sp1 ^{32}P-oligonucleotide using both HeLa (A) and SiHa (B) whole cell extracts.

The EMSA titration assays in Figure 5.11 showed that protein was able to form a complex with the Sp1 ^{32}P-labelled oligonucleotide, when compared to the absence of bands in the extract free reaction visualised in lane 1. The interactions between the whole cell extract and DNA are weak as seen by the intensity in the bands, and it was deduced by the titration assays that 80 µg of protein extract was required to produce bands at sufficient intensities and therefore this amount of extract was used in further EMSA experiments. There were some small differences between band intensities for the SiHa (A) and HeLa (B) but the pattern was very similar and differences likely occurred due to exposure or loading inconsistencies, so HeLa extracts were used for all subsequent assays.

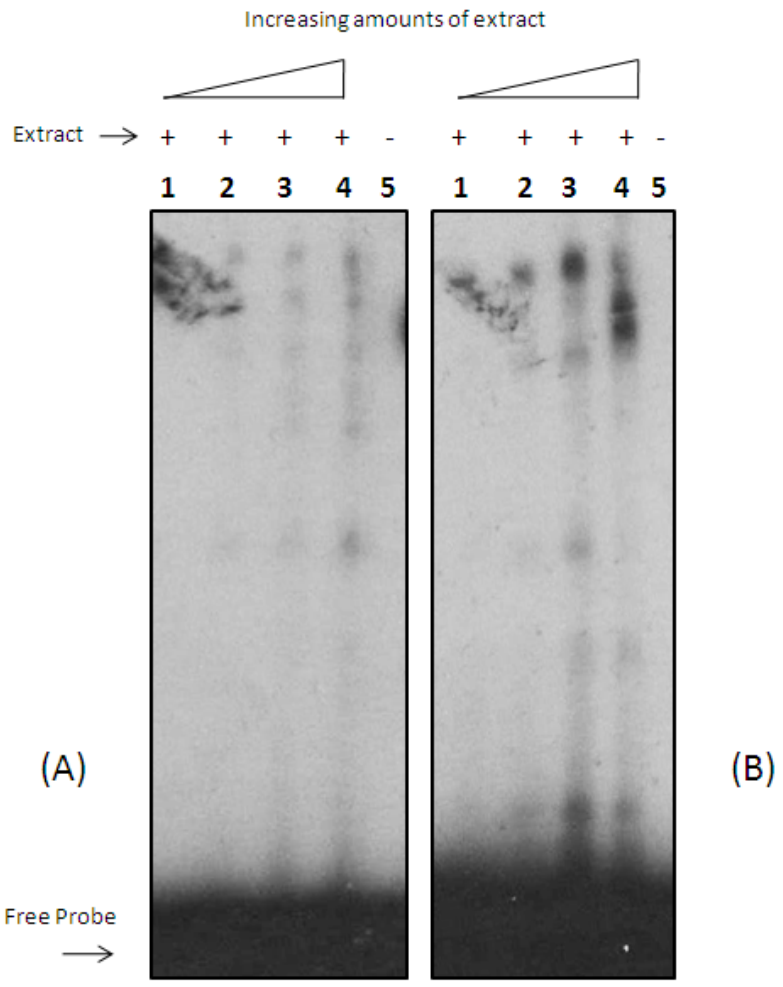

Figure 5.11 EMSA titration assays with Sp1 ^{32}P-oligonucleotide

Approximately 0.5 ng of Sp1 ^{32}P-labelled oligonucleotide was added to increasing amounts (0, 10, 20, 40, 80 µg) of HeLa (A) and SiHa (B) whole cell extracts with a total volume of 20 µL for each EMSA reaction. Half of the reaction volume was loaded onto the gel. The EMSA gel was transferred and dried onto DE-81 paper and exposed on X-ray film for 18 hours at -80ºC. The unbound oligonucleotide can be visualised at the bottom of the gel.

Lane one: Free probe only; **Lanes two, three, four and five:** HeLa (A) and SiHa (B) whole cell extracts

.

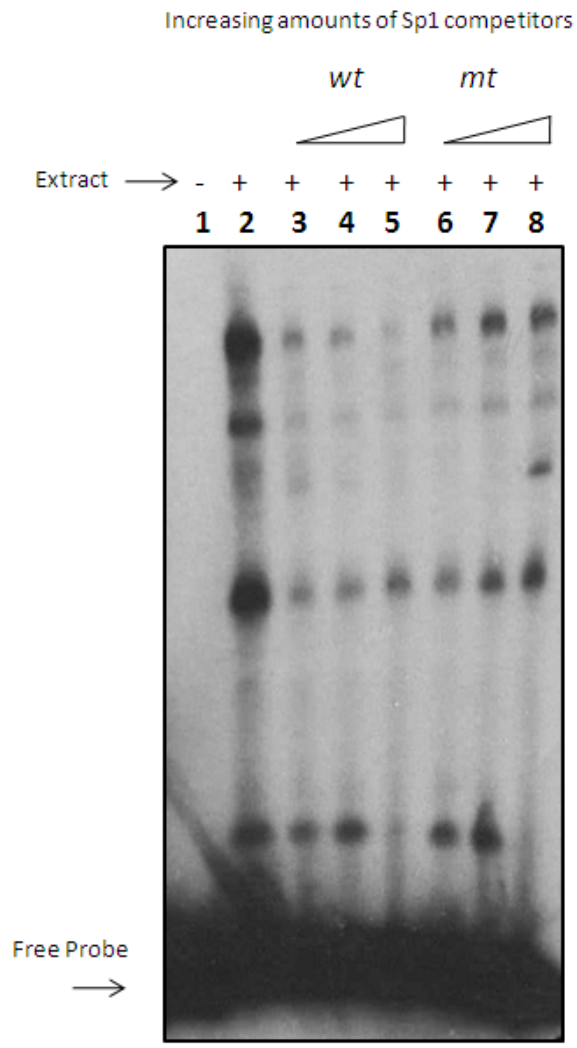

Figure 5.12 Sp1 EMSA competitor assay with Sp1 ^{32}P-oligonucleotide

Approximately 0.5 ng of Sp1 ^{32}P-oligonucleotide was added to 80 µg of HeLa whole cell extract along with increasing amounts of Sp1 wt and mt unlabelled oligonucleotides (5, 50, 100 ng) with a total volume of 20 µL for each EMSA reaction. Half of the reaction volume was loaded onto the gel. The gel was transferred and dried on DE-81 paper and exposed on X-ray film for 18 hours at -80ºC. Unbound oligonucleotide can be seen at the bottom of the EMSA gel.

Lane one: Free probe only; **Lane two:** Extract only; **Lanes three, four and five:** Extract and Sp1*wt* competitor; **Lanes six, seven and eight:** Extract and Sp1*mt* competitor.

EMSA competitor assays using Sp1*wt* (specific) and Sp1*mt* (non-specific) double-stranded oligonucleotides were used to determine if the Sp1 promoter element predicted by the AliBaba2 program bound Sp1 protein. The sequences of the competitors can be found in Table 5.4. Figure 5.12 illustrates the results of the Sp1 competitor EMSA. Lane 1 depicts the extract free reaction while lane 2 represented the control containing no DNA competitors. Lanes 3, 4 and 5 contained increasing amounts of Sp1*wt* double-stranded oligonucleotide and lanes 6, 7 and 8 contained increasing amounts of Sp1*mt* double-stranded oligonucleotide. From the figure it can be observed that the Sp1*wt* competitor competed for the binding of the protein from the whole cell extract, resulting in a reduction in band intensity. There was some decrease in band intensity seen in lanes 6, 7 and 8 but this was not consistent with increasing amounts of competitor across the lanes. This indicated either loading inconsistencies or non-specific interactions.

To further investigate the putative Sp1 element on the hADP-GK promoter, antibody supershifts using Sp1 and Sp3 antibodies were performed. Figure 5.13 presents the results of the antibody supershift with the Sp1 ^{32}P-oligonucleotide and HeLa whole cell extracts. Lane 1 contained probe only, while lane 2 was the extract control. This lane was used for the comparison of antibody reactions seen in lanes 3 to 6. Lanes 3 and 4 contained Sp1 antibody and from the gel a reduction in band intensity can be observed when compared to control lane 2. Lanes 5 and 6 contained Sp3 antibody and a possible supershift occurred as indicated by the presence of lower mobility bands at the top of the gel marked by the arrow. These results indicated that the oligonucleotide could be a potential Sp1 element or proteins binding to this region interact with Sp1 and possibly Sp3 proteins.

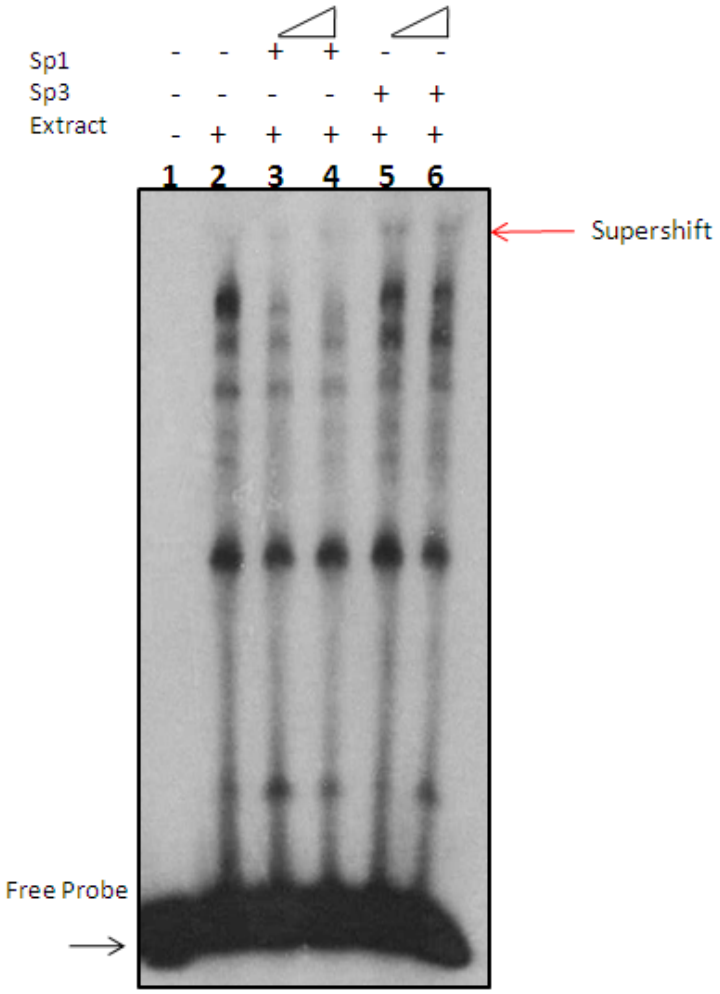

Figure 5.13 Sp1 and Sp3 antibody supershift with Sp1 ^{32}P-oligonucleotide

Approximately 0.5 ng of Sp1 ^{32}P-oligonucleotide was added to 80 µg of HeLa whole cell extract with two different amounts of Sp1 and Sp3 antibody (0.2 µg and 0.4 µg) with a total volume of 25 µL for each EMSA reaction. Ten microlitres of each reaction was loaded onto the gel. The gel was transferred and dried onto De-81 paper and exposed to X-ray film for 18 hours at -80ºC. The unbound oligonucleotide can be visualised at the bottom of the gel.

Lane one: Free probe only; **Lane two:** Extract only; **Lanes three and four:** Extract and Sp1 antibody; **Lanes five and six:** Extract and Sp3 antibody.

5.4 Discussion

The expression of a particular gene is reliant on the activity of its promoter and the specific transcription factors that bind to it. Promoter alignment and transcription factor prediction analyses identified a number of conserved putative transcription factor binding sites on the hADP-GK promoter. The analysis of the hADP-GK promoter is a crucial first step in understanding the function of hADP-GK within the cell and the potential mechanisms of its regulation. In this chapter the promoter activity and DNA binding assays for potential transcription factors were presented.

Three promoter constructs were designed across the length of the putative hADP-GK promoter for cloning, however only one construct 746 bp long was cloned successfully into the pGL3-Basic vector. This construct was used in luciferase assays to investigate promoter activity. The results from the assay showed that the promoter region closest to the ATG start codon within exon 1 was sufficient to show promoter activity through the luciferase reporter gene, compared to the no insert control vector which showed minimal activity. It is possible that this region contains the transcription start point (tsp), however further experiments would be needed to determine where the tsp is located within the hADP-GK promoter region. Deletion studies carried out by Lee and Pedersen showed that when the proximal region of the promoter closest to the tsp start point (-281 to -35) of the hexokinase type II was deleted promoter activity was completely lost. This indicates that the elements closest to the tsp in the proximal region of the promoter, including the cAMP response element (CRE), are significantly important in the activation of the hexokinase type II promoter. It is therefore possible that the same region within the hADP-GK promoter is also significant for promoter activity including the predicted CRE element.

Four potential transcription factor elements that appeared to be conserved between the human and mouse ADP-GK promoter sequences within the proximal region of promoter (746 bp from putative tsp) were investigated further using electrophoretic mobility shift assays (EMSA). These elements included two glucocorticoid receptor elements (GR1, GR2), a Sp1 element and a CRE element. Oligonucleotides were designed to span the element with 6-8 bps either side, labelled with γ^{32}P[ATP] and purified using gel electrophoresis. Scintillation

counting was performed to verify sufficient labelling occurred for each oligonucleotide; however the GR2 oligonucleotide was not sufficiently labelled (Table 4.4) and was omitted from further experiments.

The glucocorticoid receptor (GR1) which was predicted by the AliBaba 2 program was investigated by antibody supershift and competitor assays. Competitor assays using homologous and non-homologous GR, as well as Sp1 wildtype (Sp1*wt*) and mutant (Sp1*mt*) unlabeled oligonucleotides showed that the binding of protein was markedly reduced in the presence of the homologous GR oligonucleotide (Figure 5.4), which is expected, and when Sp1*wt* oligonucleotide was present (Figure 5.5). The non-homologous GR oligonucleotides did not restrict protein-DNA interactions from forming (Figure 5.4). Antibody supershift assays using Sp1, Sp3 and GR antibodies were also carried out. Figure 5.6 showed that upon addition of the Sp1 antibody a supershift occurred in the top band and also a marked reduction in band intensity. A smaller reduction in band intensity occurred with the addition of Sp3 and GR antibodies but these were likely to be due to loading inconsistencies. These results suggest that the transcription factor element is most likely an Sp1 element instead of the predicted GR element. This can be verified by the presence of an Sp1 element predicted by the AliBaba 2 program close to the predicted GR element and also included in the GR1 oligonucleotide sequence (Appendix 3). Unfortunately due to time and financial restraints the GR2 putative promoter element was not investigated further, but future work could involve re-labelling the oligonucleotide with γ^{32}P [ATP] and carrying out competitor and antibody supershift EMSAs.

Antibody supershift and competitor assays were used to investigate the potential CRE element within the hADP-GK promoter. Competitor assays using Sp1*wt*, Sp1*mt* and homologous CRE unlabeled oligonucleotides were performed. The results of the assays showed that a marked reduction in band intensity occurred upon the addition of CRE competitor which is expected (Figure 5.8), but no reduction in band intensity was observed with the addition of either Sp1*wt* or Sp1*mt* (Figure 5.9). To verify that Sp1 doesn't interact at this promoter element, Sp1 and Sp3 antibody supershift assays were performed. Figure 5.10 illustrates that the protein from the whole cell extract does not interact with either Sp1 or Sp3 antibodies due the band intensity remaining the same after the addition of the antibodies to

the reaction. The competitor and antibody supershift assays confirmed that the potential transcription element was not an Sp1 element and did not interact with either Sp1 or Sp3. To confirm that the element is indeed a CRE element, further assays with non-homologous CRE element competitors and a CRE antibody would be required. Due to time and financial constraints these experiments could not be carried out. The hexokinase type II promoter has been shown to contain a CRE element along with an activating transcription factor (ATF1) binding site which enhances the rate of transcription for the hexokinase type II gene. CREB has been shown to be phosphorylated by AMPK with hexokinase type II as a target gene (Thomson *et al*., 2008, Rempel *et al*., 1996). A similar mechanism for hADP-GK promoter activation may exist due to the presence of a putative CRE element and ATF site (Figure 4.1 C) in the hADP-GK promoter.

Finally the potential Sp1 transcription factor element was investigated using Sp1*wt* and Sp1*mt* competitor assays, as well as Sp1/Sp3 antibody supershifts. The results shown in Figure 5.12 illustrated that the Sp1*wt* competitor was able to compete for protein binding which resulted in a gradual decrease in band intensity as the amount of Sp1*wt* competitor increased. A small decrease in band intensity was observed upon the addition of Sp1*mt* to the reaction, but as the bands did not decrease significantly as competitor concentration increased, these results were likely due to non-specific interactions or inconsistencies in loading and did not indicate *bona fide* specific protein-DNA interactions. An antibody supershift EMSA with Sp1 and Sp3 was conducted to verify if the Sp1 oligonucleotide was binding the Sp1 transcription factor. From the results in Figure 5.13 it can be observed that in the presence of Sp1 antibody, the binding of protein to the Sp1 ^{32}P-oligonucleotide was substantially reduced indicating that the protein binding to the oligonucleotide was Sp1 or that the antibody can bind to the protein and restrict its ability to bind to DNA. A possible supershift was also seen in lanes 5 and 6 of Figure 5.13 indicating that Sp3 may also interact at the putative Sp1 element on the hADP-GK promoter. Further experiments would be required to identify the DNA-protein complexes forming at this Sp1 element and to confirm a role of Sp3 in the regulation of hADP-GK promoter.

Hexokinase type II was shown to be controlled by two major signal transduction pathways. The first involves the CREB family members and the other involved the Sp family. The CREB family is important in the activation of hexokinase type II in muscle, while Sp family members were shown to be important in the activation of hexokinase type II within tumours (Mathupala *et al*., 1995, Osawa *et al*., 1996). These two pathways may also be important in the regulation and activation of the hADP-GK gene, as indicated by the presence of a number of potential Sp1 and CRE elements within the proximal promoter region. CREB may bind and activate the hADP-GK promoter upon phosphorylation by AMPK which could be a direct link to cellular [AMP]/[ATP] ratios (Thomson *et al*., 2008). The ratio of [AMP]/ [ATP] is used by AMPK to metabolically sense the energetic requirements of the cell. As ATP concentrations decrease and AMP concentrations increase within the cell AMPK becomes active through phosphorylation. Downstream targets are phosphorylated by AMPK to switch the metabolic pathways from ATP utilisation to ATP conservation (Hardie, 2004, Carling, 2004). The production of AMP by hADP-GK during the phosphorylation of glucose may activate AMPK which in turn may feedback on hADP-GK through the CREB transcription factor and CRE binding element on the hADP-GK promoter.

The experiments outlined in Section 5.3 were carried out with only one set of labelled oligonucleotides and one type of whole cell extract. These experiments would need to be repeated with another set of labelled oligonucleotides and different whole cell extracts to confirm the results obtained.

Chapter 6: ADP-GK protein isolation and cellular localisation

6.1 Introduction

The expression of human ADP-dependent glucokinase (hADP-GK) has been shown experimentally by immunoblotting to be widespread across most human tissues, including cancerous tissue. Relatively large amounts of protein were found to be expressed in cytoplasmic fractions, with smaller amounts found in membrane factions (Hole, 2009). Prior to this research, it was hypothesised that the hADP-GK enzyme was likely to be a cytosolic protein due to its ability to phosphorylate glucose, as the first step in glycolysis. Other glycolytic enzymes, such as hexokinase type I and II, however, are known to interact with the mitochondrial membrane for the provision of substrate ATP and thereby ensure maximal amounts of glucose phosphorylation upon entry of glucose into the cell. To further understand the metabolic role of ADP-GK, the cellular localisation of the protein was investigated. This chapter describes the use of western blotting to visualise hADP-GK protein expression present in cellular extracts, and immunofluorescence to determine the intracellular localisation of ADP-GK within cultured cell lines.

6.2 Western blot analysis for hADP-GK protein expression

Immunoblot analysis is a technique that allows the detection of specific proteins from cell extract or tissue homogenate. Gel electrophoresis was used to separate denatured proteins which were subsequently transferred to a positively charged nylon membrane. Western blot analysis was used to specifically target hADP-GK in the cell lines used in previous experiments outlined in Chapters 3, 4 and 5 to verify the expression of hADP-GK at the protein level.

SiHa, HeLa and HCT116 cell lines were grown in culture until 80% confluence was achieved. Protein extraction was carried out using the protocol outlined in Section 2.2.14. Protein concentration was determined using a Bradford assay and/or absorbance at 280 nm using the Nanodrop spectrophotometer (Nanodrop Technologies) (Section 2.2.15.). A mouse monoclonal anti-ADP-GK antibody was used to detect hADP-GK protein at a dilution of

1/500. Rabbit secondary anti-mouse IgG antibody conjugated to horseradish peroxidase was used at a dilution of 1/4000.

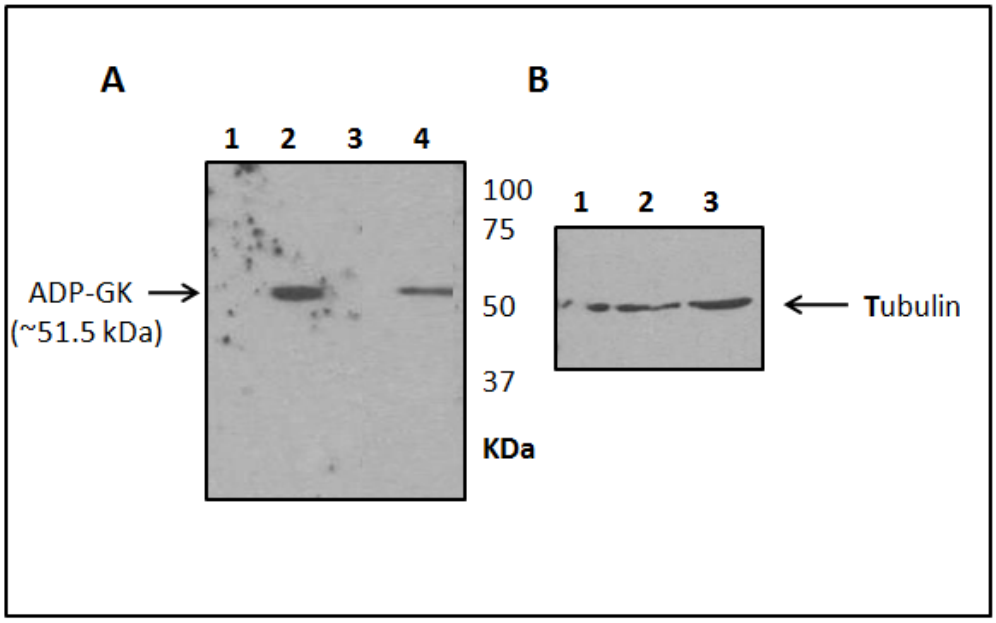

Figure 6.1 Immunoblot of human ADP-GK from cultured cell lines

An Immunoblot was carried out on whole cell extracts obtained from SiHa, HeLa and HCT116 cultured cell lines. Protein was separated by gel electrophoresis and then transferred to a positively charged nylon membrane for 1.5 hours at 450 mA. A 1/500 dilution of monoclonal mouse anti-ADP-GK antibody (A) and a 1/4000 dilution of monoclonal anti-tubulin antibody (B) was applied overnight at 4 ºC, and then a 1:4000 dilution of secondary rabbit anti-mouse antibody was applied at room temperature for 45 minutes. The membrane was exposed to X-ray film for approximately 5 minutes, and then developed in a dark room with an X-ray developer.

Lane one (A, B): Fifty microlitres of HeLa whole cell extract (10 µg/µL); **Lane two (A, B):** Fifty microlitres of SiHa whole cell extract (12 µg/µL); **Lane three (A, B):** Fifty microlitres of HCT116 whole cell extract (10 µg/uL); **Lane four (A):** Ten microlitres of lung extract (5 µg/µl).

Figure 6.1 illustrates the presence of ADP-GK in SiHa cells (Lane 2) but not the HeLa or HCT116 cultured cell lines (Lanes 1 and 3 respectively). On previous occasions a very faint band was visualised for hADP-GK in the HCT116 whole cell extract. This cell line has been altered to over-express hADP-GK protein and is a stable cell line; therefore loss of the plasmid within these cells should not occur. It is possible that the over-expression of ADP-GK has been dampened in the HCT116 cells by a silencing mechanism, and therefore over expression of hADP-GK is no longer observed. Lane 4 contains pig lung extract which has been shown to express ADP-GK (Hole, 2009), this lane was used as positive control. Tubulin was used as a loading control, from Figure 6.1 it can be seen that tubulin is expressed in all three cell lines; however in Lane 1 the presence of an air bubble has caused a defect in the band visualised.

6.3 Immunofluorescence for cellular localisation of ADP-GK in cultured cell lines

Immunofluorescence microscopy is a technique that uses fluorescently-labelled antibodies to reveal the localisation of proteins of interest. Fluorescence microscopy has the highest resolution of 0.2 µM, which is the wavelength of visible light, and is adequate to identify proteins of interest in relation to known marker proteins. Further identification of protein localisation would require alternative microscopy techniques such as confocal microscopy which would be able to visualise the protein on plane which would provide a clearer, more defined image.

Cultured SiHa and HCT116 (ADP-GK over-expressing) cell lines were used to determine the cellular localisation of hADP-GK. The cultured cells were grown overnight in chamber-welled slides in media, and then fixed to the slide using 4% paraformaldehyde and permeabilised with 0.1% SDS. Incubation overnight at 4 ºC with the primary antibodies followed the fixation of the cells. Monoclonal mouse primary ADP-GK antibody was used to detect hADP-GK at a dilution of 1/500. Fluorescein (FITC)-conjugated AffiniPure goat anti-mouse IgG secondary antibody was used at a dilution of 1/500. Mounting solution containing DAPI was applied over the slide and spread evenly using a coverslip. Detection of the hADP-GK protein within the cell was carried out using the Olympus Fluorescence

microscopy from the Manawatu Microscopy and Imaging Centre located at Massey University. Figure 6.2 illustrates the staining of ADP-GK and DAPI in both SiHa and HCT116 cell lines.

. .

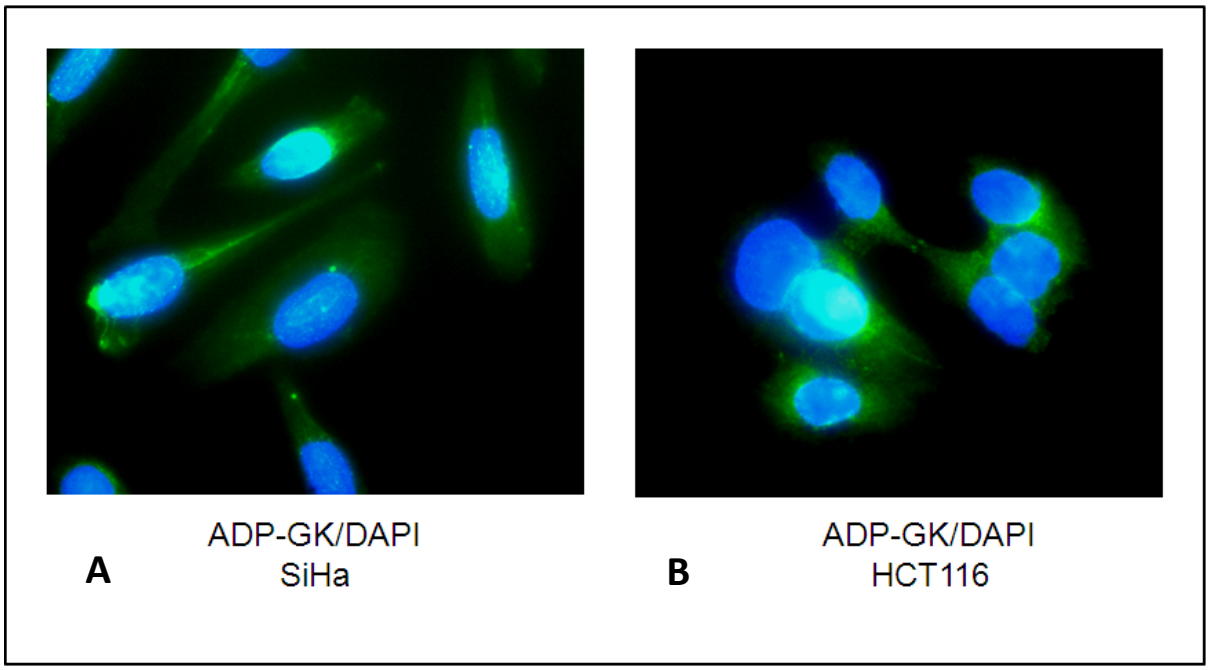

Figure 6.2 Immunofluorescence analysis of hADP-GK expression in SiHa and HCT116 cell lines

SiHa (A) and HCT116 (B) cultured cell lines were stained with mouse anti-ADP-GK primary antibody and FITC anti-mouse secondary antibody. Mounting solution containing DAPI was used to stain the cell nuclei. Cells were detected using fluorescence microscopy at 100x magnification. DAPI is stained in blue (nucleus), and hADP-GK is stained in green and can be seen to be cytosolic.

SiHa and HCT116 cell lines were tested with only primary antibody for background fluorescence. Both cell lines were stained with mouse anti-ADP-GK primary antibody (Figure 6.3) at a dilution of 1/500 and visualised under the fluorescence microscope. The results in Figure 6.3 show background only. A dilution titration was carried out to optimise dilution of antibodies for sufficient staining of each cell line.

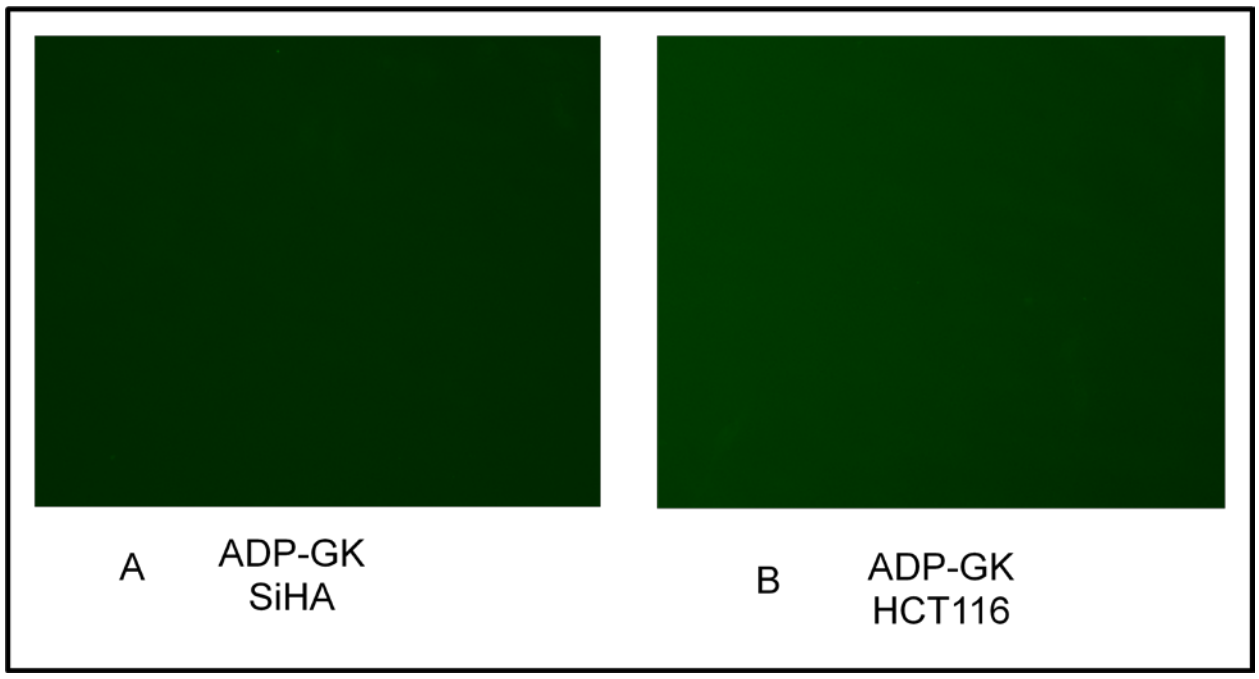

Figure 6.3 Primary antibody immunofluorescence controls in SiHa and HCT116

SiHa (A) and HCT116 (B) cultured cells were stained with mouse anti-ADP-GK primary antibody only. Cells were detected using immunofluorescence microscopy at 40x magnification.

To accurately identify the cellular localisation of hADP-GK in cultured cell lines, three known cellular marker proteins were used for double staining with the monoclonal mouse ADP-GK antibody. A polyclonal Prohibitin antibody raised in rabbit was used to identify the mitochondrial membrane. Prohibitin is also known to be transported to the nucleus, so some nuclei staining were often seen. A polyclonal pan-Cadherin antibody raised in rabbit was used to detect the plasma membrane of the cultured cells. Finally, a polyclonal Protein Disulfide Isomerase (PDI) antibody raised in rabbit was used to detect the endoplasmic reticulum. All primary antibodies were used at a dilution of 1/500. Rhodamine (TRITC)-conjugated AffiniPure goat anti-rabbit IgG secondary antibody was used at a dilution of 1/200. Figures 6.4 and 6.5 illustrate the immunofluorescence results for SiHa and HCT116 cells respectively.

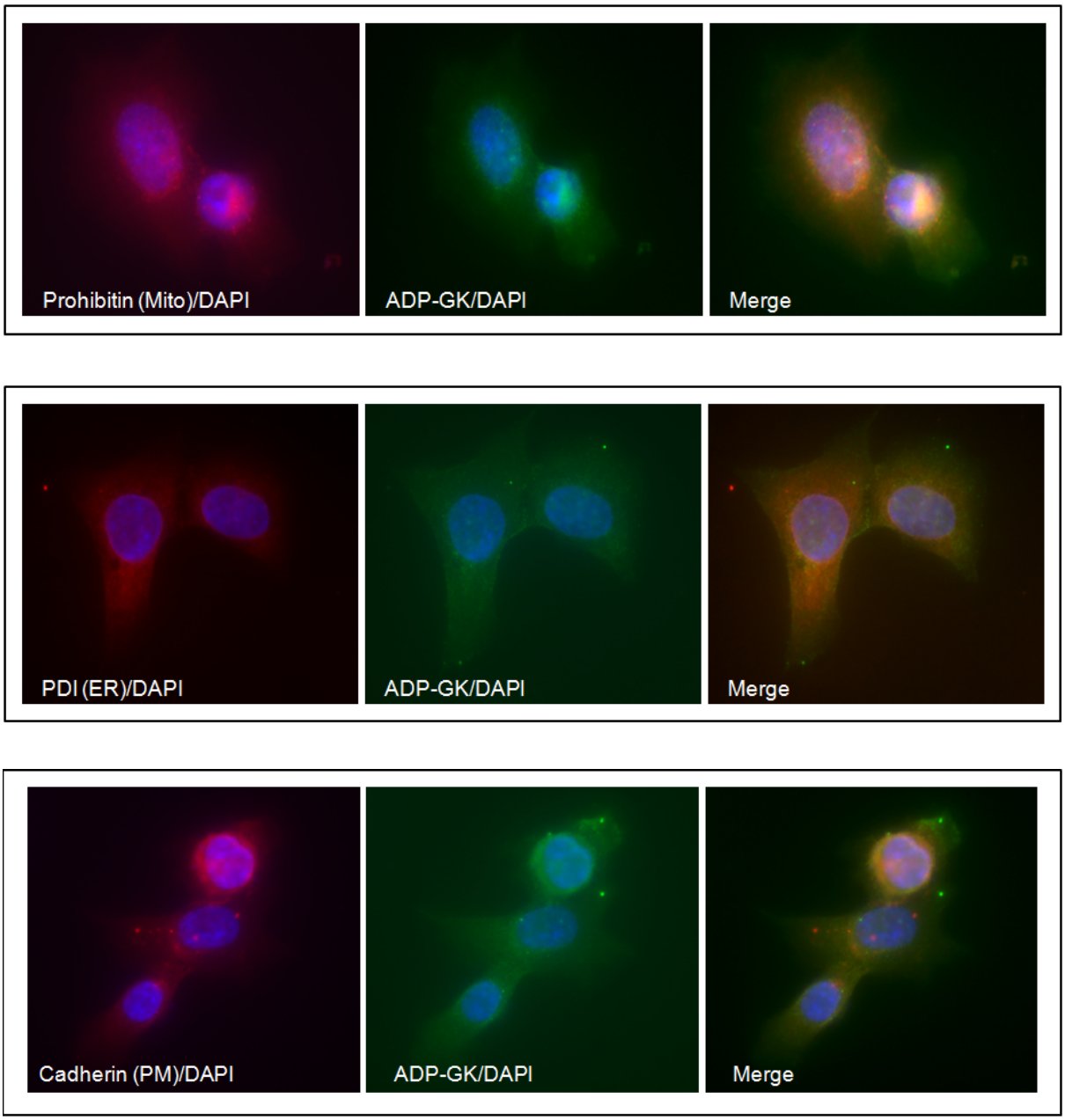

Figure 6.4 Immunofluorescence analysis of hADP-GK by co-expression in SiHa cells

SiHa cultured cells were analysed by immunofluorescence microscopy with oil immersion at 100x magnification. Monoclonal mouse anti-ADP-GK antibody and Prohibitin, PDI and Cadherin antibodies were used to detect hADP-GK and marker proteins respectively. Mounting solution containing DAPI was used to stain the cell nuclei. DAPI is shown in blue, marker proteins are shown in red, and hADP-GK is shown in green.

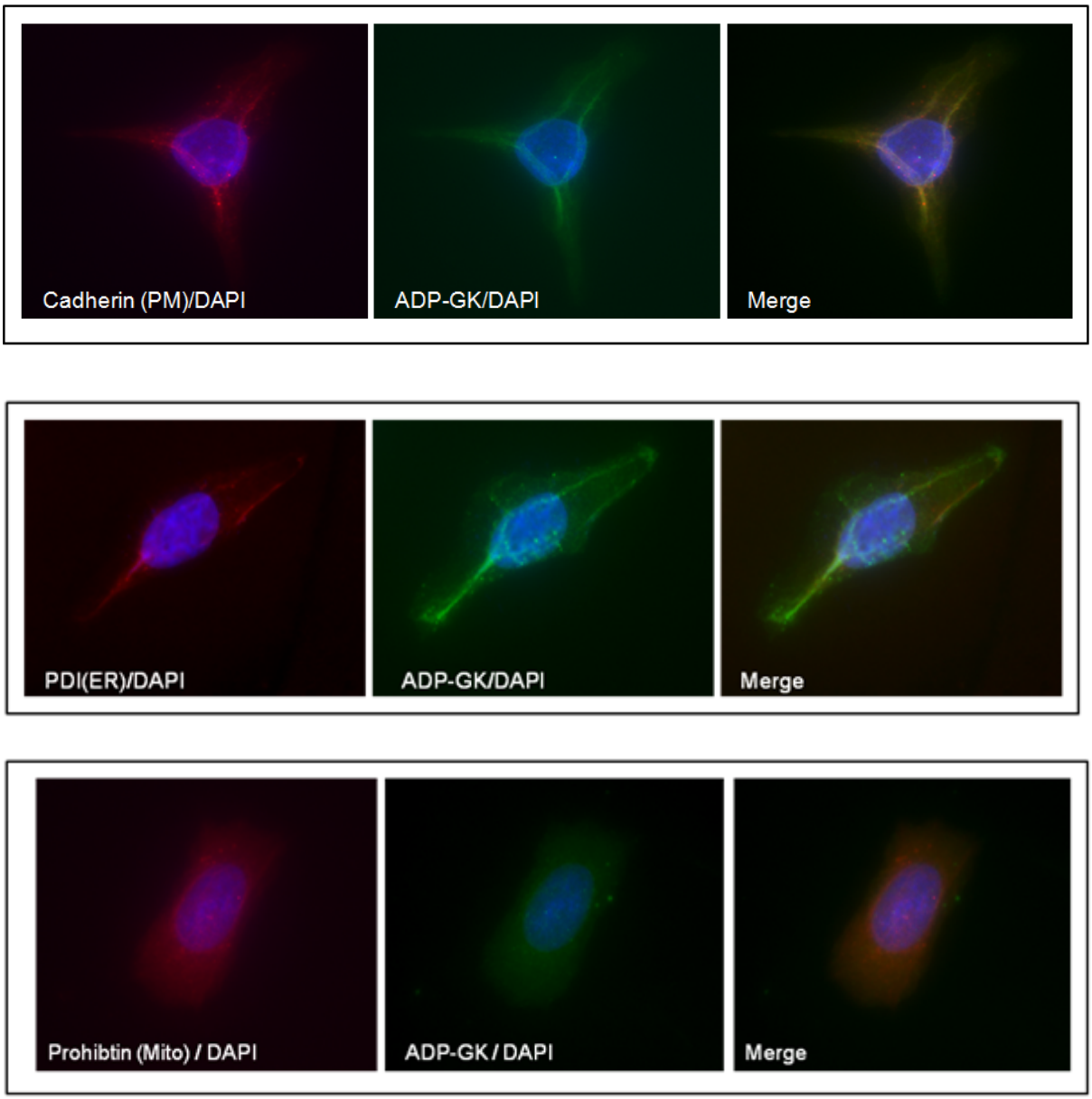

Figure 6.5 Immunofluorescence analysis of hADP-GK by co-expression in HCT116 cells

HCT116 cultured cells over-expressing hADP-GK were analysed using mouse anti-ADP-GK antibody, and marker proteins Prohibtin, PDI and Cadherin antibodies. Mounting solution containing DAPI was used to stain the cell nuclei. Magnification of microscopy was carried out at 100x with oil emersion. DAPI is shown in blue, marker proteins are shown in red, and hADP-GK is shown in green.

The results of the immunofluorescence analysis for hADP-GK expression in SiHa cell lines (Figure 6.4) suggest that hADP-GK is likely to be cytosolic with possible interactions with the mitochondria and plasma membrane, due to the co-localisation visualised. No interaction between the nucleus or endoplasmic reticulum (ER) and hADP-GK was observed. Figure 6.5 verifies the results observed in Figure 6.4 that hADP-GK is localised in the cytosol with possible interactions occurring between the mitochondrial and plasma membranes. Once again no interaction was observed between the ER or nucleus and hADP-GK.

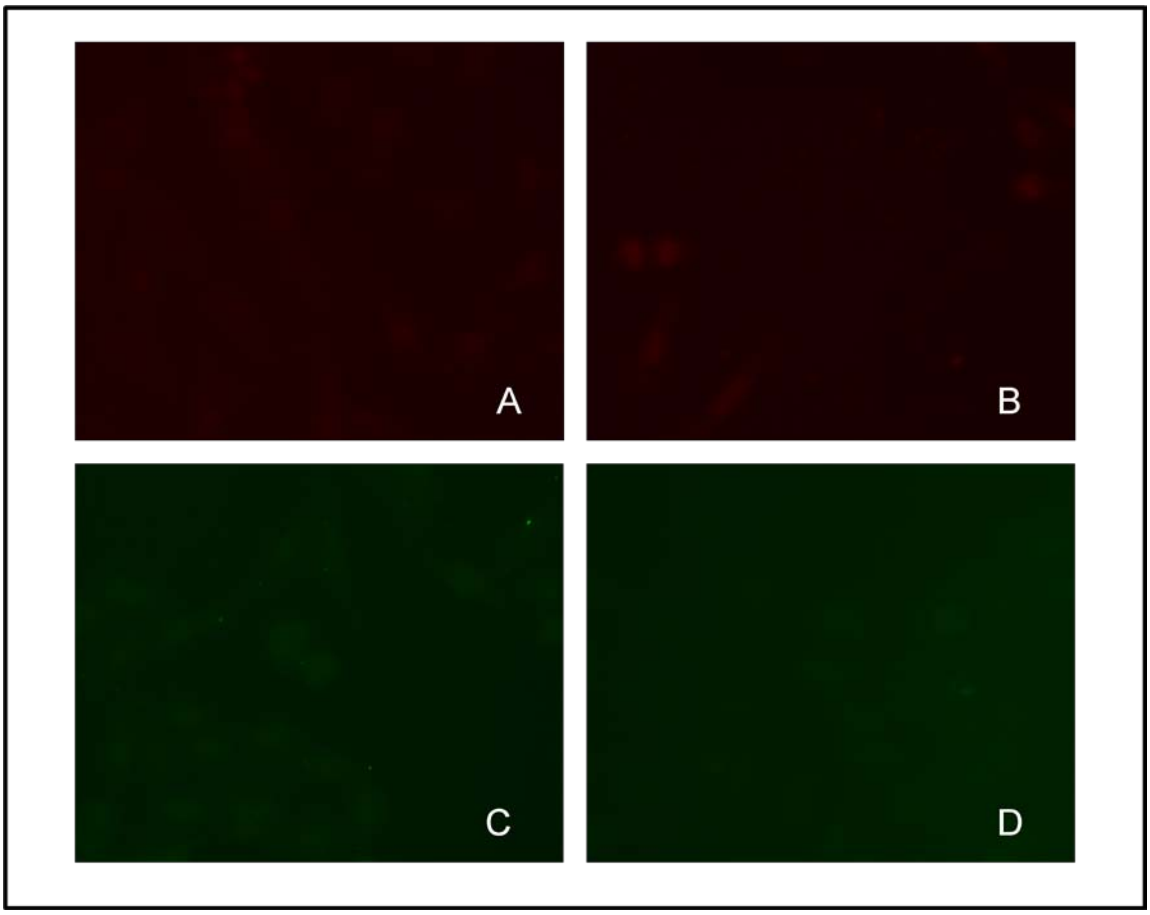

Figure 6.6 Secondary antibody immunofluorescence controls in SiHa and HeLa cells

SiHa (A & C) and HCT116 (B & D) were stained with secondary antibody only. Rhodamine (TRITC)-conjugated goat anti-rabbit secondary antibody is illustrated in A and B. Fluorescein (FITC)-conjugated goat anti-mouse secondary antibody is illustrated in C and D. Cells were detected using immunofluorescence microscopy at 40x magnification.

To ensure that the staining for hADP-GK protein and marker proteins in SiHa and HCT116 cell lines was specific, negative controls containing only secondary antibody were analysed for fluorescence. SiHa and HCT116 cell lines were stained with either FITC or TRITC secondary antibodies at a dilution of 1/200. Figure 6.6 illustrates the results of the negative control, which shows background staining only.

6.4 Discussion

Prior to this study the localisation of hADP-GK within the cell was hypothesised to be cytosolic because the cellular function of hADP-GK suggested was to be the phosphorylation of glucose upon its entry into the cell (Ronimus and Morgan, 2004). To investigate the intracellular localisation of hADP-GK, immunofluorescence microscopy was used with marker proteins. hADP-GK protein was shown to be expressed in SiHa cells through western blot analysis, therefore verifying the staining of protein visualised in Figure 6.3 and 6.2 (A). hADP-GK protein in HCT116 cells was visualised only weakly by western blot after prolonged exposure to X-ray film. This may have been caused by the loss of expression of the hADP-GK in the initially stably-expressed cell lines. Staining of hADP-GK within the HCT116 cells was still observed during immunofluorescence microscopy (Figure 6.4); however this was carried out prior to the western blot analysis.

The absence of protein visualised in HeLa extracts is interesting because the hADP-GK promoter was shown to be highly active within HeLa cells, which were used for transient transfections (Chapter 5). It would be expected that protein would be present in cells that have an active promoter, but it is possible that ADP-GK is not stable in HeLa cells. Previous studies (Hole, 2009) show different levels of expression in different tissues, different developmental stages, and normal and cancerous tissue.

The immunofluorescence microscopy experiments verified that hADP-GK is likely to be localised in the cytosol. hADP-GK appeared to co-localise with Prohibitin and pan-Cadherin, the markers for the mitochondria and plasma membranes respectively. Hexokinase type I and II have been shown to associate with a voltage dependent anion channel (VDAC), called Porin, within the mitochondrial outer membrane. This association facilitates the phosphorylation of glucose by providing a rapid supply of ATP from the process of oxidative phosphorylation within the mitochondria (Arora and Pedersen, 1988). The association with the mitochondrial membrane occurs due to a characteristic N-terminal sequence which allows selective targeting to the membrane (Tsai and Wilson, 1997). It is possible that hADP-GK also exhibits a similar sequence that may target it to the mitochondrial membrane to facilitate the phosphorylation of glucose. A similar mechanism may exist with the plasma membrane and GLUT transporters, as glucose is transported into the cell through the GLUT protein it may become quickly phosphorylated by hADP-GK to maintain a glucose gradient to ensure more is transported into the cell. Associations between hexokinase type II and GLUT 4 transporters in muscle have been shown experimentally (Jones and Dohm, 1997). No associations with the endoplasmic reticulum were observed from the fluorescence microscopy experiments.

To verify the localisation of hADP-GK in cultured cell lines, confocal microscopy would be required. Confocal microscopy is a technique that is able to provide a sharper focus for clearer images. Because of financial restrictions, confocal microscopy was not carried out. Due to the possibility of tissue specific expression a wide range of cell types should also be investigated to determine if localisation remains cytosolic or if co-localisation with cellular membranes is more predominant in specific cell types or environment states.

Chapter 7: Summary and Future Work

7.1 Overview

In the late 20th century three German scientists elucidated the pathway of glycolysis and the enzymes that catalysed each of the ten steps. For the last 70 years this catabolic process has been rigorously studied. The first step in glycolysis was shown to be catalysed by a group of enzymes called hexokinases which used ATP to phosphorylate glucose to glucose-6-phosphate. In 2004 Ronimus and Morgan characterised a novel enzyme in mice that used ADP to phosphorylate glucose, and it was hypothesised that this enzyme may have an important metabolic role in the conservation of ATP during disease states under hypoxia and low glucose conditions.

In this project the effect of glucose concentration on the expression of hADP-GK at the transcriptional level was investigated. It was hypothesised that at low glucose concentrations the expression of hADP-GK would be up-regulated, however this was not observed and instead a strict normal tissue culture glucose concentration was required for the expression of hADP-GK. To investigate the regulation of hADP-GK further, the hADP-GK promoter was cloned into a reporter gene vector and assessed for activity. Putative transcription factors were identified and investigated using electrophoretic mobility shift assays (EMSA). Finally the localisation of cellular hADP-GK protein was identified by immunofluorescence microscopy.

7.2 Summary of results

The amplification of the hADP-GK coding region by real-time qualitative PCR (qPCR) was carried out successfully. The results showed that hADP-GK expression at the transcriptional level was down-regulated compared to a constitutively expressed house-keeping gene (β-actin), when glucose concentrations were altered from normal tissue culture levels at approximately 4.6 mM. No significant differences were observed between 48, 24 and 6 hour time periods except for the 24 hour 10 mM sample which was down-regulated marginally more than the 6 and 48 hour 10 mM samples. No logical explanation can be concluded from this result, and it is likely that this result was due to intra- and inter-assay differences.

Analysis of the hADP-GK promoter using GCG version 11.1 program and the Basic Local Alignment Search Tool (BLAST) showed there was significant conservation between the human and mouse promoters, with only marginal similarity between the hexokinase type II and ADP-GK promoter in humans. The AliBaba 2 software program was used to identify putative transcription factor binding sites on the hADP-GK promoter. The transcription factor elements which appeared to be conserved between the mouse and human promoter region were chosen for further analysis. Cloning of the promoter region posed some difficulty, and only a 746 bp region of the hADP-GK promoter was successfully cloned into the pGL3-Basic reporter gene. A further attempt to clone the rest of the promoter region was unsuccessful and due to time constraints, the 746 bp construct was used for further analysis only. Luciferase assays revealed that the 746 bp promoter construct was sufficient to drive the luciferase gene when compared to a pGL3-Basic control vector. These results indicated that this region was likely to contain the putative transcription start point (tsp).

Four putative transcription factor binding sites within the 746 bp promoter construct were investigated using EMSA techniques. The transcription factor binding sites included a cAMP response element (CRE), two glucocorticoid receptor elements (GR1 and GR2) and a specificity protein 1 (Sp1) site. The results from the competitor and antibody supershift assays showed a potential CRE element and two Sp1 elements within the 746 bp core promoter region. The GR2 element unfortunately did not label sufficiently and was not used in EMSA experiments. The GR1 element was shown to be an Sp1 site instead.

Finally western blot analysis and immunofluorescence microscopy was used to investigate the expression and localisation of hADP-GK protein within cultured cell lines. hADP-GK protein was shown to be expressed in the SiHa cell line, and a faint band was seen in the HCT116 cell line. No protein was visible in the HeLa cell lines and therefore was not used in the immunofluorescence work. Immunofluorescence microscopy indicated that the hADP-GK protein was cytosolic within the cell, with a possible association with either the plasma or mitochondrial membrane.

7.3 Future direction

Human ADP-dependent glucokinase is a relatively novel enzyme and its role in metabolism and in cellular function as a whole has yet to be elucidated. It therefore opens up a wide area for future research.

The real-time qPCR experiments revealed that hADP-GK expression at the transcriptional level was not up-regulated when glucose concentrations were decreased below 5 mM. Instead the results indicated that glucose concentrations around 4.6 mM were required for the expression of hADP-GK at the transcription level, as the expression of hADP-GK was down-regulated when the concentration of glucose was altered *in vitro*. This experiment was carried out in one cell line only; it would therefore be advantageous to repeat the experiment in other cell lines, as well as investigating tissue specific expression across a wide range of tissues, as expression of hADP-GK at the protein level has already been shown to be wide-spread across mammalian tissues (Hole, 2009). Mouse tissue would be useful for this approach with a direct comparison between RNA and protein in all accessible tissues. This would provide evidence that hADP-GK may be activated in certain tissues under specific environmental conditions only, which might be predicted by the fact that a sufficient cellular mechanism for glucose phosphorylation already exists. Therefore a comparison between the expression of hexokinase type II and ADP-GK at the transcriptional level across a range of tissues would be advantageous in understanding if the two enzymes work alongside each other or in different environments. The results of this type of analysis may suggest a possible role for ADP-GK in metabolism.

The understanding of the mechanisms that regulate hADP-GK gene expression should provide insights into the cellular function of the hADP-GK enzyme and the pathway within which it is involved. The EMSA experiments carried out in this project opened up an extensive area for future work on the regulation of hADP-GK at the transcription level. The AliBaba 2 programme identified a number of putative transcription factor binding sites which could be investigated using EMSA techniques, as well as repeating the EMSA work already carried out in different extracts and with freshly labelled probes. To determine if the putative CRE site within the hADP-GK promoter does bind CREB, antibody supershift assays with

CREB antibody would need to be carried out. Re-labelling of the GR2 oligonucleotide should also be carried out to identify if the hADP-GK promoter is regulated by hormones. Co-expression vectors with Sp1, CREB (+/- phosphorylation) and GR could be used with luciferase assays to analyse the effect on the promoter activity to elucidate the regulation of hADP-GK promoter. The luciferase assays showed that the hADP-GK promoter is active *in vitro* compared to a negative control. Further work could investigate which region of the core promoter is vital for activity using a deletion series to identify a minimal promoter region. DNase I footprinting or point mutations could also be used to identify important transcription factor elements and the minimal promoter region. The binding of putative transcription factors could also be investigated *in vivo* using chromatin immunoprecipitation (ChIP) methods (Brenowitz *et al*., 2003, Weinmann and Farnham, 2002).

Recombinant mouse ADP-GK (rmADP-GK) was shown to phosphorylate glucose to glucose-6-phosphate *in vitro*. It was therefore proposed that hADP-GK protein would be localised to the cytosol *in vivo* like most glycolytic enzymes. Immunofluorescence microscopy showed hADP-GK to be cytosolic with possible associations with the mitochondrial and plasma membranes. To accurately determine the localisation of hADP-GK *in vivo* confocal microscopy should be examined which would provide a sharper focus and clearer images compared to immunofluorescence microscopy. Hexokinase type I and II have been shown to association with the mitochondrial membrane, therefore a comparison with hexokinase type II localisation with confocal microscopy would show if the two enzymes co-localise within the cell.

No previous work has investigated the regulation of hADP-GK at the protein level. Experiments investigating post-translational modifications of hADP-GK protein would provide insight into the regulation of the enzyme after translation. The crystallisation of soluble of protein has proven to be difficult; however structural analysis would provide information about the structure of the enzyme and an understanding of how the enzyme is specific for its substrate ADP. Soluble protein extracts could also be used for activity assays and investigated for post-translation modifications, such as phosphorylation.

Overall this project provided initial information on the regulation and localisation of hADP-GK *in vivo* and opened the door for further research into elucidating the role of hADP-GK in metabolism and cellular function.

References

ANDERKA, O., BOYKEN, J., ASCHENBACH, U., BATZER, A., BOSCHEINEN, O. & SCHMOLL, D. (2008) Biophysical characterization of the interaction between hepatic glucokinase and its regulatory protein : Impact pf physiological and pharmacological effectors *The Journal of Biological Chemistry,* 283**,** 31333-31340.

ARORA, K. K. & PEDERSEN, P. L. (1988) Functional significance of mitochondrial bound hexokinase in tumor cell metabolism. Evidence for preferential phosphorylation of glucose by intramitochondrially generated ATP *The Journal of Biological Chemistry,* 263**,** 17422-17428.

BENSAAD, K., TSURUTA, A., SELAK, M. A., VIDAL, M. N., NAKANO, K., BARTRONS, R., GOTTLIEB, E. & VOUSDEN, K. H. (2006) TIGAR, a p53-inducible regulator of glycolysis and apoptosis. *Cell,* 126**,** 107-120.

BRENOWITZ, M., SENEAR, D. F., SHEA, M. A. & ACKERS, G. K. (2003) Quantitative DNase footprint titration: A method for studying protein-DNA interactions. *Methods in Enzymology* 130**,** 132-181.

BUSTIN, S. A., BENES, V., GARSON, J. A., HELLEMANS, J., HUGGETT, J., KUBISTA, M., MUELLER, R., NOLAN, T., PFAFFL, M. W., SHIPLEY, G. L., VANDESOMPELE, J. & WITTWER, C. T. (2009) The MIQE guidelines: Minimum information for publication of quantitative real-time PCR experiments. *Clinical Chemistry,* 55**,** 611-622.

CARDENAS, M. L., CORNISH-BOWDEN, A. & URETA, T. (1998) Evolution and regulatory role of the hexokinases. *Biochimica et Biophysica Acta* 1401**,** 242-264.

CARLING, D. (2004) The AMP-activated protein kinase cascade--a unifying system for energy control. *Trends in Biochemical Sciences,* 29**,** 18-24.

CARO, J. (2001) Hypoxia regulation of gene transcription. *High Altitude Medicine and Biology* 2**,** 145-154.

CHEN, C., PORE, N., BEHROOZ, A., ISMAIL-BEIGI, F., MAITY, A. (2001) Regulation of glut1 mRNA by Hypoxia-inducible Factor-1: Interaction between H-ras and hypoxia *The Journal of Biological Chemistry,* 276**,** 9519-9525.

COSIO, F. G. & WILMER, W. A. (1995) Effects of high glucose concentration on c-fos: Role of protein kinase C. *Kidney International. Supplement.,* 51**,** S12-17.

DANG, C. V. & SEMENZA, G. L. (1999) Oncogenic alterations of metabolism. *Trends in Biochemical Sciences* 24**,** 68-72.

DE LA IGLESIA, N., MUKHTAR, M., SEOANE, J., GUINOVART, J. J. & AGIUS, L. (2000) The role of the regulatory protein of glucokinase in the glucose sensory mechanism of the hepatocyte. *The Journal of Biological Chemistry,* 275**,** 10597-10603.

FLURKEY, W. H. (2010) Yield of ATP molecules per glucose molecule. *Chemical Education,* 87.

GARBE, N. (2002) AliBaba2: Context specific identification of transcription factor binding sites *In Silico Biology,* 2**,** S1-15.

GATENBY, R. A. & GILLIES, R. J. (2004) Why do cancers have high aerobic glycolysis? *Nature Reviews. Cancer.,* 4**,** 891-899.

GENZEL, Y., KONIG, S. & REICHL, U. (2004) Amino acid analysis in mammalian cell culture media containing serum and high glucose concentrations by anion exchange chromatography and integrated pulsed amperometric detection *Analytical Biochemistry* 335**,** 119-125.

GESCHWIND, J. H., KO, Y. K., TORBENSON, M. S., MAGEE, C. & PEDERSEN, P. L. (2002) Novel therapy for liver cancer: Direct intra-arterial indection of a potent inhibitor of ATP production. *Cancer Research,* 62**,** 3909-3913.

GIATROMANOLAKI, A., HARRIS, A.L. (2001) Tumor hypoxia , hypoxia signalling pathways and hypoxia inducible factor expression in human cancer *Anticancer Research,* 21**,** 4317-4324.

GUPPY, M. (2002) The hypoxic core: A possible answer to the cancer paradox. *Biochemical and Biophysical Research Communications,* 299**,** 676-680.

GUPPY, M., BRUNNER, S., BUCHANAN, M. (2005) Metabolic depression: A response of cancer cells to hypoxia? *Comparative Biochemistry and Physiology, Part B,* 140**,** 233-239.

HARDIE, D. G. (2004) The AMP-activated protein kinase pathway-- new players upstream and downstream. *Journal of Cell Science* 117**,** 5479-5487.

HERMAN, M. A. & KAHN, B. B. (2006) Glucose transport and sensing in the maintenance of glucose homeostasis and metabolic harmony. *The Journal of Clinical Investigation,* 116**,** 1767-75.

HOFFMANN, M. (Ed.) (2009) *Application Manual*, Roche Diagnostics.

HOLE, R. (2009) Mammalian ADP-dependent glucokinase. *Institute of Molecular Bioscience.* Palmerston North, Massey University.

JONES, J. P. & DOHM, G. L. (1997) Regulation of glucose transporter GLUT-4 and hexokinase II gene transcription by insulin and epinephrine. *The American Journal of Physiology* 273**,** E682-687.

KAMURA, T., SATO, S., IWAI, K., CZYZYK-KRZESKA, M., CONAWAY, R. C. & CONAWAY, J. W. (2000) Activation of HIF1alpha ubiquitination by a reconstituted von Hippel-Lindau (VHL) tumor suppressor complex *Proceedings of the National Academy of Sciences of the United States of America* 97**,** 10430-10435.

KATZEN, H. M. & SCHIMKE, R. T. (1965) Multiple forms of hexokinase in the rat: Tissue distribution, age dependency and properties. *Proceedings of the National Academy of Sciences,* 54**,** 1218-1225.

KENGEN, S. W. M., TUININGA, J.E., DE BOK, F.A.M., STAMS, A.J.M., DE VOS, W.M. (1995) Purification and characterization of a novel ADP-dependent glucokinase from the hyperthermophilic archaeon *Pyrococcus furiosus The Journal of Biological Chemistry,* 270**,** 30453-30457.

KIM, J. W. & DANG, C. V. (2006) Cancer's molecular sweet tooth and the Warburg effect. *Cancer Research,* 66**,** 8927-8930.

LADEROUTE, K. R., AMIN, K., CALAOAGAN, J.M., KNAPP, M., LE, T., ORDUNA, J., FORETZ, M., VIOLLET, B. (2006) 5' AMP-activated protein kinase (AMPK) is induced by low-oxygen and glucose deprivation conditions found in solid-tumour microenvironments. *Molecular and Cellular Biology,* 26**,** 5336-5347.

LAEMMLI, U. K. (1970) Cleavage of structural proteins during the assembly of the head of bacteriophage T4 *Nature* 227**,** 680-685.

LEE, K. A., ROTH, R.A., LAPRES, J.J. (2007) Hypoxia, drug therapy and toxicity. *Pharmacology and Therapeutics,* 113**,** 229-246.

LEE, M. G. & PEDERSEN, P. L. (2003) Glucose Metabolism in Cancer *The Journal ofr Biological Chemistry,* 278**,** 41047-41058.

LU, X., GRUIA-GRAY, J., COPELAND, N. G., GILBERT, D. J., JENKINS, N. A., LONDOS, C. & KIMMEL, A. R. (2001) The murine perilipin gene: The lipid droplet-assoicated perilipins derive from tissue-specific, mRNA splice variants and define a gene family of ancient origin. *Mammalian Genome,* 12**,** 741-749.

MAGAN, N. (2009) Protein interactions at the human topoisomerase II alpha promoter. *Institute of Molecular Biosciences* Palmerston North, Massey University.

MAGNUSON, M. A. & SHELTON, K. D. (1989) An alternative promoter in the glucokinase gene is active in the pancreatic beta cell. *The Journal of Biological Chemistry,* 264**,** 15939-15942.

MANDRIOTA, S. J., TURNER, K. J., DAVIES, D. R., MURRAY, P. G., MORGAN, N. V., SOWTER, H. M., WYKOFF, C. C., MAHER, E. R., HARRIS, A. L., RATCLIFFE, P. J. & MAXWELL, P. H. (2002) HIF activation identifies early lesions in VHL kidneys: Evidence for site-specific tumor suppressor function in the nephron. *Cancer Cell,* 1**,** 459-468.

MANKOFF, D. A. & BELLON, J. R. (2001) Positron-emission tomographic imaging of cancer: Glucose metabolism and beyond *Siminars in Radiation Oncology,* 11**,** 16-27.

MARIN-HERNANDEZ, A., RODRIGUEZ-ENRIQUEZ, S., VITAL-GONZALEZ, P. A., FLORES-RODRIGUEZ, F. L., MACIAS-SILVA, M., SOSA-GARROCHO, M. & MORENO-SANCHEZ, R. (2006) Determining

and understanding the control of glycolysis in fast-growth tumor cells: Flux control by an over-expressed but strongly product-inhibited hexokinase. *FEBS Journal* 273**,** 1975-1988.

MATHUPALA, S. P., REMPEL, A. & PEDERSEN, P. L. (1995) Glucose catabolism in cancer. *The Journal of Biological Chemistry,* 270**,** 16918-16925.

MATHUPALA, S. P., REMPEL, A. & PEDERSEN, P. L. (1997) Aberrant glycolytic metabolism of cancer cells: A remarkable coordination of genetic, transcriptional, post-translational and mutational events that lead to a critical role for type II hexokinase. *Journal of Bioenergetics and Biomembranes* 29**,** 339-343.

MATSCHINSKY, F. M., MAGNUSON, M. A., ZELENT, D., JETTON, T. L., DOLIBA, N., HAN, Y., TAUB, R. & GRIMSBY, J. (2006) The network of glucokinase-expressing cells in glucose homeostasis and the potential of glucokinase activators for diabetes therapy *Diabetes,* 55**,** 1-12.

MAXWELL, P. H., PUGH, C. W. & RATCLIFFE, P. J. (2001) Activation of the HIF pathway in cancer. *Current Opinion in Genetics and Development* 11**,** 293-299.

NAKASHIMA, R. A., PAGGI, M. G. & PEDERSEN, P. L. (1988) Purification and characterization of a bindable form of mitochondrial bound hexokinase from the highly glycolytic AS-30D rat hepatoma cell line. *Cancer Research,* 48**,** 913-919.

ORNSTIEN, L. (1964) Disc electrophoresis. I. Background and theory. *Annals of the New York Academy of Sciences* 121**,** 321-349.

OSAWA, H., ROBEY, R. B., PRINTZ, R. L. & GRANNER, D. K. (1996) Identification and characterization of basal and cyclic AMP response elements in the promoter of the rat hexokinase type II gene *The Journal of Biological Chemistry,* 271**,** 17296-17303.

OVSTEBO, R., HAUG, K. B., LANDE, K. & KIEFULF, P. (2003) PCR-based calibration curves for studies of quantitative gene expression in human monocytes: Development and evaluation *Clinical Chemistry,* 49**,** 425-432.

PASTEUR, L. (1861) *Comp. Rend. Acad. Sci*,52, 1260-1264.

PASTORINO, J. G., SHULGA, N. & HOEK, J. B. (2002) Mitochondrial binding of hexokinase II inhibits Bax-induced cytochrome c release and apoptosis *The Journal of Biological Chemistry,* 277**,** 7610-7618.

PEDERSEN, P. L. (2007) Warburg, me and Hexokinase 2: Multiple discoveries of key molecular events underlying one of cancers' most common phenotypes, the "Warburg Effect", i.e., elevated glycolysis in the presence of oxygen. *J Bioenerg Biomembr,* 39**,** 211-222.

PEDERSEN, P. L., MATHUPALA, S. P., REMPEL, A., GESCHWIND, J. F. & KO, Y. H. (2002) Mitochondrial bound type II hexokinase: A key player in the growth and survival of many cancers and an ideal prospect for therapeutic intervention. *Biochimica et Biophysica Acta* 1555**,** 14-20.

PRELLER, A. & WILSON, J. E. (1992) Localization of the type III isozyme of hexokinase at the nuclear periphery. *Archives of Biochemistry and Biophysics,* 294**,** 482-492.

RATTAN, R., GIRI, S., SINGH, A. K. & SINGH, I. (2005) 5-Aminoimidazole-4-carboxamide-1-beta-D-ribofuranoside inhibits cancer cell proliferation *in vitro* and *in vivo* via AMP-activated protein kinase *The Journal of Biological Chemistry,* 280**,** 39582-39593.

REMPEL, A., MATHUPALA, S. P. & PEDERSEN, P. L. (1996) Glucose catabolism in cancer cells: Regulation of the type II hexokinase promoter by glucose and cyclis AMP. *FEBS Letters,* 385**,** 233-237.

RONIMUS, R. S. & MORGAN, H. W. (2004) Cloning and biochemical characterization of a novel mouse ADP-dependent glucokinase *Biochemical and Biophysical Research Communications,* 315**,** 652-658.

SEAGROVES, G. L., RYAN, T. N., LU, H., WOUTERS, B. G., KNAPP, M., THIBAULT, P., LADEROUTE, K. & JOHNSON, R. S. (2001) Transcription factor HIF-1 is a necessary mediator of the Pastuer effect in mammalian cells *Molecular and Cellular Biology,* 21**,** 3436-3444.

SEBASTIAN, S., EDASSERY, S. & WILSON, J. E. (2001) The human gene for the type III isozyme of hexokinase: Structure, basal promoter, and evolution. *Archives of Biochemistry and Biophysics,* 395**,** 113-120.

SEMENZA, G. L. (2007) HIF-1 mediates the Warburg effect in clear cell renal carcinoma *J Bioenerg Biomembr,* 39**,** 231-234.

SEMENZA, G. L., ROTH, P. H., FANG, H. & WANG, G. L. (1994) Transcriptional regulation of genes encoding glycolytic enzymes by hypoxia-inducible factor 1. *The Journal of Biological Chemistry,* 269**,** 23757-23763.

THOMSON, D. M., HERWAY, S. T., FILLMORE, N., KIM, H., BROWN, J. R. & WINDER, W. W. (2008) AMP-activated protein kinase phosphorylates transcription factors of the CREB family. *J Appl Physiol,* 104**,** 429-438.

TSAI, H. J. & WILSON, J. E. (1995) Functional organization of mammalian hexokinases: Characterization of chimeric hexokinases constructed from the N- and C-terminal domains of the rat type I and type II isozymes *Archives of Biochemistry and Biophysics,* 316**,** 206-214.

TSAI, H. J. & WILSON, J. E. (1996) Functional organization of mammalian hexokinases: Both N- and C-terminal halves of the rat type II isozyme possess catalytic sites. *Archives of Biochemistry and Biophysics,* 329**,** 17-23.

TSAI, H. J. & WILSON, J. E. (1997) Functional organization of mammalian hexokinases: Characterization of the rat type III isozyme and its chimeric forms, constructed N- and C-

terminal halves of the type I and type II isozymes *Archives of Biochemistry and Biophysics,* 338**,** 183-192.

VAN SCHAFTINGEN, E., DETHEUX, M. & VEIGA DA CUNHA, M. (1994) Short-term control of glucokinase activity: Role of a regulatory protein. *Federation of American Societies for Experimental Biology,* 8**,** 414-419.

VISSERS, M. C. M., GUNNINGHAM, S. P., MORRISON, M. J., DACHS, G. U. & CURRIE, M. J. (2007) Modulation of hypoxia-inducible factor-1 alpha in cultured primary cells by intracellular ascorbate *Free Radical Biology and Medicine,* 42**,** 765-772.

WALLACE, D. C. (2005) Mitochondria and cancer: Warburg addressed. *Cold Spring Harbor Symposia on Quantitative Biology* 70**,** 363-374.

WARBURG, O. (1956) On the origin of cancer cells. *Science,* 123.

WEINMANN, A. S. & FARNHAM, P. J. (2002) Identification of unknown target genes of human transcription factors using chromatin immunoprecipitation. *Methods,* 26**,** 37-47.

WILFINGER, W. W., MACKEY, K. & CHOMCZYNSKI, P. (1997) Effect of pH and ionic strength on the spectrophotometric assessment of nucleic acid purity. *BioTechniques* 22**,** 478-481.

WILSON, J. E. (1997) An introduction to the isoenzymes of mammalian hexokinase types I-III. *Biochemical Society Transactions* 25**,** 103-107.

WILSON, J. E. (2003) Isozymes of mammalian hexokinase: Structure, subcellular localization and metabolic function. *The Journal of Experimental Biology,* 206**,** 2049-2057.

WON, J. W., RHEE, B. D. & KO, K. S. (2009) Glucose-responsive gene expression system for gene therapy. *Advanced Drug Delivery Reviews* 61**,** 633-640.

ZELENT, D., GOLSON, M. L., KOEBERLEIN, B., QUINTENS, R., VAN LOMMEL, L., BUETTGER, C., WEIK-COLLINS, H., TAUB, R., GRIMSBY, J., SCHUIT, F., KAESTNER, K. H. & MATSCHINSKY, F. M. (2006) A glucose sensor role for glucokinase in anterior pituitary cells. *Diabetes* 55**,** 1923-1929.

ZU, X. L. & GUPPY, M. (2004) Cancer metabolism: Facts, fantasy and fiction. *Biochemical and Biophysical Research Communications* 313**,** 459-465.

Appendix 1: Vectors

1.1 pGEM®T Vector

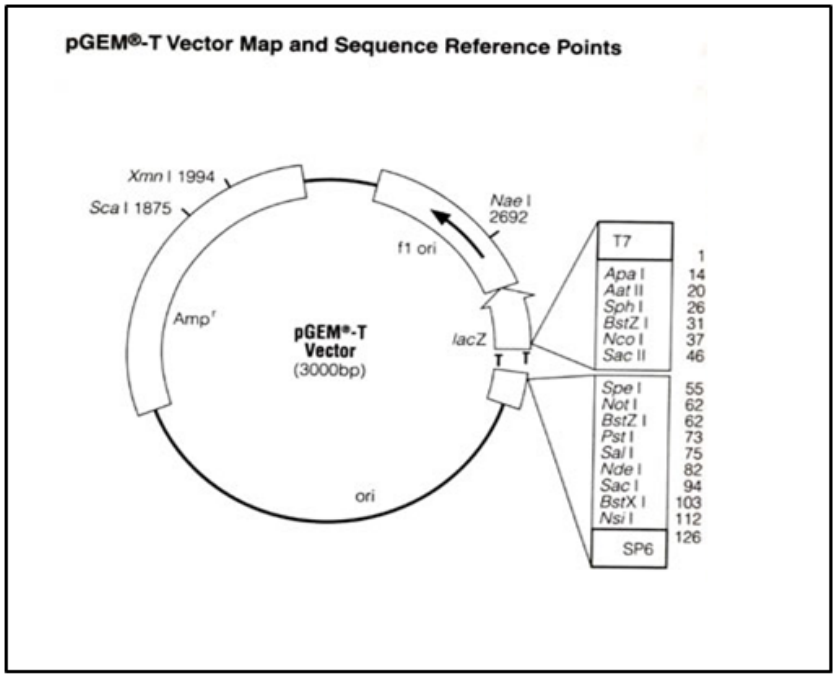

1.2 pGL3-Basic Vector

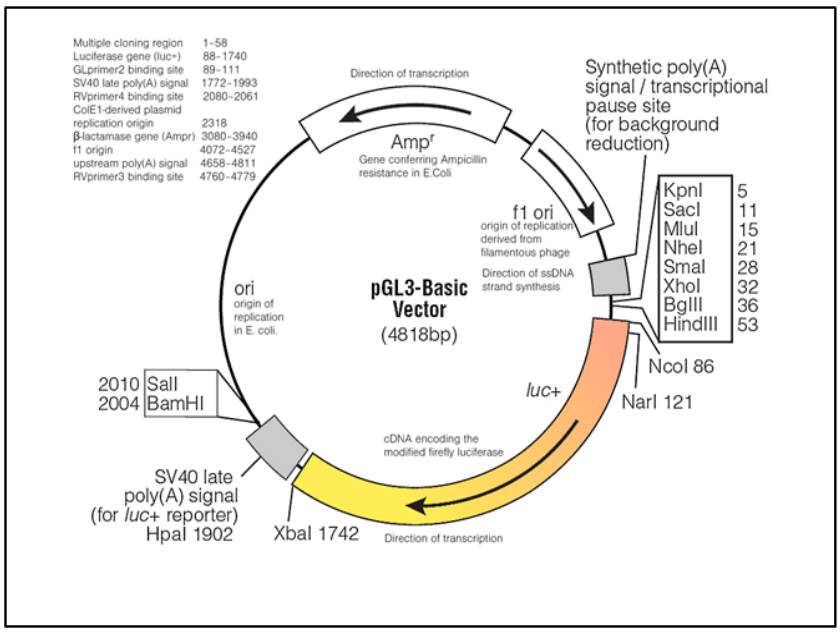

Appendix 2: Sequencing chromatograms

2.1 644 forward sequencing chromatogram

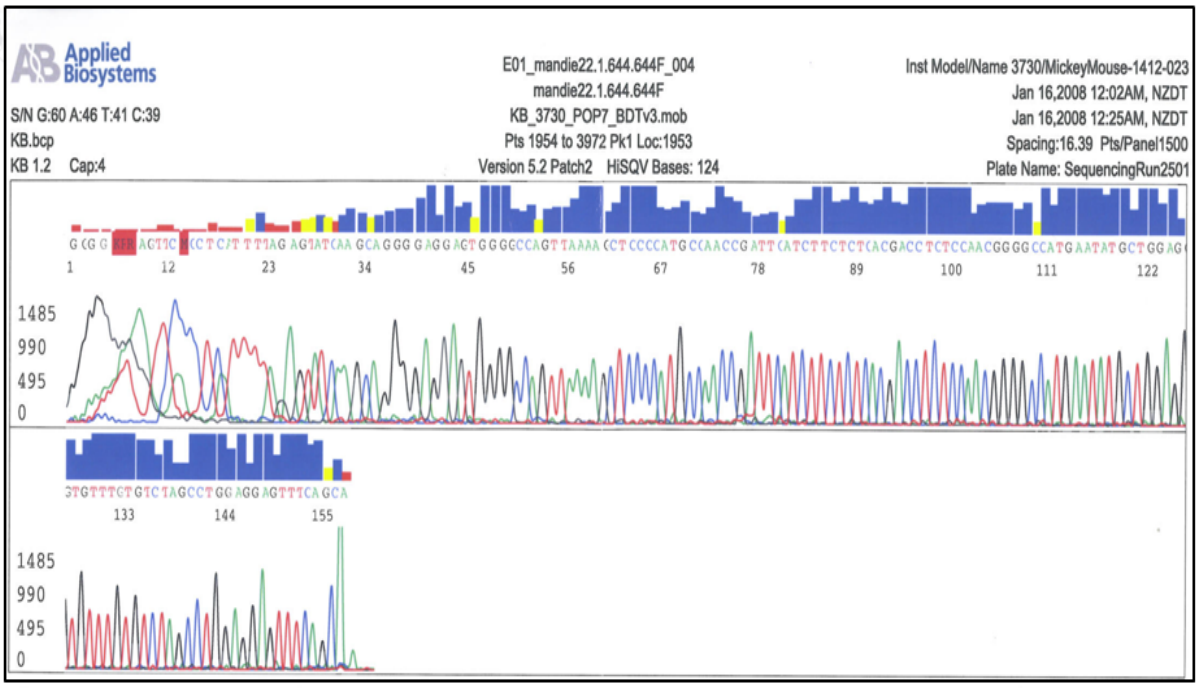

2.2 F1 RV3 sequencing chromatogram

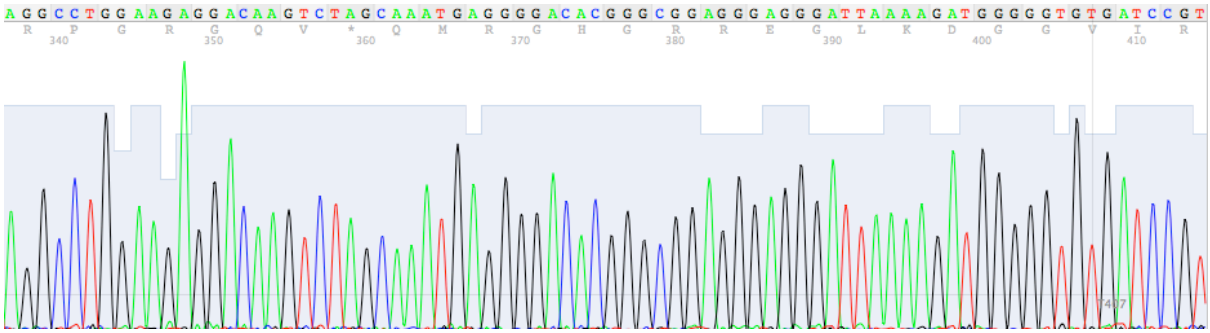

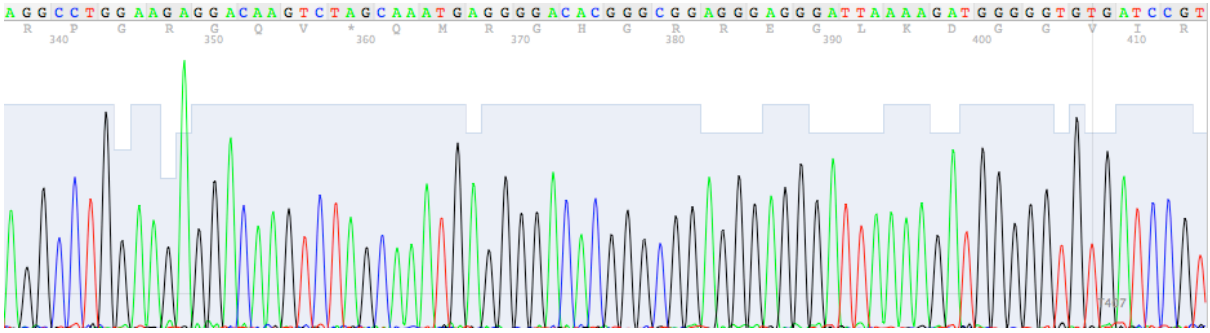

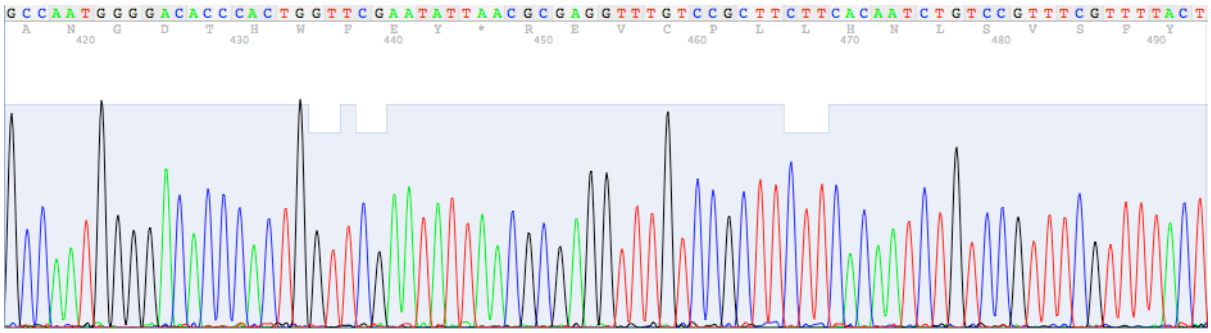

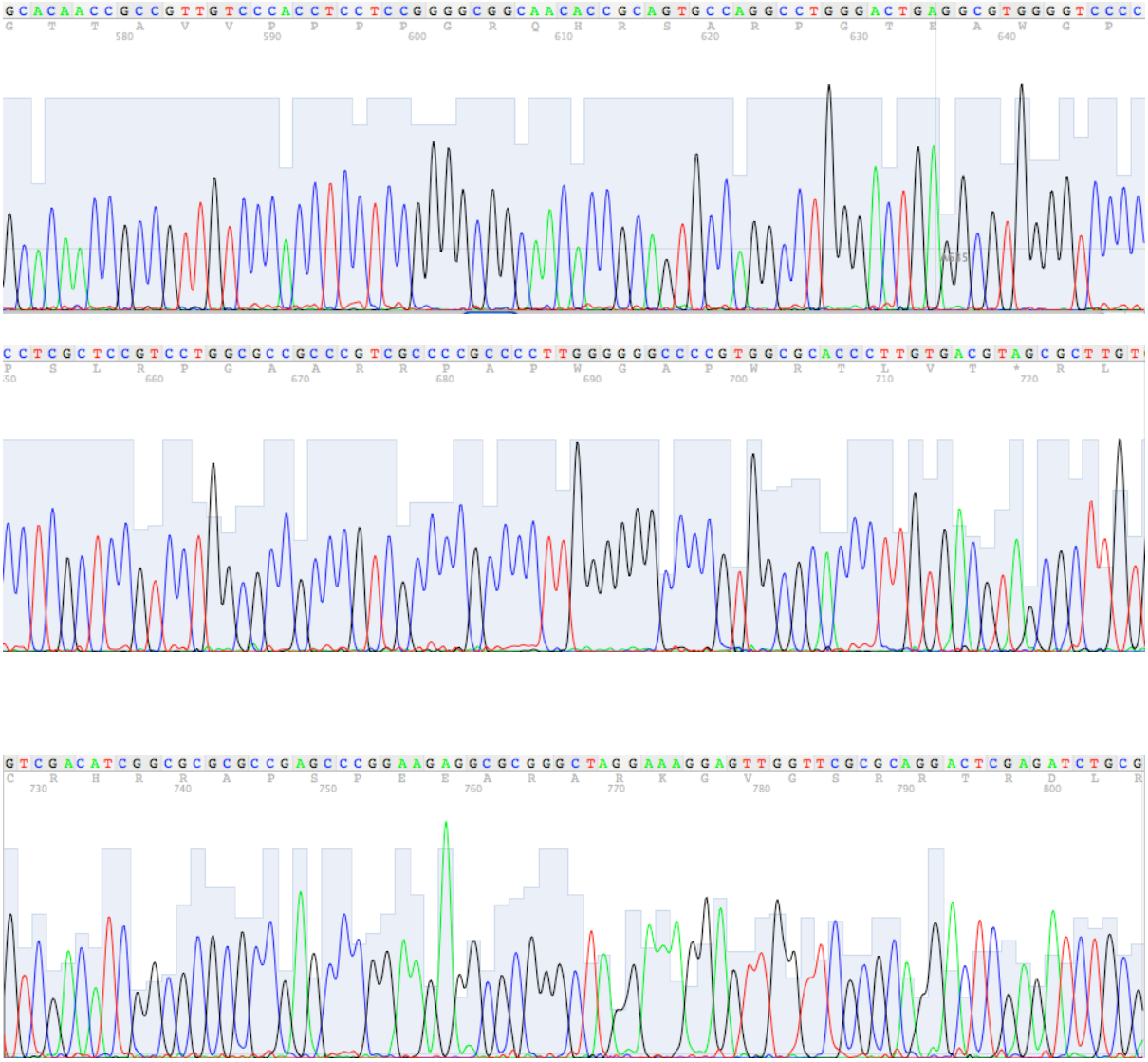

Appendix 3: AliBaba 2 transcription factor element analysis

```
seq(    0..   59)  ttgcctctgaattttctagaaccaaattgcttttcttctctcatttcaaggtcctaggag
Segments:
3.4.1.0    10   19              ====HSF===
1.1.3.0    17   26                    =C/EBPalp=
3.1.1.2    24   33                          ====Ftz===
================================================================================
seq(   60..  119)     agagaaccaataggaaaggccatgtctggaagcaatttgggtgggggcgggggtgtctt
Segments:
9.9.590    72   81               =NF-kappaB
2.3.1.0    77   86                    ====Sp1===
3.1.2.2    93   102                             ===Oct-1==
2.3.1.0    100  113                                ======Sp1=====
9.9.561    101  110                                 ==NF-muE1=
2.3.2.1    102  111                                  ==Krox-20=
2.3.2.3    102  111                                  ====WT1===
9.9.270    104  113                                    ====ETF===
================================================================================
seq(  120..  179)     gaggcctgcccagcccagccctttcctctttgttcagcctaggcaaaggagccacagctg
Segments:
2.3.1.0    121  130    ====Sp1===
2.3.1.0    127  140          ======Sp1=====
9.9.539    130  139             ====NF-1==
3.5.2.0    141  150                       ====PU.1==
1.3.1.4    170  179                                              ====AP-4==
================================================================================
seq(  180..  239)     cccactcagagctgttttaattgtccccagaaacctaacttctagaaaaacaattggctt
Segments:
3.1.1.2    193  202               ===Zen-1==
3.4.1.0    216  225                          ====HSTF==
2.3.2.2    222  231                               =====Hb===
2.4.1.0    228  237                                    ====p40x==
9.9.539    233  242                                        ====NF-
1.1.3.0    235  244                                          ===C/
3.1.2.2    235  244                                          ===Oc
================================================================================
seq(  240..  299)     gcaaaggattccagactctctgaacagatagatgatcagaatcttttctgattttcgtta
Segments:
9.9.539    233  242   1==
1.1.3.0    235  244   EBP==
3.1.2.2    235  244   t-1==
1.1.1.1    254  263               ===c-Jun==
2.1.1.1    261  270                     =====GR===
2.2.1.1    263  272                       ===GATA-1=
3.1.2.2    286  295                                         ===Oct-1==
4.1.1.0    286  295                                         =NF-kappaB
================================================================================
seq(  300..  359)     aggaaatatttcaagagggactgtggcaccaagacagtgaatgcctgcccctgagccccg
Segments:
1.1.3.0    300  309   =C/EBPalp=
2.3.1.0    311  325            =======Sp1=====
1.1.3.0    321  330                     =C/EBPbeta
2.3.1.0    342  352                                    =====Sp1===
3.1.2.2    343  352                                     ===Oct-1==
```

```
================================================================================
seq(  360..  419)     atgagaaggaattaagggccctgtgactctgtatgtgaccagaagccacatcaggctccg
Segments:
3.1.1.2     366  375         ====Ftz===
2.1.1.4     376  385                  =====ER===
2.1.2.3     377  386                   =REV-ErbA=
1.3.1.2     378  387                    ====USF===
9.9.29      381  390                       ====AP-1==
1.1.1.2     382  391                        ===c-Fos==
2.3.1.0     413  426                                                  ======S
================================================================================
seq(  420..  479)     ccaggcctggcaactgtccctggtgttctgttcttcacctcctgcggctcctgactcttc
Segments:
2.3.1.0     413  426   p1=====
2.1.1.1     445  454                            =====GR===
2.1.2.1     454  463                                    =RAR-alph=
2.1.2.3     454  463                                    =T3R-alpha
3.5.2.0     454  463                                    ===Elk-1==
9.9.45      454  463                                    ===ARP-1==
1.2.1.0     455  464                                     =====E1===
1.2.2.0     455  464                                     ===CeMyoD=
2.3.1.0     458  467                                        ====Sp1===
1.1.1.1     468  477                                                ===c-Jun==
2.3.1.0     468  477                                                ====Sp1===
1.1.1.5     469  478                                                 ===Pap1+==
9.9.29      469  478                                                 ====AP-1==
================================================================================
seq(  480..  539)     agttctcagttggaattgaggtcagctctctcgtttccttgtctggccccttcaccacc
Segments:
2.3.3.0     495  504                 =CPE_bind=
4.3.2.0     515  524                                    ====SRF===
9.9.539     515  524                                    ====NF-1==
2.3.1.0     520  533                                        ======Sp1=====
2.3.2.3     522  531                                          ====BRF1==
2.3.1.0     523  534                                           =====Sp1====
2.3.1.0     526  535                                              ====Sp1===
================================================================================
seq(  540..  599)     cacaatgcaaacccacactgagtgactaaccagcaagaggcccacagcaggtcccatagc
Segments:
2.2.1.1     540  549   ===GATA-1=
3.1.2.2     541  550    ===Oct-1==
9.9.29      555  568                 ======AP-1====
1.1.1.1     560  569                      ====JunD==
2.3.1.0     572  585                               ======Sp1=====
1.2.1.0     584  593                                     =====E1===
1.5.1.0     593  602                                           ====EF-
================================================================================
seq(  600..  659)     aaccagaggggccaagcttgctaccacagcccacaacatgccaacaccccatttagact
Segments:
1.5.1.0     593  602   C==
2.3.1.0     604  616       ======Sp1====
9.9.173     606  615         ====CTF===
2.3.3.0     607  616          ====MIG1==
9.9.537     608  617           ====NF-1==
9.9.539     610  619             ====NF-1==
2.3.1.0     625  634                            ====Sp1===
9.9.539     635  644                                    ====NF-1==
2.3.2.2     652  661                                                =====Hb=
```

```
================================================================================
seq(  660..  719)     tttacatgagaaataaacatccactttgttcaactgctgttgttttgtctctgtgactaa
Segments:
2.3.2.2    652  661   ==
3.1.2.2    662  671     ===Oct-1==
2.1.1.1    681  690                        =====GR===
1.1.1.5    710  719                                                ====CPC1==
9.9.32     710  719                                                ====AP-1==
================================================================================
seq(  720..  779)     atcaacaattctggcaaatctagaaagaagcagaagaattaggtgcaaagtgctggaagt
Segments:
1.1.3.0    729  738            =C/EBPalp=
3.1.2.2    744  753                              ===Oct-1==
1.1.3.0    758  767                                          =C/EBPalp=
================================================================================
seq(  780..  839)     ttagcagcctctcgtgggagcaagaaagccccaggcaggtttctgtccacatcactttaa
Segments:
9.9.590    802  811                          =NF-kappaB
2.3.1.0    806  815                              ====Sp1===
4.3.2.0    822  831                                              ====SRF===
================================================================================
seq(  840..  899)     tgtggagcactctcctagtcctctagatctgtctgttctatcaccttcccacagttcagc
Segments:
================================================================================
seq(  900..  959)     ttcctgtgctccccaaaacttcaccttggaaacatatttaactggttctgacctttagcc
Segments:
1.6.1.0    906  915         =AP-2alph=
1.1.3.0    924  933                              =C/EBPalp=
3.1.1.7    933  942                                       =embryo_D=
3.1.1.2    935  944                                         ====Ftz===
3.1.1.8    935  944                                         ====Eve===
2.1.2.1    945  955                                                  =RAR-alpha1
2.1.1.4    946  955                                                   =====ER===
2.1.2.10   946  955                                                   ====COUP==
2.1.2.3    946  958                                                   ===T3R-alpha=
1.1.3.0    959  968                                                                =
================================================================================
seq(  960.. 1019)     ttgtgtgactttgtgggtccacagccaatatcaaataactacagacaacagaaacttggt
Segments:
1.1.3.0    959  968   C/EBPalp=
1.6.1.0    974  983                =AP-2alph=
1.1.3.0    988  997                                =C/EBPalp=
3.1.1.12   993  1002                                     ===HNF-1C=
4.3.1.1    1017 1026                                                        ===
4.3.1.2    1017 1026                                                        ===
================================================================================
seq( 1020.. 1079)     taaaattctcaatagagggaaatgatcgctggacagtcagcagactcgctgttttcaggt
Segments:
4.3.1.1    1017 1026  MEB-1==
4.3.1.2    1017 1026  =GLO===
9.9.590    1033 1042              =NF-kappaB
2.1.2.3    1072 1081                                                  ====T3R=
2.1.1.4    1072 1083                                                  ======ER
2.3.3.0    1073 1082                                                   =CPE_bi
9.9.853    1073 1082                                                   =T3R-be
1.3.1.4    1077 1086                                                      ===
1.2.2.0    1078 1087                                                       ==
1.3.1.2    1078 1087                                                       ==
```

```
================================================================================
seq( 1080.. 1139)     cagctgctggctcagtcccctctgggtgccagggaaacctgacagctgagggttgtgaga
Segments:
2.1.2.3    1072 1081  ==
2.1.1.4    1072 1083  ====
2.3.3.0    1073 1082  nd=
9.9.853    1073 1082  ta1
1.3.1.4    1077 1086  =AP-4==
1.2.2.0    1078 1087  ==MyoD==
1.3.1.2    1078 1087  ==USF===
1.2.1.0    1080 1089  =====E1===
1.1.3.0    1084 1093      =C/EBPalp=
2.3.1.0    1090 1101           =====Sp1====
4.1.1.0    1093 1102              =NF-kappa=
9.9.539    1102 1111                       ====NF-1==
2.3.1.0    1104 1113                         ====YY1===
9.9.590    1107 1116                            =NF-kappaB
1.2.2.0    1119 1128                                     ====MyoD==
================================================================================
seq( 1140.. 1199)     agaagcagtttctctaggaactgactgacatgtctccctaaggagagagaagtgacaggc
Segments:
3.4.1.0    1143 1152     ====HSF===
3.4.1.0    1151 1160             ====HSTF==
2.3.1.0    1168 1177                       ====Sp1===
1.2.8.0    1175 1184                            ===Olf-1==
================================================================================
seq( 1200.. 1259)     aactctagggaagatggctttcatggcttcataaagatctgactggctctttggcttctt
Segments:
2.3.1.0    1208 1217          ====YY1===
9.9.173    1239 1248                                ====CTF===
9.9.539    1250 1259                                         ====NF-1==
1.1.3.0    1255 1264                                              =C/EB
================================================================================
seq( 1260.. 1319)     ttccaaggtagcccaaatctgttcctgtgtgaatatctttgtcgaaagggatggcatggt
Segments:
1.1.3.0    1255 1264  Palp=
2.1.1.1    1276 1285                =====GR===
3.1.2.2    1290 1299                      ===Oct-1==
2.3.1.0    1319 1328                                                        =
================================================================================
seq( 1320.. 1379)     caggtaggctgggtaggatgaactgcgggaaggtagatgaccaggatggggaagttctga
Segments:
2.3.1.0    1319 1328  ===Sp1===
2.3.1.0    1327 1336         ====Sp1===
2.3.3.0    1340 1349                 ====ACE2==
2.3.2.2    1350 1359                       ====Odd===
9.9.590    1367 1376                                =NF-kappaB
================================================================================
seq( 1380.. 1439)     tgaggtggggctgaggagaatgaagactaatgcccaagatcaaagttagggaaataaagt
Segments:
2.3.1.0    1381 1395   =======Sp1=====
9.9.77     1382 1391    =CACCC-bi=
1.1.3.0    1386 1395        =C/EBPalp=
3.6.1.0    1395 1404                ====TEC1==
3.1.1.2    1404 1413                      ====Ftz===
2.1.1.1    1415 1424                           =====GR===
================================================================================
```

```
seq( 1440.. 1499)     ttcgctgccaagtccaaaggtcagggtcacagtggaaaactggacacaaagccaaggtca
Segments:
9.9.539    1443 1453     ====NF-1===
2.1.2.3    1452 1461              =T3R-alpha
2.1.2.10   1453 1462               ====COUP==
2.1.1.4    1454 1463                =====ER===
2.1.2.1    1454 1463                =RAR-alph=
9.9.45     1454 1463                ===ARP-1==
1.1.1.6    1455 1464                 =ATF-3del=
2.1.2.2    1456 1465                  =RXR-alpha
2.1.1.4    1463 1472                       =====ER===
1.1.3.0    1480 1489                                  ===C/EBP==
3.1.1.2    1485 1494                                      ====Ftz===
================================================================================
seq( 1500.. 1559)     ggagccgagagaattggaaaagtggaaacaaaccagggaacaagactaggccgggcattg
Segments:
1.1.3.0    1512 1521              =C/EBPdel=
1.1.3.0    1512 1522              ==C/EBPbeta
2.3.1.0    1546 1557                                              =====Sp1====
================================================================================
seq( 1560.. 1619)     tggctgatgagaatgagctggtacccagcctagcttcactgtctctcaacctagcctcat
Segments:
9.9.539    1579 1588                    ====NF-1==
================================================================================
seq( 1620.. 1679)     gcacagaaaagtatcagcgaagagagggctgggtttaagtgatgtcaccaaggggaaca
Segments:
1.1.3.0    1620 1629  =C/EBPalp=
2.3.1.0    1643 1652                       ====Sp1===
1.1.1.6    1658 1667                                 ==CRE-BP1=
2.3.3.0    1658 1667                                 =CPE_bind=
9.9.29     1658 1667                                 ====AP-1==
1.1.2.0    1658 1668                                 ====CREB===
================================================================================
seq( 1680.. 1739)     aaagaaagcagcgtttctcaacccaggtccataactctcgtgttgtgcacaagattgtgt
Segments:
4.4.1.0    1686 1695        =====E2===
1.1.3.0    1691 1700             =C/EBPalp=
1.1.3.0    1731 1740                                                  =C/EBPbet
3.1.2.1    1736 1745                                                      ===P
================================================================================
seq( 1740.. 1799)     acattttccagagtttgttaaagggaacagcgcccccaaaagggttaaagtttgattgtg
Segments:
1.1.3.0    1731 1740  a
3.1.2.1    1736 1745  it-1a=
2.1.1.1    1761 1770                  =====GR===
2.3.1.0    1767 1778                       =====Sp1====
1.1.3.0    1778 1787                                 =C/EBPalp=
1.1.3.0    1789 1803                                            ===C/EBPalp
================================================================================
seq( 1800.. 1859)     gaataatctggttatccagaagagaacgatctctgcgggctctcctgtctcgacgaagtc
Segments:
1.1.3.0    1789 1803  ha==
1.1.3.0    1824 1833                    =C/EBPalp=
2.1.1.2    1854 1863                                                  =====P
================================================================================
seq( 1860.. 1919)     ctttagtggctgagggtctcggccaccttccaaaggggcggaatccccctgcctcgcgta
Segments:
2.1.1.2    1854 1863  R===
```

```
1.1.3.0    1865 1874       =C/EBPalp=
2.3.1.0    1890 1901                                  =====Sp1====
4.1.1.0    1897 1906                                        ===c-Rel==
9.9.590    1901 1910                                           =NF-kappaB
2.3.1.0    1903 1914                                             =====Sp1====
================================================================================
seq( 1920.. 1979)     ccccaggggtctcggcagcgccgctattctgtgagcctattcctctcagaagcgccgagc
Segments:
2.3.1.0    1925 1934       ====Sp1===
2.3.1.0    1933 1942              ====Sp1===
2.3.1.0    1954 1963                                    ====Sp1===
2.2.1.1    1959 1968                                        ===GATA-1=
================================================================================
seq( 1980.. 2039)     actaggcctggaagaggacaagtctagcaaatgaggggacacgggcggagggagggatta
Segments:
2.3.1.0    1984 1998      =======Sp1=====
1.1.3.0    2002 2014                        ==C/EBPdelta=
3.1.2.2    2008 2017                             ===Oct-1==
1.3.1.2    2015 2024                                   ====USF===
2.3.1.0    2015 2027                                   ======Sp1====
2.3.1.0    2015 2029                                   =======Sp1=====
2.3.1.0    2021 2030                                        ====Sp1===
2.3.1.0    2027 2036                                            ====Sp1===
================================================================================
seq( 2040.. 2099)     aaagatgggggtgtgatccgtgccaatggggacacccactggttcgaatattaacgcgag
Segments:
2.3.1.0    2041 2055   =======Sp1=====
9.9.77     2043 2052     =CACCC-bi=
3.5.1.2    2044 2053      ====RAP1==
2.3.1.0    2047 2056         ====Sp1===
9.9.539    2056 2065                 ====NF-1==
2.3.1.0    2071 2080                           ====Sp1===
3.1.1.12   2085 2094                                    ===HNF-1==
================================================================================
seq( 2100.. 2159)     gtttgtccgcttcttcacaatctgtccgtttcgttttactgcgaaagcaaatgtgttccc
Segments:
2.3.1.0    2106 2115        ====YY1===
1.1.3.0    2112 2125              ===C/EBPalpha=
2.1.1.1    2116 2125                 =====GR===
1.1.3.0    2144 2153                                    =C/EBPdel=
2.3.1.0    2157 2166                                                 ===
================================================================================
seq( 2160.. 2219)     atccctctatttggggatacgattagagttccgggaaggggtgcagcgcccggactggc
Segments:
2.3.1.0    2157 2166  =Sp1===
4.3.2.0    2163 2172     ====SRF===
9.9.1299   2187 2196                          ====MPBF==
2.3.1.0    2191 2203                             ======Sp1====
9.9.77     2194 2203                                =CACCC-bi=
2.3.1.0    2198 2207                                    ====Sp1===
2.3.1.0    2208 2217                                            ====Sp1===
1.1.3.0    2213 2225                                                ==C/EBP
================================================================================
seq( 2220.. 2279)     acaaccgccgttgtcccacctcctccggggcggcaacaccgcagtgccaggcctgggact
Segments:
1.1.3.0    2213 2225  alpha=
2.3.1.0    2236 2250                 =======Sp1=====
2.3.1.0    2244 2254                        =====Sp1===
```

```
1.1.3.0    2274 2283                                                                =C/EBP
2.3.1.0    2279 2290                                                                   =
================================================================================
seq( 2280.. 2339)     gaggcgtggggtccccccctcgctccgtcctggcgccgcccgtcgccccgccccttggggg
Segments:
1.1.3.0    2274 2283  alp=
2.3.1.0    2279 2290  ====Sp1====
2.3.1.0    2290 2303           ======Sp1=====
9.9.270    2292 2301             ====ETF===
1.1.3.0    2305 2314                        =C/EBPalp=
2.3.1.0    2308 2319                           =====Sp1====
2.3.1.0    2322 2334                                    ======Sp1====
2.3.2.1    2323 2332                                     ==Krox-20=
2.3.2.3    2323 2332                                     ====GLI3==
9.9.270    2323 2332                                     ====ETF===
9.9.539    2332 2341                                              ====NF-1
1.6.1.0    2333 2342                                               =AP-2al
2.3.1.0    2334 2348                                                ======
================================================================================
seq( 2340.. 2399)     gccccgtggcgcaccttgtgacgtagcgcttgtgtcgacatcggcgcgcgccgagcccg
Segments:
9.9.539    2332 2341  ==
1.6.1.0    2333 2342  ph=
2.3.1.0    2334 2348  =Sp1=====
1.1.1.6    2358 2367                ==CRE-BP1=
9.9.51     2358 2367                ====ATF===
2.3.1.0    2382 2391                                    ====Sp1===
2.3.1.0    2388 2400                                         ======Sp1===
2.3.1.0    2399 2413                                                   =
================================================================================
seq( 2400.. 2459)     gaagaggcgcgggctaggaaaggagttggttcgcgcaggtgcggcgcctgggtccccatg
Segments:
2.3.1.0    2388 2400  =
2.3.1.0    2399 2413  ======Sp1=====
2.3.1.0    2437 2451                                      =======Sp1=====
================================================================================
seq( 2460.. 2519)     gcgctgtggcgcggctccgcgtacgcgggcttcctggcgctggccgtgggctgcgtcttc
Segments:
1.1.3.0    2462 2471    =C/EBPbeta
2.3.1.0    2465 2479       =======Sp1=====
2.3.1.0    2495 2504                                  ====Sp1===
9.9.539    2497 2506                                    ====NF-1==
1.6.1.0    2501 2510                                        =AP-2alph=
2.3.1.0    2502 2514                                         ======Sp1====
9.9.29     2507 2516                                              ====AP-1==
2.3.1.0    2512 2521                                                   ====Sp1=
1.2.2.0    2516 2525                                                      ===C
================================================================================
seq( 2520.. 2579)     ctgctggagccagagctgccaggctcggcgctgcgctctctctggagctcgctgtgtctg
Segments:
2.3.1.0    2512 2521  ==
1.2.2.0    2516 2525  eMyoD=
2.3.1.0    2521 2530   ====Sp1===
2.3.1.0    2539 2548                ====Sp1===
1.1.1.1    2556 2565                                  ===c-Jun==
2.3.1.0    2575 2589                                                 =====
1.6.1.0    2576 2585                                                  =AP-
================================================================================
```

```
seq( 2580.. 2639)     gggcccgcgcctgcgccccgggacccgtctcccccgagggccggttggcggcagcctgg
Segments:
2.3.1.0    2575 2589  ==Sp1=====
1.6.1.0    2576 2585  2alph=
2.3.1.0    2581 2590   ====Sp1===
2.3.2.3    2581 2590   ====WT1===
9.9.637    2586 2595        ===NRF-1==
9.9.1197   2586 2595        ===NRF-1==
2.3.1.0    2590 2603            ======Sp1=====
2.3.3.0    2592 2601              ====MIG1==
1.6.1.0    2593 2606               ======AP-2====
2.3.1.0    2596 2606                  =====YY1===
2.3.1.0    2603 2612                        ====Sp1===
1.1.1.6    2606 2615                           ==CRE-BP1=
2.3.2.3    2606 2615                           =Tra-1_(s=
2.3.3.0    2608 2617                             =CPE_bind=
2.3.1.0    2612 2625                                 ======Sp1=====
9.9.539    2627 2636                                                ====NF-1==
2.3.1.0    2638 2647                                                      ==
================================================================================
seq( 2640.. 2699)     gacgcgcttatcgtgcggccagtccggcgctggcgccgcgtggcagtggggtgagtgcca
Segments:
2.3.1.0    2638 2647  ==Sp1===
2.3.1.0    2655 2664                ====Sp1===
2.3.1.0    2669 2678                      ====Sp1===
2.3.1.0    2680 2690                           =====Sp1===
2.3.1.0    2687 2696                                 ====Sp1===
1.1.1.5    2688 2697                                  ====CPC1==
9.9.539    2691 2700                                     ====NF-1=
================================================================================
seq( 2700.. 2759)  acggggcctgggtctctgagcctccgaggtcggccttggaggtcgggcggagccgcgcag
Segments:
9.9.539    2691 2700  =
2.3.1.0    2700 2711  =====Sp1====
1.3.2.1    2701 2710   ===c-Myc==
1.3.2.2    2701 2710   ====Max1==
1.6.1.0    2702 2711    =AP-2alph=
2.3.1.0    2719 2728                ====Sp1===
2.3.1.0    2726 2735                      ====Sp1===
2.3.1.0    2743 2754                            =====Sp1====
9.9.726    2749 2758                                 =represso=
================================================================================
seq( 2760.. 2819)     aaacagggcttctcagaggtccccgggaggcgctgctgtc
Segments:
2.3.1.0    2781 2795                   =======Sp1=====
```

Appendix 4: Promoter alignment

4.1 Human and mouse ADP-GK

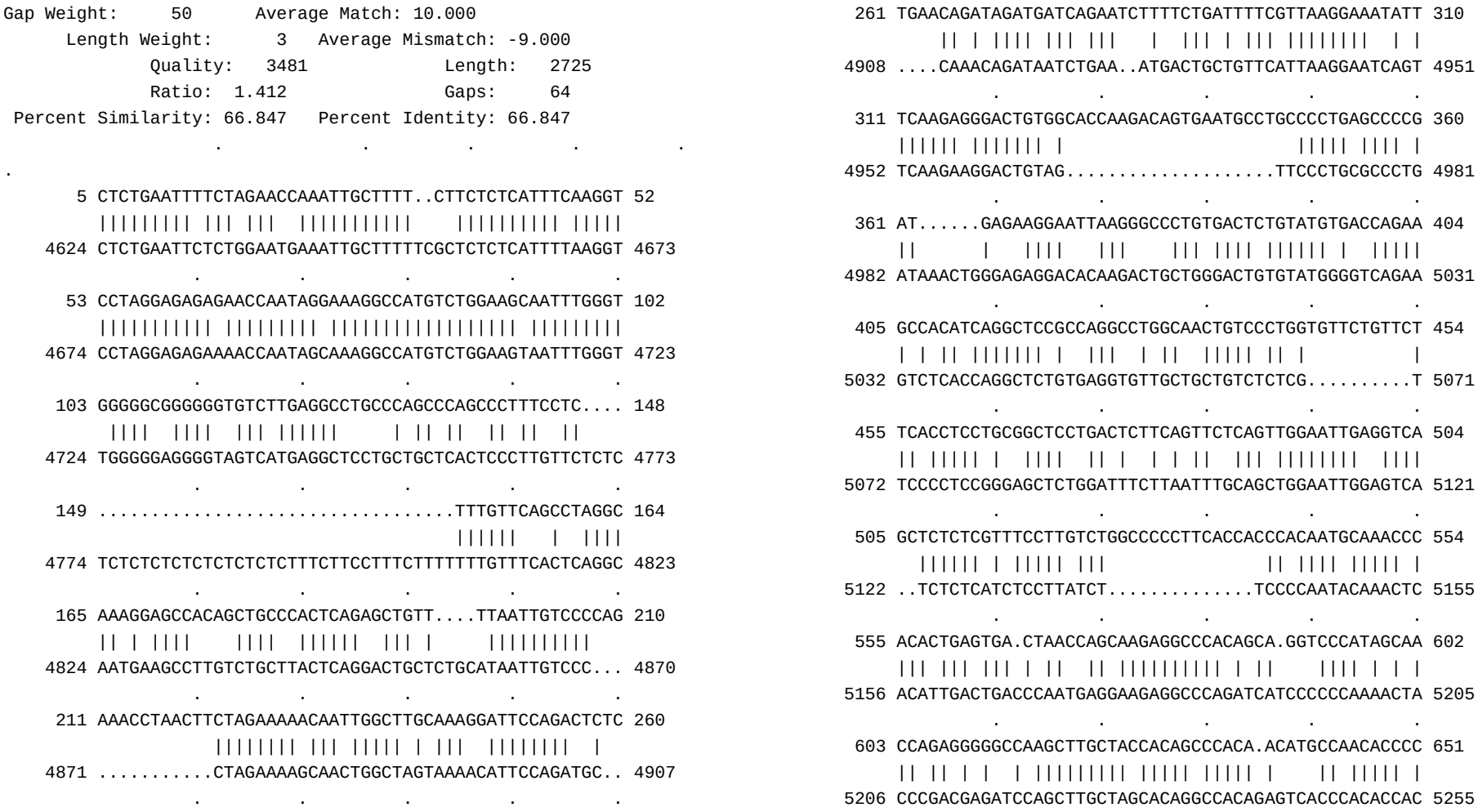

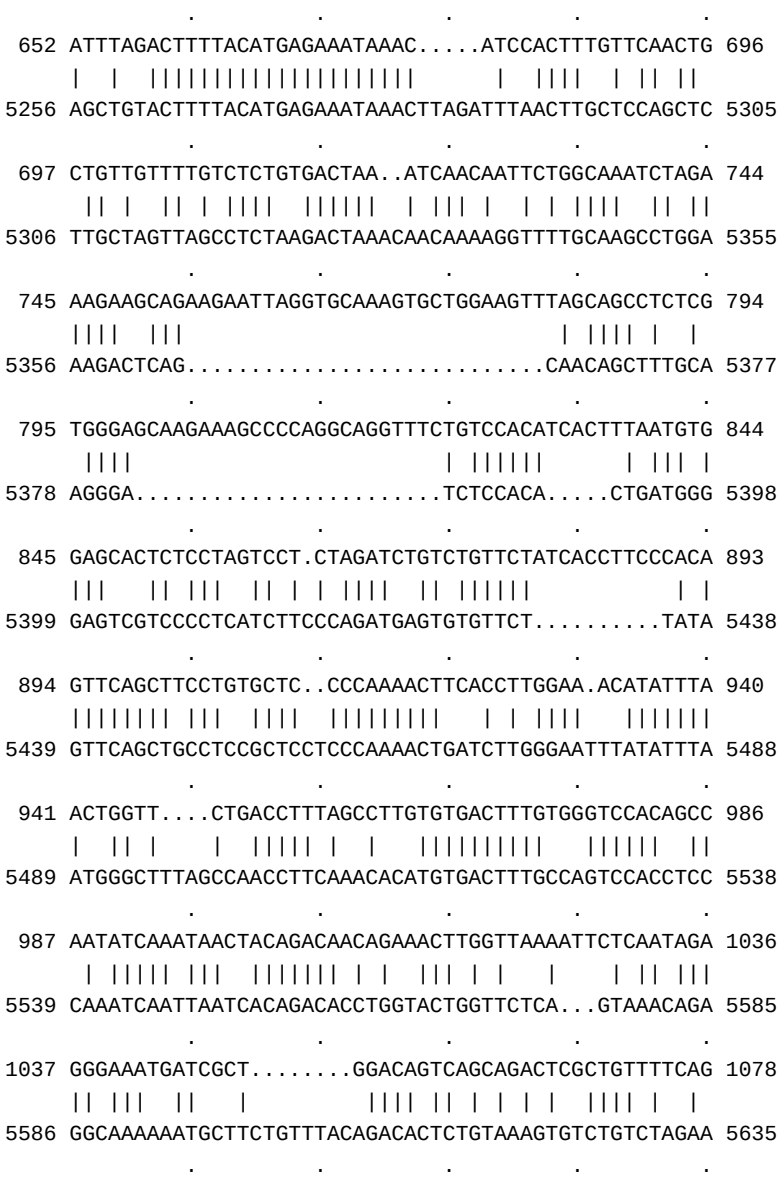
652 ATTTAGACTTTTACATGAGAAATAAAC.....ATCCACTTTGTTCAACTG 696
5256 AGCTGTACTTTTACATGAGAAATAAACTTAGATTTAACTTGCTCCAGCTC 5305
697 CTGTTGTTTTGTCTCTGTGACTAA..ATCAACAATTCTGGCAAATCTAGA 744
5306 TTGCTAGTTAGCCTCTAAGACTAAACAACAAAAGGTTTTGCAAGCCTGGA 5355
745 AAGAAGCAGAAGAATTAGGTGCAAAGTGCTGGAAGTTTAGCAGCCTCTCG 794
5356 AAGACTCAG.....CAACAGCTTTGCA 5377
795 TGGGAGCAAGAAAGCCCCAGGCAGGTTTCTGTCCACATCACTTTAATGTG 844
5378 AGGGA.....TCTCCACA.....CTGATGGG 5398
845 GAGCACTCTCCTAGTCCT.CTAGATCTGTCTGTTCTATCACCTTCCCACA 893
5399 GAGTCGTCCCCTCATCTTCCCAGATGAGTGTGTTCT.....TATA 5438
894 GTTCAGCTTCCTGTGCTC..CCCAAAACTTCACCTTGGAA.ACATATTTA 940
5439 GTTCAGCTGCCTCCGCTCCTCCCAAAACTGATCTTGGGAATTTATATTTA 5488
941 ACTGGTT....CTGACCTTTAGCCTTGTGTGACTTTGTGGGTCCACAGCC 986
5489 ATGGGCTTTAGCCAACCTTCAAACACATGTGACTTTGCCAGTCCACCTCC 5538
987 AATATCAAATAACTACAGACAACAGAAACTTGGTTAAAATTCTCAATAGA 1036
5539 CAAATCAATTAATCACAGACACCTGGTACTGGTTCTCA...GTAAACAGA 5585
1037 GGGAAATGATCGCT.....GGACAGTCAGCAGACTCGCTGTTTTCAG 1078
5586 GGCAAAAAATGCTTCTGTTTACAGACACTCTGTAAAGTGTCTGTCTAGAA 5635

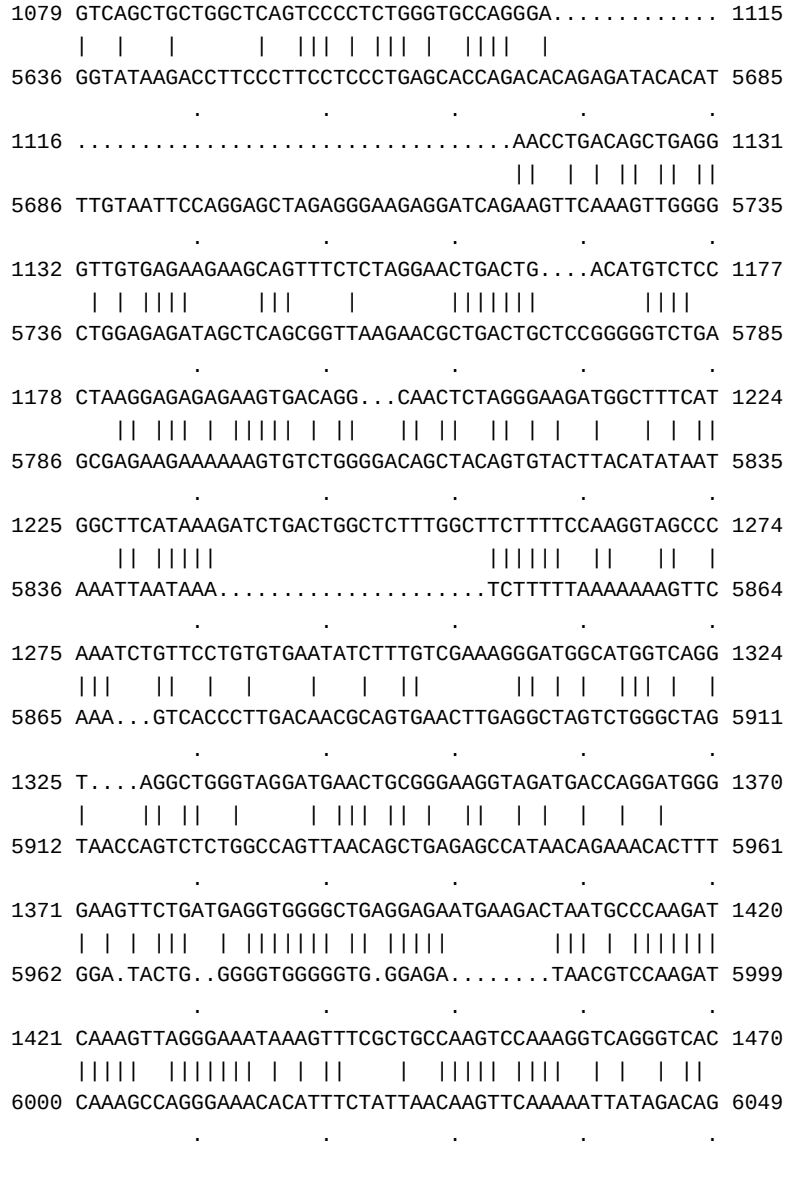
1079 GTCAGCTGCTGGCTCAGTCCCCTCTGGGTGCCAGGGA..... 1115
5636 GGTATAAGACCTTCCCTTCCTCCCTGAGCACCAGACACAGAGATACACAT 5685
1116 .....AACCTGACAGCTGAGG 1131
5686 TTGTAATTCCAGGAGCTAGAGGGAAGAGGATCAGAAGTTCAAAGTTGGGG 5735
1132 GTTGTGAGAAGAAGCAGTTTCTCTAGGAACTGACTG....ACATGTCTCC 1177
5736 CTGGAGAGATAGCTCAGCGGTTAAGAACGCTGACTGCTCCGGGGGTCTGA 5785
1178 CTAAGGAGAGAGAAGTGACAGG...CAACTCTAGGGAAGATGGCTTTCAT 1224
5786 GCGAGAAGAAAAAAAGTGTCTGGGGACAGCTACAGTGTACTTACATATAAT 5835
1225 GGCTTCATAAAGATCTGACTGGCTCTTTGGCTTCTTTTCCAAGGTAGCCC 1274
5836 AAATTAATAAA.....TCTTTTTAAAAAAAGTTC 5864
1275 AAATCTGTTCCTGTGTGAATATCTTTGTCGAAAGGGATGGCATGGTCAGG 1324
5865 AAA...GTCACCCTTGACAACGCAGTGAACTTGAGGCTAGTCTGGGCTAG 5911
1325 T....AGGCTGGGTAGGATGAACTGCGGGAAGGTAGATGACCAGGATGGG 1370
5912 TAACCAGTCTCTGGCCAGTTAACAGCTGAGAGCCATAACAGAAACACTTT 5961
1371 GAAGTTCTGATGAGGTGGGGCTGAGGAGAATGAAGACTAATGCCCAAGAT 1420
5962 GGA.TACTG..GGGGTGGGGGTG.GGAGA.....TAACGTCCAAGAT 5999
1421 CAAAGTTAGGGAAATAAAGTTTCGCTGCCAAGTCCAAAGGTCAGGGTCAC 1470
6000 CAAAGCCAGGGAAACACATTTCTATTAACAAGTTCAAAAATTATAGACAG 6049

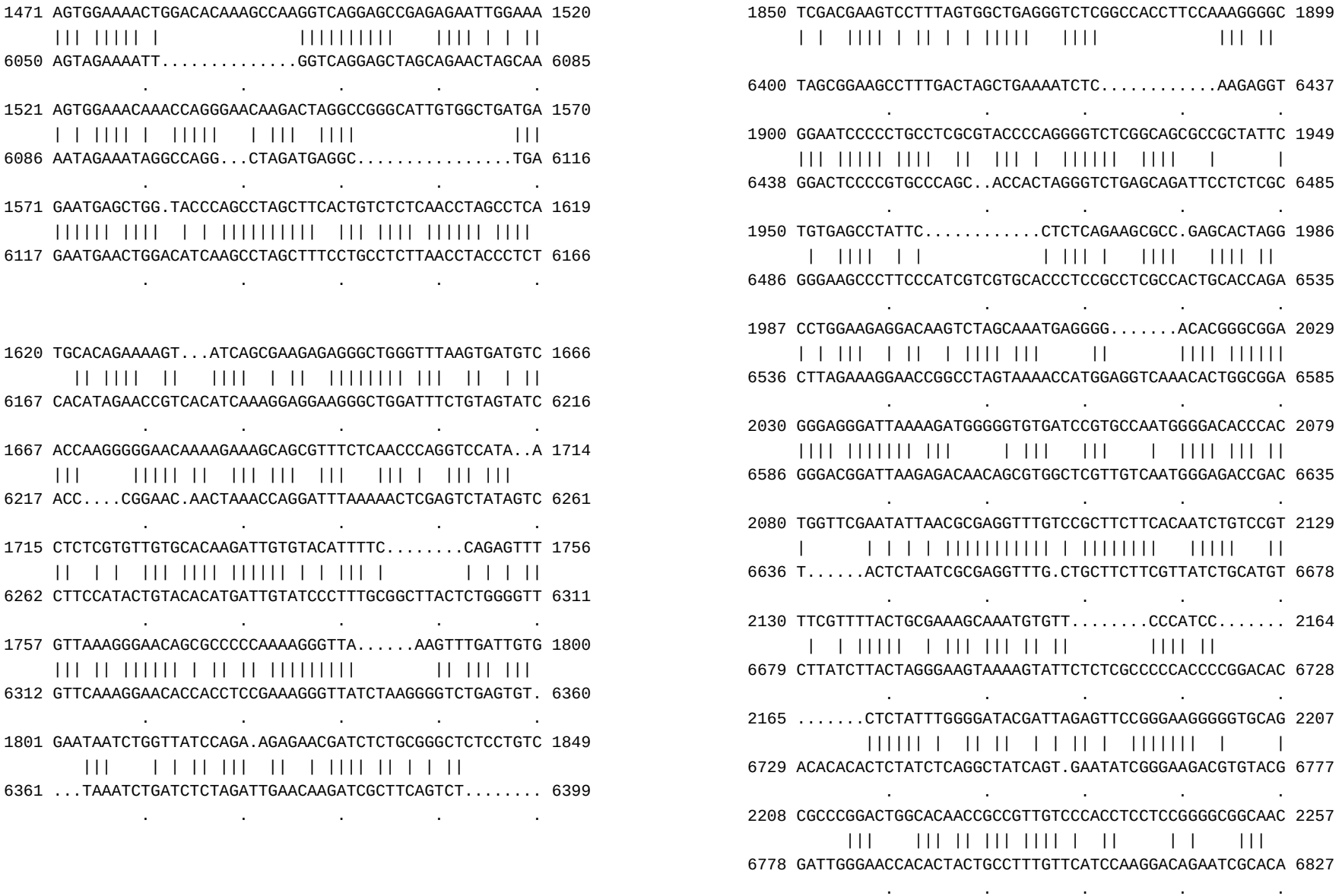
1471 AGTGGAAAACTGGACACAAAGCCAAGGTCAGGAGCCGAGAGAATTGGAAA 1520
6050 AGTAGAAAATT.....GGTCAGGAGCTAGCAGAACTAGCAA 6085
1521 AGTGGAAACAAACCAGGGAACAAGACTAGGCCGGGCATTGTGGCTGATGA 1570
6086 AATAGAAATAGGCCAGG...CTAGATGAGGC.....TGA 6116
1571 GAATGAGCTGG.TACCCAGCCTAGCTTCACTGTCTCTCAACCTAGCCTCA 1619
6117 GAATGAACTGGACATCAAGCCTAGCTTTCCTGCCTCTTAACCTACCCTCT 6166
1620 TGCACAGAAAAGT...ATCAGCGAAGAGAGGGCTGGGTTTAAGTGATGTC 1666
6167 CACATAGAACCGTCACATCAAAGGAGGAAGGGCTGGATTTCTGTAGTATC 6216
1667 ACCAAGGGGGAACAAAAGAAAGCAGCGTTTCTCAACCCAGGTCCATA..A 1714
6217 ACC....CGGAAC.AACTAAACCAGGATTTAAAAACTCGAGTCTATAGTC 6261
1715 CTCTCGTGTTGTGCACAAGATTGTGTACATTTTC.....CAGAGTTT 1756
6262 CTTCCATACTGTACACATGATTGTATCCCTTTGCGGCTTACTCTGGGGTT 6311
1757 GTTAAAGGGAACAGCGCCCCCAAAAGGGTTA.....AAGTTTGATTGTG 1800
6312 GTTCAAAGGAACACCACCTCCGAAAGGGTTATCTAAGGGGTCTGAGTGT. 6360
1801 GAATAATCTGGTTATCCAGA.AGAGAACGATCTCTGCGGGCTCTCCTGTC 1849
6361 ...TAAATCTGATCTCTAGATTGAACAAGATCGCTTCAGTCT..... 6399
1850 TCGACGAAGTCCTTTAGTGGCTGAGGGTCTCGGCCACCTTCCAAAGGGGC 1899
6400 TAGCGGAAGCCTTTGACTAGCTGAAAATCTC.....AAGAGGT 6437
1900 GGAATCCCCCTGCCTCGCGTACCCCAGGGGTCTCGGCAGCGCCGCTATTC 1949
6438 GGACTCCCCGTGCCCAGC..ACCACTAGGGTCTGAGCAGATTCCTCTCGC 6485
1950 TGTGAGCCTATTC.....CTCTCAGAAGCGCC.GAGCACTAGG 1986
6486 GGGAAGCCCTTCCCATCGTCGTGCACCCTCCGCCTCGCCACTGCACCAGA 6535
1987 CCTGGAAGAGGACAAGTCTAGCAAATGAGGGG.......ACACGGGCGGA 2029
6536 CTTAGAAAGGAACCGGCCTAGTAAAACCATGGAGGTCAAACACTGGCGGA 6585
2030 GGGAGGGATTAAAAGATGGGGGTGTGATCCGTGCCAATGGGGACACCCAC 2079
6586 GGGACGGATTAAGAGACAACAGCGTGGCTCGTTGTCAATGGGAGACCGAC 6635
2080 TGGTTCGAATATTAACGCGAGGTTTGTCCGCTTCTTCACAATCTGTCCGT 2129
6636 T......ACTCTAATCGCGAGGTTTG.CTGCTTCTTCGTTATCTGCATGT 6678
2130 TTCGTTTTACTGCGAAAGCAAATGTGTT........CCCATCC....... 2164
6679 CTTATCTTACTAGGGAAGTAAAAGTATTCTCTCGCCCCCACCCCGGACAC 6728
2165 .......CTCTATTTGGGGATACGATTAGAGTTCCGGGAAGGGGGTGCAG 2207
6729 ACACACACTCTATCTCAGGCTATCAGT.GAATATCGGGAAGACGTGTACG 6777
2208 CGCCCGGACTGGCACAACCGCCGTTGTCCCACCTCCTCCGGGGCGGCAAC 2257
6778 GATTGGGAACCACACTACTGCCTTTGTTCATCCAAGGACAGAATCGCACA 6827

```
2258 AC.......CGCAGTGCCAGGCCTGGGACTGAGGCGTGGGGTCCCCCCTC 2300
     ||       | ||| |||||  |   |||| |  |   | |  |||||
6828 ACAGCGTCGCCCAGCGCCAGCGCCAAGACTTAAACAGAGCGAACCCCCAA 6877
             .         .         .         .         .
2301 GCTCCGTCCTGGCGCCGCC.............................. 2319
        | | |||| || || |
6878 CGCCAGCCCTGTCGTCGTCCCGCCTCCAGCCCACCCATAGCTCCACCCAT 6927
             .         .         .         .         .
2320 ...................CGTCGCCCCGCCCCTTGGGGGG....CCCC 2345
                        ||| || |||||| | ||| ||     ||
6928 AACTGGGGCTGCAGTTCCGTCGTAGCTCCGCCCATCGGGAGGAAGAGCCT 6977
2346 GTGGCGCACCCTTGTGACGTAGCGCTTGTGTCGACATCGGCGCGCGCCGA 2395
     ||||||| |   |||||||  |||    ||| || || || |||||| |
6978 GTGGCGCGCGGGTGTGACGTTACGC..ACGTCTACGTCAGCACGCGCCCA 7025
             .         .         .         .         .
2396 GCCCGGAAGAGGCGCGGGCTAGGAAAGGAGTTGGTTCGCGCAGGTGCGGC 2445
     ||  ||| |||||||| ||   |||||||    ||   | | ||||||||
7026 GCTGGGAGGAGGCGCGAGCCGAGAAAGGATCCTGTAGCCACCGGTGCGGC 7075
             .         .
2446 GCCTGGGTCCCCATGGCGCTGTGGC 2470
     |  || || | |||||||||||||
7076 G.GTGTGTGCACATGGCGCTGTGGC 7099
```

4.2 ADP-GK and hexokinase type II

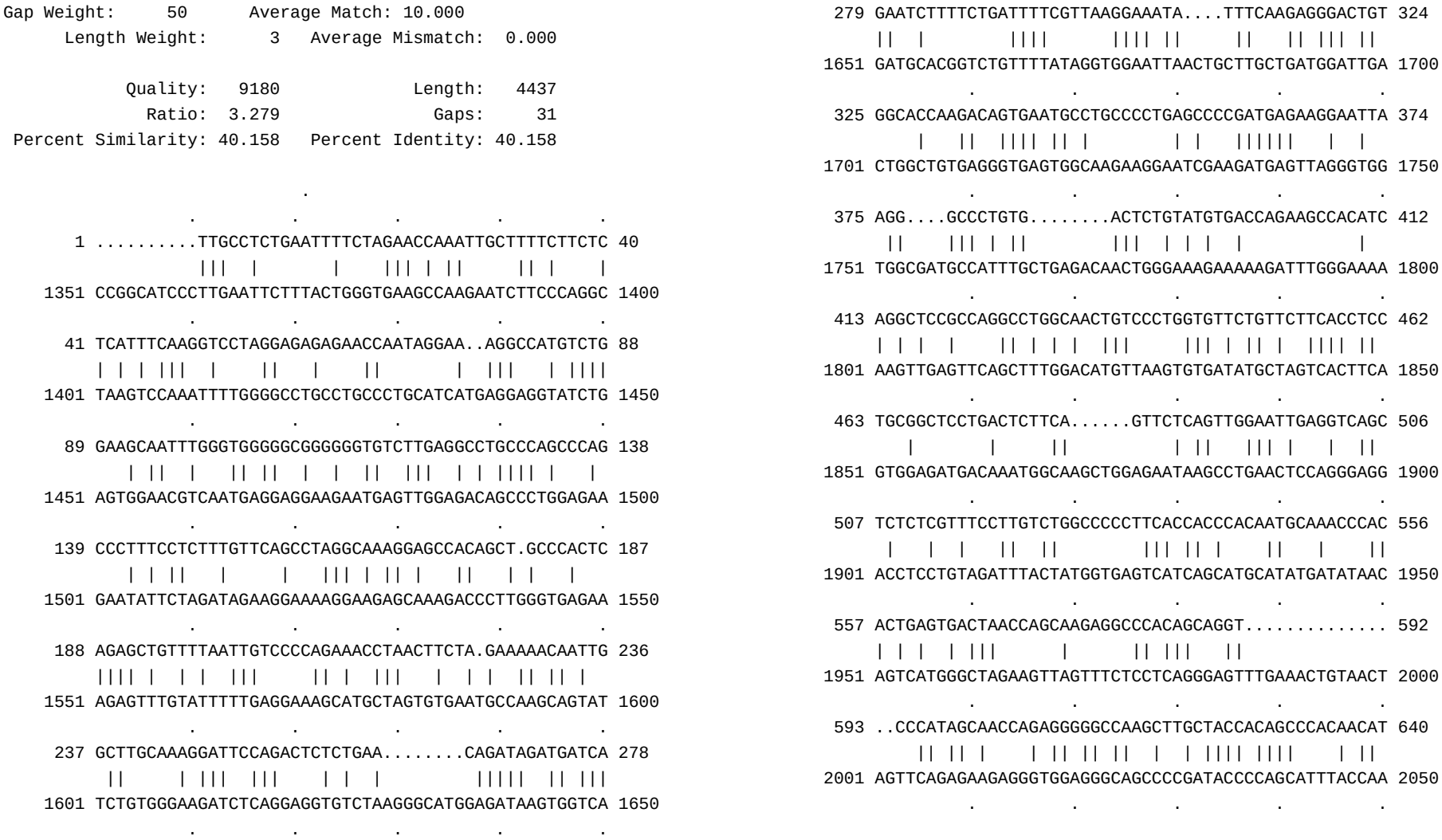

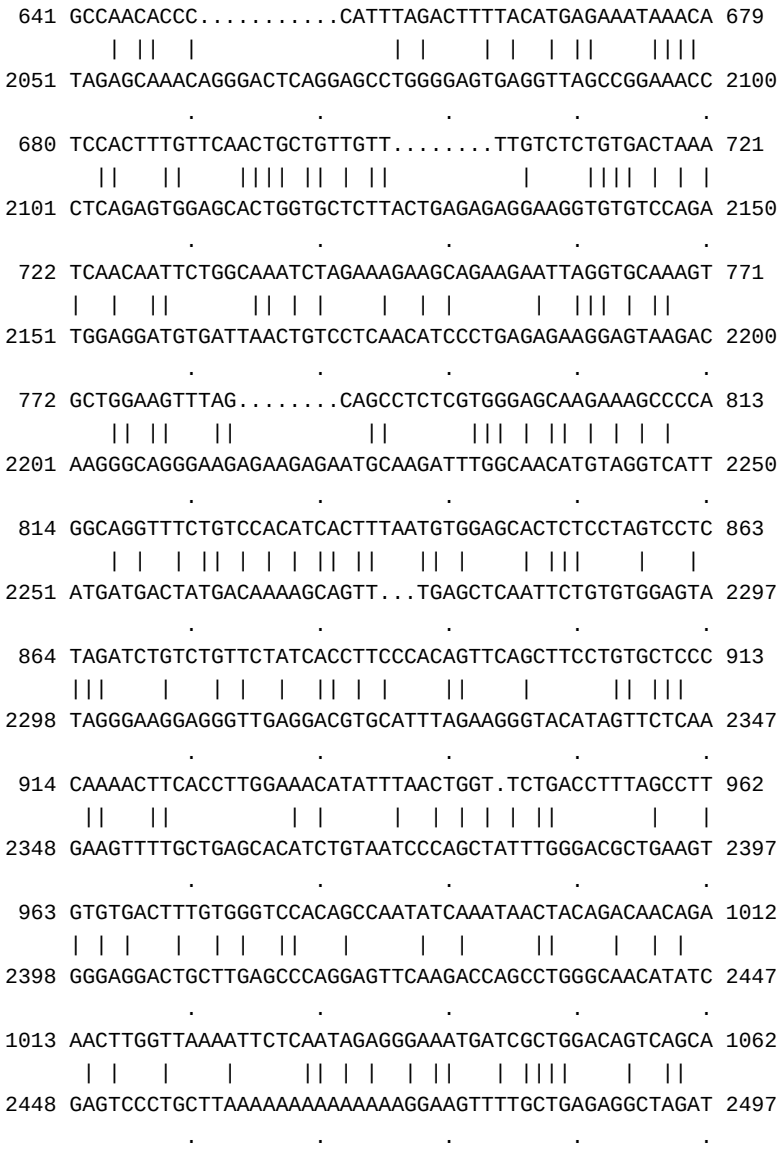

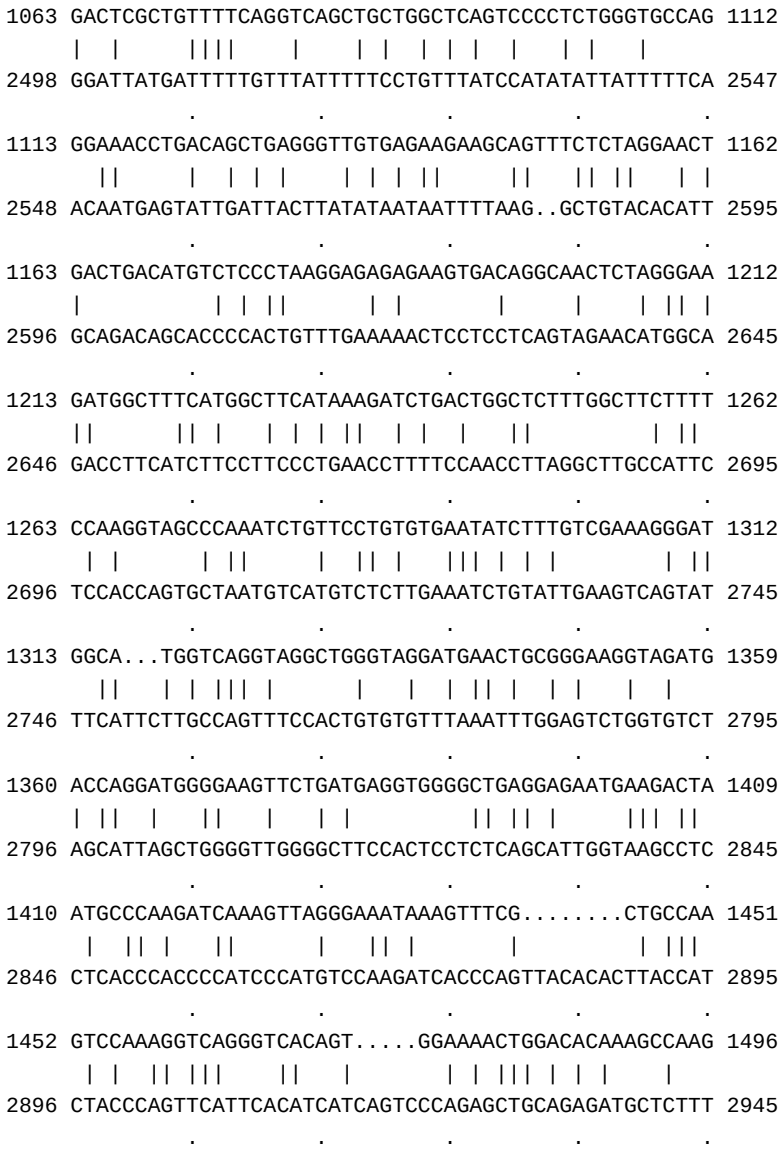

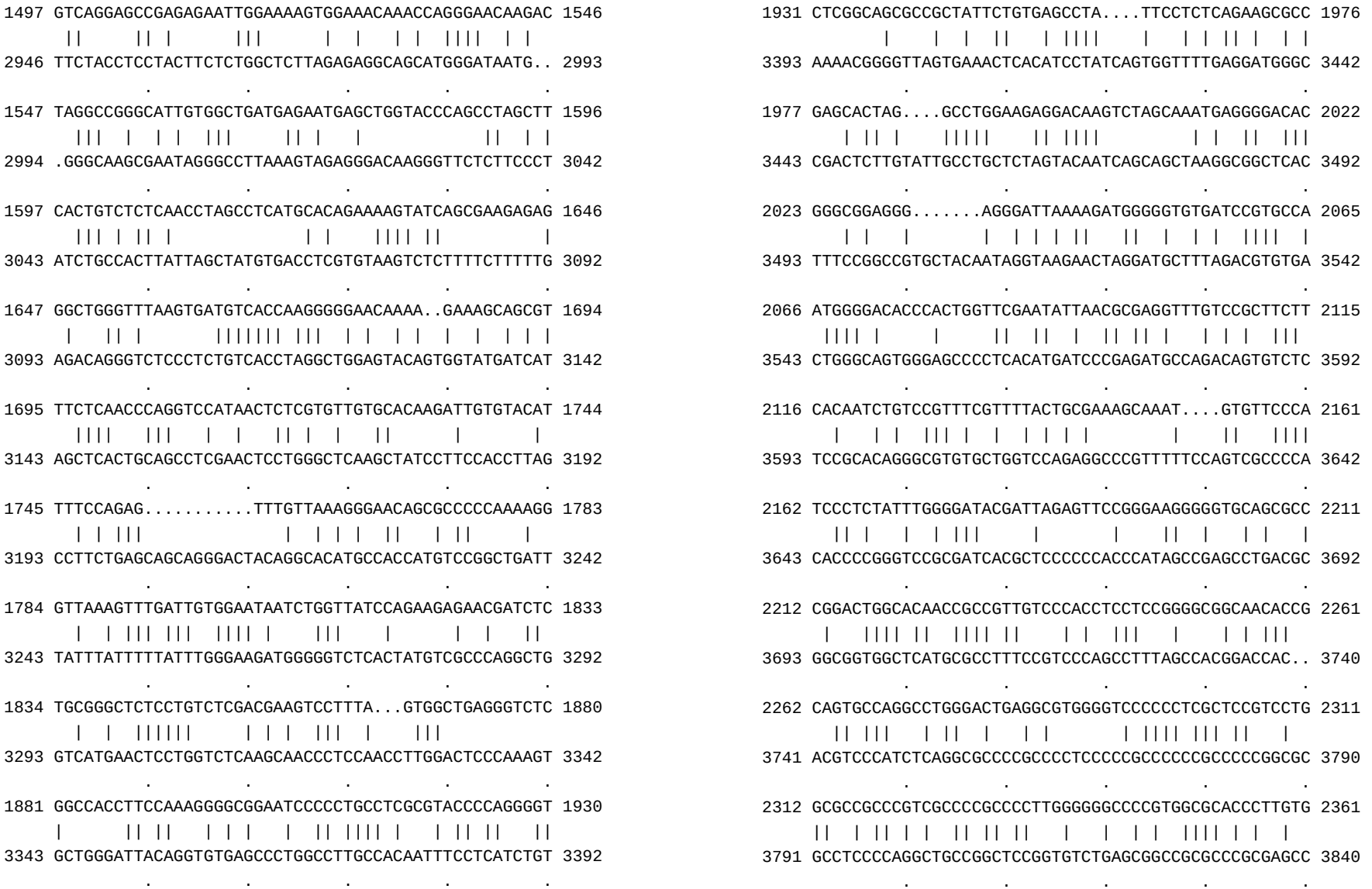

```
2362 ACGTAGCGCTTGTGTCGACATCGGCGCGCGCCGAGCCCGGAAGAGGCGCG 2411
           |         || |  |  |   |||    | |  | |  |  || |
    3841 GTGAGCGATGATTGGCTGCGCCACGGCGGCGGGCGGTCCGTGGGCGCACA 3890
                 .         .         .         .         .
    2412 GGCTAGGAAAGGAGTTGGTTCGCGCAGGTGCGGCGCCTGGGTCCCCATGG 2461
           |       |          | ||  | ||    |   | |||  |
    3891 CACCCTCCCCGCGCAGCCAATGGGCGTGCGCACGTCACTGATCCGGAGCC 3940
                 .         .         .         .         .
    2462 CGCTGTGGCGCGGCTCCGCGTACGCGGGCTTCCTGGCGCTGGCCGTGGGC 2511
         ||| |    || || || |         | |  | ||      |   |||
    3941 CGCGGGCCGGCAGCCCCTCAATAAGCCACATTGTTGCATGAAACTCCGGC 3990
                 .         .         .         .         .
    2512 TGCGTCTTCCTGCTGGAGCCAGAGCTGCCAGGCTCGGCGCTGCGCTCTCT 2561
           |   |||     | ||    |||| ||   |||    |   |   ||
    3991 GCAGGAGTCC....CGGGCTGCCGCTGGCAACATCG..TGTCACCCAGCT 4034
                 .         .         .         .         .
    2562 CTGGAGCTCGCTGTGTCTGGGGCCCGCGCCTGCGCCCCCG...GGACCCG 2608
           | |  ||   | | | | | | |||||||| |   | |   || |||
    4035 AAGAAAATCCGCGGGCCCGAGCCACGCGCCTGTGAATCGGAGAGGTCCCA 4084
                 .         .         .         .         .
    2609 TCTCCCCCGAGGGCCGGTTGGCGGCAGCCTGGGACGCGCTTATCGTGCGG 2658
           |||  | ||  | |      |   | |   | |          | |
    4085 CTGCCCGAGTGGAGCCGGGCTGAGATTCTTCTCAAGTTGAGCCTCAGTGA 4134
                 .         .         .         .         .
    2659 CCAGTCCGGCGCTGGCGCCGCGTGGCAGTGGGGTGAGTGCCAACGGGGCC 2708
          |     | ||  |    ||| | |  |||||   |  |   |||  |||
    4135 TCCTGTGGCCGAAGTTAGCGCCTTGACGTGGGACAACCGGACACGTCGCC 4184
                 .         .         .         .         .
    2709 TG..GGTCTCTGAGCCTCCGAGGTCGGCCTTGGAGGTCGGGCGGAGCCGC 2756
          |  |    ||||| | ||          |  || | |      |
    4185 AGGAGAGAACTGAGGCGCCTTCTAGCAGTTGTGACGCCAAAATCACGTCT 4234
                 .         .         .         .         .
    2757 GCAGAAACAGGGCTTCTCAGAGGTCCCCGGGAGGCGCTGCTGTC...... 2800
          | || ||  |    ||| |    ||  | |   |   || |
    4235 CCGGAGACCCGCGCCCTCCGCCAGCCGGGCGCACCCTCGCCGGTAGCCTT 428
```

Appendix 5: BLAST promoter similarity in mammalian species

Descriptions

Legend for links to other resources: U UniGene E GEO G Gene S Structure M Map Viewer

Sequences producing significant alignments:

(Click headers to sort columns)

AC009712.22	Homo sapiens chromosome 15, clone RP11-361M10, complete sequence	1847	1847	100%	0.0	100%	
AK095995.1	Homo sapiens cDNA FLJ38676 fis, clone IMR322000383	1831	1831	100%	0.0	99%	U
AK127877.1	Homo sapiens cDNA FLJ45982 fis, clone PROST2017729	1748	1748	94%	0.0	99%	U
AC210935.3	Pongo abelii BAC clone CH276-332K1 from chromosome 15, complete sequence	1700	1700	100%	0.0	97%	
BC018074.1	Homo sapiens ADP-dependent glucokinase, mRNA (cDNA clone IMAGE:4791959), complete cds	1700	1700	92%	0.0	99%	U G
NR_023318.1	Homo sapiens ADP-dependent glucokinase (ADPGK), transcript variant 2, transcribed RNA	994	994	53%	0.0	100%	G
BC044589.1	Homo sapiens ADP-dependent glucokinase, mRNA (cDNA clone IMAGE:5269974)	898	898	48%	0.0	100%	U G
NR_023319.1	Homo sapiens ADP-dependent glucokinase (ADPGK), transcript variant 3, transcribed RNA	604	604	32%	1e-169	100%	G
NM_031284.4	Homo sapiens ADP-dependent glucokinase (ADPGK), transcript variant 1, mRNA	601	601	32%	1e-168	100%	U E G
XM_001175160.1	PREDICTED: Pan troglodytes ADP-dependent glucokinase, transcript variant 2 (ADPGK), mRNA	595	595	32%	6e-167	99%	G
AK055526.1	Homo sapiens cDNA FLJ30964 fis, clone HEART2000035, weakly similar to Transacylases	592	592	32%	8e-166	100%	U G
XM_001093274.1	PREDICTED: Macaca mulatta ADP-dependent glucokinase (ADPGK), mRNA	529	529	32%	7e-147	96%	U G
BC006112.1	Homo sapiens ADP-dependent glucokinase, mRNA (cDNA clone MGC:12975 IMAGE:3347312), complete cds	497	497	26%	2e-137	100%	U E G
XM_001175157.1	PREDICTED: Pan troglodytes ADP-dependent glucokinase, transcript variant 1 (ADPGK), mRNA	488	488	27%	1e-134	98%	G
AK075560.1	Homo sapiens cDNA PSEC0260 fis, clone NT2RP3004059	484	484	26%	1e-133	100%	U E G
EU831454.1	Synthetic construct Homo sapiens clone HAIB:100066483; DKFZo008E0617 ADP-dependent glucokinase protein (ADPGK) gene, encodes complete protein	435	435	23%	1e-118	99%	G
EU831541.1	Synthetic construct Homo sapiens clone HAIB:100066570; DKFZo004E0618 ADP-dependent glucokinase protein (ADPGK) gene, encodes complete protein	435	435	23%	1e-118	99%	G
CU675251.1	Synthetic construct Homo sapiens gateway clone IMAGE:100019680 5' read ADPGK mRNA	433	433	23%	5e-118	100%	
AC134894.4	Mus musculus BAC clone RP24-260P1 from chromosome 9, complete sequence	287	287	27%	4e-74	85%	
AC160111.2	Mus musculus BAC clone RP24-144L16 from chromosome 9, complete sequence	287	287	27%	4e-74	85%	
NM_001100723.1	Rattus norvegicus ADP-dependent glucokinase (Adpgk), mRNA	267	267	26%	6e-68	85%	U E G
BC021526.1	Mus musculus ADP-dependent glucokinase, mRNA (cDNA clone MGC:38532 IMAGE:5353637), complete cds	261	261	25%	3e-66	85%	U E G
AK149942.1	Mus musculus bone marrow macrophage cDNA, RIKEN full-length enriched library, clone:G530106P09 product:RbBP-35 homolog [Homo sapiens], full insert sequence	261	261	25%	3e-66	85%	U G
AK167634.1	Mus musculus 11 days pregnant adult female placenta cDNA, RIKEN full-length enriched library, clone:I530025L22 product:RbBP-35 homolog [Homo sapiens], full insert sequence	261	261	25%	3e-66	85%	U G
AK169590.1	Mus musculus 2 days neonate thymus thymic cells cDNA, RIKEN full-length enriched library, clone:E430001A13 product:RbBP-35 homolog [Homo sapiens], full insert sequence	261	261	25%	3e-66	85%	U G
AK048904.1	Mus musculus 0 day neonate cerebellum cDNA, RIKEN full-length enriched library, clone:C230080G04 product:RIKEN cDNA 2610017G09 gene, full insert sequence	261	261	25%	3e-66	85%	E G
AK011434.1		261	261	25%	3e-66	85%	U E